**Title**
Reproductive, Metabolic, and Autonomic Networks Across the Female Lifespan



**Author**
Grant, Azure

**Publication Date**
2021

Peer reviewed|Thesis/dissertation

# Reproductive, Metabolic, and Autonomic Networks Across the Female Lifespan

By

Azure Grant

A dissertation submitted in partial satisfaction of the

requirements for the degree of

Doctor of Philosophy

in

Neuroscience

in the

Graduate Division

of the

University of California, Berkeley

Committee in charge:

Professor Lance J. Kriegsfeld, Co-Chair

Professor Linda Wilbrecht, Co-Chair

Professor Frédéric Theunissen

Professor Andrew Ahn

Summer 2021

# Abstract

Reproductive, Metabolic, and Autonomic Networks Across the Female Lifespan

By

Azure Grant

Doctor of Philosophy in Neuroscience

University of California, Berkeley

Professor Lance J. Kriegsfeld, Co-Chair

Professor Linda Wilbrecht, Co-Chair

Mammalian physiology is exquisitely tuned to anticipate and synchronize with environmental oscillations. These oscillations appear to occur in a networked fashion across systems and timescales, such that information about difficult-to-measure systems (e.g., reproductive) may be garnered from easy-to-measure systems (e.g., autonomic, and thermoregulatory). These network dynamics and their implications for health require deep exploration. The goals of this dissertation are to 1) investigate the relationship among reproductive, metabolic, and autonomic rhythms at the hourly to ovulatory timescales, and 2) investigate the conditions under which peripheral timeseries features may serve as proxies for hormonal status. This dissertation traverses discrete stages of reproductive life: adolescence, adulthood, and menopause; as well as the impacts of exogenous network perturbations at each stage of life. Chapter 1 reviews central mechanisms of coupled oscillations in the reproductive and thermoregulatory systems. Chapters 2 and 3 investigate the development of thermoregulatory rhythms across adolescence, their dependence on endogenous and exogenous reproductive hormones, their interaction with natural and artificial environments, and derive peripheral features to monitor reproductive development in the rat. Chapter 4 extends these findings to adult women and investigates shared rhythmicity among autonomic and thermoregulatory outputs and sex hormones for the purposes of LH surge prediction or identification of its absence in menopause. With an eye toward future developments in sex hormone replacement, Chapter 5 compares the effects of the most advanced forms of continuous hormone replacement therapy on biological rhythms in metabolic output. These studies inform our understanding of the structure of reproductive, metabolic, and autonomic networks across life, and reveal translational tools for reproductive health.

## Dedication

*For Benjamin, who decided to be in it for the long haul.*

*For my parents, who support me fiercely in all endeavors.*

*For my best friends: you have filled the last 15 years with joy and curiosity.*

*And for all those who practice everyday science.*

## Acknowledgements

*Thank you to my mentors, labs, peers, and program.*

*Lance Kriegsfeld:* I did not know at age 19 that I had happened into a lab that would change my life. I had met a mentor who would shepherd me safely from being a kid who liked research, to a slightly older kid who loves research, and does it a bit better now. You have infused humor, rigor, sensitivity, tolerance, precision, and care into the past 7 years. Due to your intellectual guidance through several developmental, as well as career, milestones, I will undoubtedly carry your influence and idiosyncrasies throughout my life and work. I am incredibly fortunate to learn from you.

*Linda Wilbrecht:* Without your guidance and support, I would probably not have stayed in graduate school! You exemplify so many attributes I wish to develop: kindness, deep knowledge, youthful curiosity, close listening, culturing understanding and growth among your students, tenacity, and motherhood. I will always look to you as an example and feel humbled that you chose to take me on as your student.

*Frédéric Theunissen:* Thank you for making the time to listen to my ideas, question them, read my writing, and even to tape a temperature sensor to your wrist on a trans-continental trip. I greatly admire how you ask questions, and the easy-going, yet rigorous lab culture you create.

*Andrew Ahn:* You were my socially distanced mentor before it was cool! It is rare to meet someone who so closely combines one's research interests. Thank you for helping expose me to network physiology, introducing me to new friends and colleagues, and supporting me with kindness and tons of time from the East coast.

*Kate Wilsterman:* I think I'll be looking up to you for the rest of my career. Thank you for all the days of writing, editing, running, relaxing, reflecting, commiserating, and laughing. Your sprint to academic success has inspired me across my undergraduate and graduate career.

*Neta Gotlieb:* I met you on my first day as an undergrad in the lab in 2014! Your smile, creativity, kindness, passion, and determination to make progress in basic and translational reproductive health, and your support as we move on to the next stages of our career are invaluable. I hope to have you as a colleague and friend for life.

*Dax Ovid and Adam Orford:* thank you for exemplifying an academic couple appreciating all the bay has to offer with good humor, for the hikes and the discussions, and for supporting me on two continents.

*Dana Lewis:* Thank you for teaching me to tackle my first multi-person grant and introducing me to the world of type-1-diabetes and large community data collection. Your positive attitude, deep competence, and consistency were essential to my graduate career.

*Candace Groskreutz:* You make this graduate program work.

To those who supported me earliest in my education. *Jacqueline Lincoln*, who taught me about neuroplasticity long before I could take a biology class, and who rewarded curiosity and spontaneity in a small town. *Erik Wasinger*, whose lab gave me my first chance to do research; you were the first person to make me believe that research was my future. And thank you to *Daniela Kaufer*, for supporting me as a new undergraduate.

*Thank you to my family and friends.*

*Momma*: You believe in me more than most any mom believes in their child. You nurtured and fought for me through every hurdle growing up, and through my finding independence. You are a reader of minds, a fighter, a brain, a beauty, and an infuser of art and structure into every situation you encounter.

*Dad*: Thank you for teaching me to struggle with problems, to sleep on them, and to try again in the morning. Thank you for teaching me when to struggle, and when to ask for help. Thank you for being the calming force, and for exemplifying what life is like when one successfully juggles engineering, athleticism, music, tolerance, and relaxation.

*Grandma*: You were my earliest exposure to medicine and biological rhythms in the way that mom was my first exposure to anatomy and form. I am shaped by your raucous sense of humor, your no-nonsense taking care of bodies, and your love and marvel for the natural world.

*Auntie Jayle*: Thank you for taking care of me whenever I'll let you, and for providing the retreat from the world needed to finish this dissertation.

*Jenn, Richard, and Jimmy*: Thank you for accepting me into the fold and being there for me whenever I need it.

*Larry, Janet, Michi, Joseph, Lili, Sebe, Tom, and Jan*: Thank you for expanding my family more than I ever anticipated. You exemplify the full range of intellectual and social endeavors, and are role models for poise, success, and enjoyment at any age.

*Gary Wolf, Christa Aboitiz, and Inez Aboitiz-Wolf*: Thank for your mentorship, perspective, meals, and friendship; and for continually educating me on the history, culture, and practice of science.

*Brad and Nenelle Bunnin:* Much of this PhD was conducted in your downstairs apartment, or in your backyard. You two are and will be lifelong role models of family, career, and kind curiosity.

I could write a second dissertation on: *Cypress, Camellia, Sura, Celia, Lau, Adam, and Brianna*. You are my tethers. Watching you all mature and change since we were children has kept me motivated, awed, having too much fun, and feeling like we're in it together.

And, finally, *Benjamin*: you are the best partner that I could hope for. We have been through so many transitions together that you have shown me the meaning of change. But you have also shown me that, with a little savvy, we can see what changes may come next and, together, prepare.

Table of Contents

**Reproductive, Metabolic, and Autonomic Networks Across the Female Lifespan** ..... **1**
Abstract ..... 1
Dedication ..... i
Acknowledgements ..... ii
**1. Neural Substrate for Ultradian Coupling Among Reproductive and Thermoregulatory Circuits** ..... **1**
1.1 Abstract ..... 1
1.2 Introduction ..... 2
1.3 Hypothalamic Organization of Reproduction ..... 3
1.4 Hypothalamic Organization of Thermoregulation ..... 4
1.5 Interaction Among Thermoregulatory and Reproductive Circuits ..... 5
1.6 Modulating URs by Phase of Cycle: A Job for the Dopaminergic Ultradian Oscillator, TIDA Neurons, and the Arcuate Pulse Generator? ..... 6
1.7 Could Coupling be Decentralized? ..... 9
1.8 Summary and Conclusions ..... 10
1.9 References ..... 11
**2. Adolescent Development of Biological Rhythms: Estradiol Dependence and Effects of Combined Contraceptives** ..... **20**
2.1 Abstract ..... 20
2.2 Introduction ..... 21
2.3 Materials and Methods ..... 23
2.4 Results ..... 26
2.5 Discussion and Conclusions ..... 34
2.6 Acknowledgements ..... 37
2.7 Supplemental Figures ..... 37
2.8 References ..... 41
**3. Sex Differences in Pubertal Circadian and Ultradian Rhythm Development Under Naturalistic Conditions** ..... **53**
3.1 Abstract ..... 53
3.2 Introduction ..... 54
3.3 Materials and Methods ..... 55
3.4 Results ..... 58
3.5 Discussion and Conclusions ..... 64

3.6 Acknowledgements ..... 65
3.7 Supplemental Figures ..... 65
3.8 References ..... 67
**4. Ultradian Rhythms of Heart Rate Variability and Distal Body Temperature Anticipate Onset of the Luteinizing Hormone Surge ..... 72**
4.1 Abstract ..... 72
4.2 Introduction ..... 73
4.3 Materials and Methods ..... 75
4.4 Results ..... 78
4.5 Discussion and Conclusions ..... 83
4.6 Acknowledgements ..... 86
4.7 Supplemental Figures ..... 87
4.8 References ..... 91
**5. Multi-Timescale Rhythmicity of Blood Glucose and Insulin Delivery Reveals Key Advantages of Hybrid Closed Loop Therapy ..... 99**
5.1 Abstract ..... 99
5.2 Introduction ..... 100
5.3 Materials and Methods ..... 101
5.4 Results ..... 103
5.5 Discussion and Conclusions ..... 106
5.6 Acknowledgements ..... 108
5.7 Supplemental Figures ..... 109
5.8 References ..... 111

# 1. Neural Substrate for Ultradian Coupling Among Reproductive and Thermoregulatory Circuits

## 1.1 Abstract

**Background:** Temporal coupling among reproductive and thermoregulatory outputs has been reported in females for over a century[1–6]. These systems exhibit inter-dependent, stereotyped biological rhythms at multiple timescales, including ultradian rhythms (UR; within-a-day), circadian rhythms (CR; daily), and multi-day ovulatory rhythms (ORs). However, the mechanisms underlying these coupled oscillations, or if coupling occurs on a continuous basis, are not well understood.

**Motivation and Methods:** Today, numerous digital tools aim to provide proxy measures for female reproductive state by presuming reproductive-thermoregulatory coupling across timescales and conditions. Due, in part, to the unknown origins of *high frequency* coupling among these outputs, little is known about the timescales and life stages under which these tools are accurate. One possibility is that coupling is generated at the level of the hypothalamus via direct synaptic communication among regions that temporally organize reproduction and thermoregulation. Alternately, peripherally observed coupling may be orchestrated indirectly through shared effects on metabolism, locomotor activity, and other factors. In this review, we compile evidence of neural substrate for coupling among central circuits governing reproduction and thermoregulation at the UR timescale. We include integration of dominant hypotheses about UR generation as pertains to reproduction, including the arcuate pulse generator and the dopaminergic ultradian oscillator.

**Conclusions:** We find strong evidence of structural and functional hypothalamic coupling among thermoregulatory and reproductive circuits, with potential ovulatory phase modulation from the VTA and TIDA dopaminergic populations. Future work is needed to map the continuous dynamics of reproductive-thermoregulatory coupling across the lifespan, as well as the conditions that may decouple these circuits. It is likely that observations of temporal coupling among hormones in the blood and temperature outputs reflect central coupling, but that desynchronizing influences including chronic jetlag or metabolic disease may complicate interpretation of temperature-based proxies for reproductive state.

## 1.2 Introduction

Neural Origins of Coupled Ultradian Oscillations. Endocrine and thermoregulatory outputs exhibit coordinated rhythmicity at the within-a-day (ultradian; UR)[7–9], daily (circadian; CR)[10], and ovulatory (OR) timescales in females[11–13]. Peripherally observed coupling has led to the hypothesis that neuroendocrine physiology operates as a network of coupled oscillators across reproductive, metabolic, autonomic, cognitive, and behavioral outputs[2,4–6,14–16]. If this coupled oscillator (CO) hypothesis is accurate at the fastest relevant timescale, *ultradian*, then surrogate measures, such as continuous body temperature (CBT), could be used to glean information about more difficult-to-measure reproductive outputs. Although numerous commercial tools are developed on the assumption that this hypothesis is true and applicable to all individuals, the origin of coupling, degree of functional coupling in real-world settings, and impacts of life stage are unknown. This review draws together evidence for and against the CO hypothesis as pertains to the connection between female reproductive and thermoregulatory neurocircuitry, as well as potential impacts on real-world applications.

What Do We Know About Coupling? The study of temporal coupling among peripheral and reproductive output goes back over a century to the Dutch gynecologist and author Theodor Van de Velde. In 1904, Van de Velde documented the potential use of daily oral temperature for monitoring reproductive activity at long timescales, including the ovulatory cycle, pregnancy, and the transition to menopause[1,13]. He described that temperature rises approximately around the time of expected ovulation in premenopausal women, and that temperature exhibits a sustained rise in early pregnancy. However, it was unclear if this coupling between reproductive state and thermoregulation, which played out on the order of months, indicated that coupling also took place on more rapid timescales. The subsequent century of study in reproductive neuroendocrinology, thermoregulation, and biological rhythms revealed not only that temperature and reproductive output exhibit URs, CRs, and ORs; but that these rhythms may be coupled *from hour to hour.* Such rapid coupling could hypothetically provide faster, more precise readouts of reproductive state and, as described below, enable peripheral *prediction* of future reproductive state. As a result, females comprise a fascinating opportunity to understand endocrine and metabolic network dynamics[5,67,17–21].

Utility of the Coupled Oscillator Hypothesis. If patterns of *hormonal* change over time (URs, CRs, and ORs) are strongly coupled to patterns in easy-to-measure outputs, like CBT, then wearable sensors could be adapted to provide useful information about reproductive state. Potential applications include personalized prediction or detection of pubertal onset and progression, ovulation, pregnancy and miscarriage, labor, post-partum recovery and family health, infertility, aging, and guidance for hormone replacement. Of these potential applications, only daily-resolution ovulatory cycle monitoring has been realized at scale[22]. Daily oral temperature, also known as basal body temperature (BBT), is commonly used as an approximate, retrospective indication of ovulation timing for purposes of family planning[1,11–13,23–25]. However, recent work suggests that it may be possible to anticipate ovulation via analysis of ultradian rhythmicity in CBT[7,8,26]. Although this evidence is promising, assuming that the CO hypothesis therefore holds broadly across individuals and stages of reproductive life could lead to inferences made from wearables that are suboptimal at best and damaging at worst. To move beyond phenomenology,

it is necessary to review the evidence for central coupling among reproductive and thermoregulatory measures. Doing so can help to identify questions for future study that will contextualize the development of peripheral markers for reproductive health across life.

Central or Peripheral Substrate for Reproductive and Thermoregulatory Coupling. If peripherally observed co-pulsatility arises from direct connections among hypothalamic reproductive and thermoregulatory regions, then there is strong support for the development of surrogate markers of reproductive state. Conversely, if it does not appear that coupling among reproductive and thermoregulatory output arises from central circuitry, then peripheral coupling must occur via co-modulation of other systems. This would suggest that a more tangential, or dissociable connection among these outputs, and therefore encourage more caution in the interpretation of peripheral signals in reference to reproductive function[27]. In either case, proxy-based predictors and detectors of female reproductive status would need to be identified and validated across stages of life, as hypothalamic circuits regulating both reproduction and body temperature undergo marked developments in puberty, pregnancy, and menopause, and in cases of pharmaceutical use[28–30]. These markers will also require validation in heterogeneous populations, as ethnicity[31] and behavior[32–34] impact rhythmic stability and reproductive function.

## 1.3 Hypothalamic Organization of Reproduction

The Hypothalamic-Pituitary-Gonadal Axis. Hypothalamic reproductive circuits form the apex of the hypothalamic-pituitary-gonadal (HPG) axis. Multiple hypothalamic subregions coordinate the release of reproductive neuropeptides and hormones[35], including kisspeptin (KP) within the arcuate (ARC), medial preoptic area (MPOA), and anteroventral paraventricular nuclei (AVPV); gonadotropin releasing hormone (GnRH) within the MPOA/AVPV; and RFRP-3 within the dorsomedial nucleus (DMN)[36,37]. These populations integrate with the central clock in the suprachiasmatic nucleus (SCN) and extrahypothalamic regions to generate an exquisitely coordinated pulsatile, circadian, ovulatory phase, and environmentally integrated GnRH signal. GnRH is released to the portal vasculature of the anterior pituitary[37–41], where it triggers the release of luteinizing hormone (LH) and follicle stimulating hormone (FSH). LH and FSH act on the gonads to stimulate the synthesis and release of sex steroids. Sex steroids and gonadotropins provide feedback both locally and long range to the pituitary and hypothalamus to regulate HPG activity from the pulsatile to the ovulatory, and longer timescales[35,39].

URs are integral to the functioning of the HPG axis across the ovulatory cycle[39,42]. Each KP-induced GnRH UR or "pulse" consists of a short, ~2 minute square wave of elevation, a 4 or 5 minute variable plateau, and a precipitous ~3 minute decline[43–45]. This pattern repeats with stereotyped frequency modulation across the ovulatory cycle. The pulsatile signal generated by these complex interactions propagates directly down the HPG axis, resulting in URs of LH, FSH, estrogen, progesterone, and testosterone[5,42,46]. This patterning is required for normal pituitary gonadotropin secretion[47,48], and its disruption contributes to the phenotypes of menopause[49], polycystic ovarian syndrome (PCOS)[49–51], hypothalamic amenorrhea[52,53], and hypogonadotropic hypogonadism[54–56].

In a typical ovulatory cycle, HPG pulse frequency increases from about once per 1-2 hours, to slightly less than once per hour across the pre-ovulatory or follicular phase[5,42]. This change is coincident with rising levels of estradiol that peak prior to ovulation, and low progesterone. Sufficiently elevated estradiol and circadian factors[57,58] then integrate to initiate an LH surge: the trigger for ovulation[59]. Notably, despite apparent circadian coordination of ovulation timing[57], and reports of post-ovulatory reduced circadian amplitude of CBT CRs[21], CR stability does not appear to change stereotypically across the ovulatory cycle (See: Chapter 4[7]). Following the LH surge and ovulation, pulsatility slows down to one pulse per 3 or 4 hours[5,44,60]. This post-ovulatory phase (called the luteal phase in humans) is associated with elevated progesterone, and a relatively small elevation in estradiol. In the absence of pregnancy, progesterone, and estradiol decline in the latter portion of the luteal phase, and the cycle begins again with rising estradiol and increasing hormonal pulse frequency. The circuitry undergirding the canonical ovulatory pattern of HPG pulsatility influences not only reproduction, but thermoregulation, and broad coordination of URs.

The Arcuate Kisspeptin Pulse Generator. Ultradian rhythmicity in the HPG axis appears to originate from an ARC pulse generator[39 61] which, incidentally, has been proposed as a broader source of hormonal and behavioral URs[61]. Recently, Liu et al., demonstrated that ARC Kisspeptin/Neurokinin/Dynorphin, or KNDy, neurons make close, non-synaptic appositions to GnRH "dendrons", which are unique structures positioned at the median eminence (ME) resembling both an axon and dendrite[62]. KP alone among the peptides released from KNDy neurons activates these dendrons[62]. Additionally, KNDy neurons exhibit synchronized bursting that is correlated with pulsatile LH secretion[63]. Tuning KNDy activity artificially results in corresponding changes to LH concentrations: selective activation of KNDy neurons in mice generates LH pulses[64], and their selective suppression inhibits LH pulses[63]. Although these circuits are frequently studied in rodents and ewes, KP neurons in the rostral POA, infundibular nucleus, and ARC[65] also appear to take on the role of pulse generation in humans[66–68]. Together, these observations support the link between periodic KP stimulation of GnRH dendrons as a generator of pulsatility across the HPG axis.

Additional work supports that GnRH neurons cannot generate *in vivo* oscillatory dynamics without KP and extra-hypothalamic input[69]. Although there is some evidence across species for synchronous pulsatility 1 or 2 times per hour from cultured GnRH neurons, isolated cultures from various ages and species do not reflect *in-vivo* dynamics[70–75]. Synchronized activity has not yet been observed in slice, and optogenetic stimulation of synchronous bursts in GnRH neurons fails to evoke LH secretion[76]. Together, the ARC appears to impose pulsatility on GnRH neurons, and therefore on the entire HPG axis. Much remains to be learned about how synchronicity is maintained within the pulse generator, as well as mechanisms behind the stereotyped pattern of pulsatility observed across the ovulatory cycle [39,77].

## 1.4 Hypothalamic Organization of Thermoregulation

Body Temperature Dynamics: The Core and Shell. CBT is a non-stationary signal that is influenced by a variety of temporal, endocrine, autonomic, behavioral, and species-specific factors. Female mammalian CBT exhibits URs, CRs, and ORs; as well as distinct rhythmic structures at different

locations on the body. Although each part of the body comprises a "micro-climate", body temperature is traditionally divided into the skin or "shell", and the "core" or interior of the body[78,79]. Briefly, during the active phase, core temperature is elevated relative to the shell[80,81]. During the inactive phase, vasodilation sends blood from the core to the shell, thereby reducing core temperature and heating the shell by dissipating heat through it[82,83]. In larger mammals, including humans, the gradient from shell to core is more exaggerated than in smaller animals, such as mice and rats[84–86], suggesting that findings from rodents' core and shell may not translate directly to human core and shell temperature[21,80]. For simplicity, the present discussion will be limited to central regulation of core temperature[7,25,87]. For reviews on behavioral and environmental, as opposed to endogenous rhythmic, influences on body temperature, see[21,80,88,89].

Warm and Cold Sensitive Neurons. Thermoregulation is predominantly influenced by neural populations within the MPOA/AVPV[83]. "Warm sensitive" neurons, named due to their activation at high temperatures via TRP receptors, make up ~30% of the MPOA[90]. "Cold sensitive" neurons, activated at low temperatures, comprise a smaller population, about ~5-10% of the MPOA,[90] and extend into the ventral lateral preoptic nucleus[91]. Additionally, GABAergic interneurons within the POA serve to inhibit warm sensitive neurons in response to cold stimuli[92], and warm sensitive neurons reciprocally inhibit cold sensitive neurons[90]. Environmental feedback to thermoregulatory populations comes from sensory neurons in the trigeminal and dorsal root ganglia. These cells sample temperature from specific tissues in the abdomen, spine, skin, and within the brain itself[83,93–95] (reviewed in[96]).

## 1.5 Interaction Among Thermoregulatory and Reproductive Circuits

Phenomenology of Ovulatory Cycle Impacts on Body Temperature. The previous century's[1] documentation of covariance among reproductive hormones and body temperature were made largely using BBT in humans, and various surface or implantable sensors in animals, collectively giving rise to the term "in heat" for an ovulating, sexually receptive female[97]. Acutely, estradiol promotes vasodilation and progesterone promotes vasoconstriction[82]. Accordingly, estradiol lowers core and skin temperature in females[98–100], and ovariectomized mice (in which the dominant estradiol source is removed) exhibit a sustained increase in tail temperature that can be reversed with estradiol treatment[101]. In males, testosterone acutely raises muscle temperature while lowering adipose temperature, but can also be aromatized to estradiol, thereby affecting body temperature through similar mechanisms as estradiol in females[102,103]. Conversely, progesterone, either alone or combined with estrogen, raises body temperature. In rodents, the preovulatory spike in estradiol and progesterone on estrous days is associated with a plateau of high CBT [8,26,104]. This phenomenon has also been observed in humans following ovulation[7,25]. Although recent work claims to identify various patterns of pre-ovulatory temperature depression followed by peri-ovulatory temperature rise, confounding factors (e.g., conflation of LH surges with true ovulation) have thus far limited the interpretation of these enticing findings[19,105–108]. Finally, described below, changes in thermogenesis associated with sex steroids likely occur through co-influence on hypothalamic neurons that regulate pulsatile release of GnRH as well as body temperature, and through direct synaptic coupling[98,99].

Kisspeptin and GnRH Input to Thermosensitive Neurons and Non-Thermosensitive Neurons Lower Body Temperature. A distinct population of non-thermosensitive NK3 neurons in the MPOA receive projections from ARC KNDy neurons[109]. NK3 neurons reduce core temperature when activated by KNDy input[109]. Moreover, GnRH and estrogen[93,110] excite warm sensitive neurons, presumably lowering body temperature in a pulsatile fashion[110]. Finally, although not yet shown to be centrally mediated, the pituitary hormone prolactin, which is temporally coupled to pulsatile estrogen and LH release, reduces body temperature[111].

Progesterone and Prostaglandins Inhibit Warm Sensitive Neurons to Raise Body Temperature. Progesterone inhibits warm sensitive neurons in slice and *in vitro*, resulting in elevation of body temperature[88,112,113]. Additionally, prostaglandin E2, which is released in response to progesterone (and, canonically, in sickness), inhibits warm sensitive neuron activity by binding to EP3 receptors, thereby raising body temperature[88,114].

Temperature Sensitive Neurons in the POA Exhibit Pulsatile Activity. The POA exhibits URs, CRs, and ORs[115,116]. Activity across the rat POA, which includes both reproductive and thermoregulatory populations, is pulsatile during estrus and diestrus[115], with some POA neurons exhibiting ultradian sleeping bouts associated with REM, and sinusoidal ultradian waking bouts[116]. Additionally, temperature sensitive neurons are reciprocally affected by ARC[117]. Arcuate KP neurons project to both warm and cold populations, and stimulation of the ARC results in inhibition of thermosensitive POA neurons, [117] suggesting that the pulsatile activity from this population may impose pulsatile structure on the activity of warm and cold populations *in vivo*[109]. Additionally, about half of temperature sensitive MPOA neurons are affected by estrogen or testosterone[93]. If warm and cold neurons are also sensitive to sex steroids, this would suggest that sex steroid pulsatility could reinforce temperature pulsatility directly. Moreover, in ovariectomized animals, temperature sensitive cells in the POA are both less active and exhibit an altered activity profile[118]. Additionally, their activity may be raised by phytoestrogen-rich black cohosh and by direct estrogen replacement[119]. Together, the activity profile and reciprocal connections among thermoregulatory neurons in the POA, reproductive circuits in the ARC, and sex steroids, suggest that reproductive-thermoregulatory coupling is both centrally generated and peripherally reinforced.

## 1.6 Modulating URs by Phase of Cycle: A Job for the Dopaminergic Ultradian Oscillator, TIDA Neurons, and the Arcuate Pulse Generator?

Soper and Weick determined in 1980 that an extrahypothalamic region projecting to the anterior ARC was necessary for maintenance of LH pulsatility in ovariectomized rats[69]. This indicated that hypothalamic pulsatility is dependent on extrahypothalamic regions, despite the existence of the ARC pulse generator[27].This observation indicated that an additional party is necessary to link UR generation across the ARC pulse generator and POA. Twenty five years after Soper and Weick, the ventral tegmental area (VTA) was compellingly presented as an tunable regulator of UR in dopamine, behavior, and temperature[16,120]. This system, dubbed the “Dopamine Ultradian Oscillator”, or DUO, may be responsible for reinforcement of URs and modulation of UR periodicity across the ovulatory cycle.

The Dopamine Ultradian Oscillator. From 2015 to 2017, Blum, Storch, and Bourguignon reported that the VTA exhibits URs in dopamine that are tightly correlated to URs in CBT and locomotor activity[16,120]. Additionally, they showed that natural and pharmacological increase in dopamine lengthens UR period, whereas natural and pharmacological decrease in dopamine shortens UR period[16,120]. Subsequent experiments established that the VTA is a key area for generation and coordination of URs across systems, including motivation, locomotor activity, feeding, and hippocampal activity[16,120,121]. Moreover, the VTA sends projections to the anterior, lateral, and posterior hypothalamus[122]. Reciprocally, the pro-opiomelanocortin (POMC)[123,124] neurons of the ARC both send projections to the VTA[125], inhibiting dopaminergic activity, and express the KP receptor. Finally, AGRP/NPY[125] neurons (canonically opposing the actions of POMC neurons) project to the VTA. The combination of KP-sensitive POMC input, and AGRP/NPY input to the VTA suggest potential bi-directional influence of the ARC on VTA activity. Finally, the Nucleus Accumbens (NAcc) projections to both the VTA and ventromedial ARC may reinforce coupling (reviewed in[61]). Together, dopaminergic URs could be an important reinforcer of reproductive-thermoregulatory coupling and have direct synaptic substrate for communicating with pertinent hypothalamic circuits. However, an additional dopaminergic population within the hypothalamus itself must be considered in order to integrate reproductive, thermoregulatory, and ovulatory-phase-dependent URs.

Tuberoinfundibular Dopaminergic Neurons. An additional population of tuberoinfundibular dopaminergic (TIDA) neurons within the ARC both acts on KNDy neurons and releases dopamine to the ME[126]. This input is essential for normal reproductive function, and exerts pulsatile inhibition on dopamine's antagonist: temperature-reducing prolactin[127128]. As reviewed in Nestor et al., 2018[129] in the case of anestrous ewes: dopamine inhibits GnRH by suppressing KNDy neuron activity via D2 receptors[130–132], E2 increases expression of D2, and D2 antagonist infusion in the ARC increases LH pulse frequency[130,132,133]. Although Nestor et al., were not able to find reports of URs in TIDA neurons, this activity is highly likely to be pulsatile in order for the pulsatile pattern of KNDy and GnRH activity to occur. Moreover, 70% of prolactin pulses occur coincident with LH pulses, supporting coupled timing of dopamine and KP pulsatility[42]. These findings indicate that TIDA dopaminergic output, KNDy, GnRH, LH, and prolactin likely exhibit synchronized URs. Finally, Stagkourakis et al., recently showed that D2R autoreceptor activation in TIDA neurons increases oscillatory period[126]. Although this finding occurred at a different timescale (seconds to minutes), the effect is consistent with the impact of dopamine on UR periodicity in the VTA. Together, the role of dopamine from TIDA neurons may accord with the potential role of the VTA in reinforcement of coupling among pulses of reproductive and body temperature, as well as potentially contribute to modulation of UR period across the ovulatory cycle, discussed below.

Modulation of Ultradian Period by Phase of Ovulatory Cycle. The mechanisms underlying stereotyped modulation of UR periodicity across the ovulatory cycle are yet unexplained, but Prendergast and Zucker recently proposed that changes in dopaminergic tone across the ovulatory cycle could be responsible[61]. If so, one would expect higher dopaminergic tone to be coincident with times of UR period lengthening of body temperature, and hormonal output, as well as elevated temperature level (i.e., the post-ovulatory luteal phase). Likewise, one would expect reduced dopaminergic tone to be associated with increasing frequency of these URs (i.e.,

the phenotype observed in the preovulatory follicular phase). Consistent with this, prolactin – a

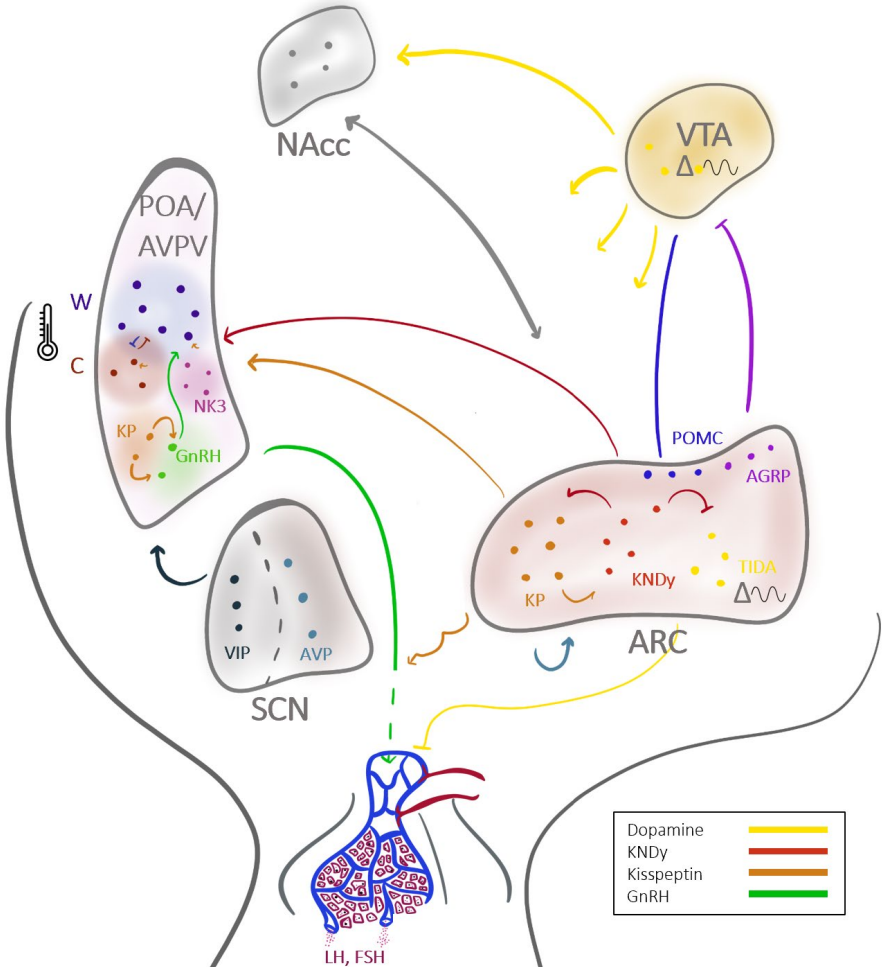


**Figure 1. Schematic of Ultradian Interactions Among Reproductive and Thermoregulatory Output.** An expanded model of hypothalamic and subcortical structures proposed to enable ultradian coupling of reproductive and thermoregulatory outputs (See: Prendergast and Zucker, 2016; Storch et al., 2014; Grant et al., 2018; for original models). The ARC pulse generator interacts with the POA/AVPV to convey a pulsatile GnRH signal to the anterior pituitary, in turn stimulating pulsatile release of LH and FSH. KNDy input to TIDA neurons may impose a similar inhibitory dopaminergic influence on prolactin secretion. These reproductive UR networks project directly to warm (W) and cold (C) neurons in the POA/AVPV, as well as to temperature-regulating NK3 POA neurons. The SCN, dopaminergic ultradian oscillator of the VTA, and NAcc may to impose both time of day (SCN) and time of cycle (VTA, NAcc) interactions on reproduction and body temperature. This action may be achieved through their influence on the ARC pulse generator, POA/AVPV KP and GnRH populations, reciprocal interaction with ARC POMC and AGRP neurons, and VTA projections to diverse hypothalamic subregions. *Abbreviations: arcuate (ARC), preoptic area (POA), anterior ventral periventricular area (AVPV), kisspeptin neurokinin dynorphin (KNDy), tuberoinfundibular dopaminergic (TIDA), neurokinin 3 (NK3), suprachiasmatic nucleus (SCN), ventral tegmental area (VTA), nucleus accumbens (NAcc), gonadotropin releasing hormone (GnRH), luteinizing hormone (LH), follicle stimulating hormone (FSH), pro-opiomelanocortin (POMC), agouti-related peptide (AGRP).*

dopamine antagonist, is highest around ovulation (when URs are fastest and dopaminergic tone likely reduced), and lower during the early follicular phase (when URs are relatively slower and dopaminergic tone is likely increased)[134]. Moreover, in natural systems, it appears that increases

in dopaminergic tone are inversely proportional to increases in LH pulse frequency, whether that dopamine is released from the VTA or TIDA neurons. Together, recent work reinforces the intriguing possibility is that the DUO[120] and the ARC hypotheses of ultradian rhythm generation[61] could be united – presumably by direct or indirect communication among the ARC pulse generator, VTA, and TIDA populations[61].

## 1.7 Could Coupling be Decentralized?

It appears feasible that a) central reproductive and thermoregulatory circuits are coupled within the hypothalamus and that b) dopaminergic circuitry within the hypothalamus, VTA, and NAcc intermediary could provide substrate for modulation of ultradian frequency of temperature and reproductive output across the ovulatory cycle. However, it is possible that the appearance of co-pulsatility is achieved by decentralized means. Numerous other factors contribute to thermoregulation in a manner that may be decoupled from reproductive status. For example, brown adipose tissue deposition is positively correlated with progesterone across the cycle, and inversely correlated with estrogen in the follicular phase, yet is heavily influenced by cortisol[135,136]. Unlike the HPG axis, URs in the hypothalamic-pituitary-adrenal (HPA) axis can be preserved in the absence of URs in their hypothalamic releasing hormone[27]. As HPA axis activity contributes to the regulation of body temperature[137,138], and has been observed to potentially time-lock with ultradian rhythms of CBT[139], central reproductive-thermoregulatory coupling is not likely to generate an isolated, 1:1 relationship between these systems. Variable additional impacts of stress, environment, and behavior on thermoregulation and reproduction have been reviewed recently[88,140,141], and are required to contextualize our understanding of coupling between these systems.

If co-pulsatility among reproductive and thermoregulatory outputs is not centrally generated, or even contains a strong peripheral component, then it is more likely that peripheral factors could perturb coupling. This outcome could lead to challenges or misinterpretations of a temperature signal that was used to infer information about reproduction, especially in cases of rhythmic instability (e.g., in shift workers, during late pregnancy and the post-partum period, in PCOS, in diabetes, in HPA axis disorders, or during the perimenopausal period)[7,142,143]. In particular, the unpleasant side effects of rhythmic disruptors, such as jetlag, are due to dissociation of rhythmicity among different systems in the body. When the body is required to “adjust” to a new time zone, different systems adjust at different rates, leading to decoupling and suboptimal function during the readjustment period, and the canonical malaise of jetlag[144–146]. Although physical time zone shifts are the most well-known example of rhythmic disruption, many common behaviors and medical interventions are associated with internal desynchrony. These include light at night, late meals, pharmaceuticals such as hormonal contraception or cortisone, and early school times, which together impose “pharmaceutical” or “social” jetlag on an alarming proportion of the population[147–151]. The result of these other forms of jetlag appear to exert de-coupling events on systems throughout the body, including the HPG and HPA axes, and thermoregulation[7,139]. A likely result of these de-coupling events is that the numerous systems contributing to patterns of CBT may be misaligned in many individuals and may therefore be more difficult to rely on as direct proxies for reproductive function. For this reason, it is

important to treat the likelihood of central substrate for temperature-reproductive ultradian or coupling with caution until even more direct observations of co-pulsatility within the hypothalamus, or continuous comparisons of temperature and pituitary/peripheral hormones can be made.

## 1.8 Summary and Conclusions

Reproductive and thermoregulatory hypothalamic output is pulsatile and appears to have the neural substrate to create coupled ultradian oscillations. Multiple hypotheses have been proposed for how such coupling may be achieved, including the ARC pulse generator, the DUO, and decentralized mechanisms. We propose that pulsatility is likely to be of central origin in the case of reproductive-thermoregulatory coupling, and that peripheral factors likely reinforce this coupling and may play a larger role in other hypothalamic-pituitary axes. Moreover, future studies may resolve the DUO and ARC pulse generation hypotheses into one coupled system, as there appears to be neural substrate for communication among the ARC pulse generator, the ARC TIDA system, and the VTA. If these systems work together, then the tunability of ultradian periodicity by the VTA and/or TIDA neurons may underly ovulatory cycle frequency modulation of ultradian rhythms. There is strong evidence to support the development of *continuous* temperature-based proxies for reproductive system output, but these proxies may be disrupted by desynchronizing behavioral, environmental, or pharmacological interventions. Applications may span from assessing changes to continuous patterns of hormones across adolescence, fertility and infertility, pregnancy, and menopause.

## 1.9 References


1. Van de Velde, T. Ueber den Zusammenhang zwischen Ovarialfunction, Wellenbewegung und Menstrualblutung, und ueber die Entstehung des sogenannten Mittelschmerzes / von Th. H. Van de Velde. *Wellcome Collection* https://wellcomecollection.org/works/tcxermmu (1904).
2. Brandenberger, G., Simon, C. & Follenius, M. Ultradian endocrine rhythms: A multioscillatory system. *J. Interdiscip. Cycle Res.* **18**, 307–315 (1987).
3. Brodsky, V. Y. Circahoralian (Ultradian) metabolic rhythms. *Biochem. Mosc.* **79**, 483–495 (2014).
4. Goh, G. H., Maloney, S. K., Mark, P. J. & Blache, D. Episodic Ultradian Events—Ultradian Rhythms. *Biology* **8**, 15 (2019).
5. Grant, A. D., Wilsterman, K., Smarr, B. L. & Kriegsfeld, L. J. Evidence for a Coupled Oscillator Model of Endocrine Ultradian Rhythms. *J. Biol. Rhythms* 748730418791423 (2018) doi:10.1177/0748730418791423.
6. Shannahoff-Khalsa, D. S., Kennedy, B., Yates, F. E. & Ziegler, M. G. Ultradian rhythms of autonomic, cardiovascular, and neuroendocrine systems are related in humans. *Am. J. Physiol.* **270**, R873-887 (1996).
7. Grant, A. D., Newman, M. & Kriegsfeld, L. J. Ultradian rhythms in heart rate variability and distal body temperature anticipate onset of the luteinizing hormone surge. *Sci. Rep.* **10**, 20378 (2020).
8. Smarr, B. L., Grant, A. D., Zucker, I., Prendergast, B. J. & Kriegsfeld, L. J. Sex differences in variability across timescales in BALB/c mice. *Biol. Sex Differ.* **8**, 7 (2017).
9. Sanchez-Alavez, M., Alboni, S. & Conti, B. Sex- and age-specific differences in core body temperature of C57Bl/6 mice. *Age Dordr. Neth.* **33**, 89–99 (2011).
10. Kerdelhué, B. *et al.* Timing of initiation of the preovulatory luteinizing hormone surge and its relationship with the circadian cortisol rhythm in the human. *Neuroendocrinology* **75**, 158–163 (2002).
11. de Mouzon, J., Testart, J., Lefevre, B., Pouly, J. L. & Frydman, R. Time relationships between basal body temperature and ovulation or plasma progestins. *Fertil. Steril.* **41**, 254–259 (1984).
12. Farris, E. J. Basal body temperature throughout pregnancy; a report upon two patients. *Hum. Fertil.* **12**, 106–109 (1947).
13. Van de Velde, T. *Ideal Marriage*. (Elsevier, 1926). doi:10.1016/C2013-0-06602-9.
14. Van Cauter, E. Diurnal and Ultradian Rhythms in Human Endocrine Function: A Minireview. *Horm. Res. Paediatr.* **34**, 45–53 (1990).
15. Conway-Campbell, B. L. *et al.* Glucocorticoid ultradian rhythmicity directs cyclical gene pulsing of the clock gene period 1 in rat hippocampus. *J. Neuroendocrinol.* **22**, 1093–1100 (2010).
16. Bourguignon, C. & Storch, K.-F. Control of Rest:Activity by a Dopaminergic Ultradian Oscillator and the Circadian Clock. *Front. Neurol.* **8**, 614 (2017).
17. Bartsch, R. P., Liu, K. K. L., Bashan, A. & Ivanov, P. C. Network Physiology: How Organ Systems Dynamically Interact. *PloS One* **10**, e0142143 (2015).

18. Bashan, A., Bartsch, R. P., Kantelhardt, J. W., Havlin, S. & Ivanov, P. C. Network physiology reveals relations between network topology and physiological function. *Nat. Commun.* **3**, 702 (2012).
19. Goodale, B. M. *et al.* Wearable Sensors Reveal Menses-Driven Changes in Physiology and Enable Prediction of the Fertile Window: Observational Study. *J. Med. Internet Res.* **21**, e13404 (2019).
20. Webster, W., Godfrey, E. M., Costantini, L. & Katilius, J. Passive fertility prediction using a novel vaginal ring and smartphone application. *Fertil. Steril.* **104**, e98 (2015).
21. Webster, W. W. & Smarr, B. Using Circadian Rhythm Patterns of Continuous Core Body Temperature to Improve Fertility and Pregnancy Planning. *J. Circadian Rhythms* **18**, 5 (2020).
22. Bull, J. R. *et al.* Real-world menstrual cycle characteristics of more than 600,000 menstrual cycles. *Npj Digit. Med.* **2**, 1–8 (2019).
23. Buxton, C. L. & Atkinson, W. B. Hormonal factors involved in the regulation of basal body temperature during the menstrual cycle and pregnancy. *J. Clin. Endocrinol. Metab.* **8**, 544–549 (1948).
24. Cohen, J., Iffy, L. & Keyser, H. H. Basal body temperature recordings in spontaneous abortion. *Int. J. Gynaecol. Obstet. Off. Organ Int. Fed. Gynaecol. Obstet.* **14**, 117–122 (1976).
25. Maijala, A., Kinnunen, H., Koskimäki, H., Jämsä, T. & Kangas, M. Nocturnal finger skin temperature in menstrual cycle tracking: ambulatory pilot study using a wearable Oura ring. *BMC Womens Health* **19**, 150 (2019).
26. Prendergast, B. J., Beery, A. K., Paul, M. J. & Zucker, I. Enhancement and Suppression of Ultradian and Circadian Rhythms across the Female Hamster Reproductive Cycle. *J. Biol. Rhythms* **27**, 246–256 (2012).
27. Walker, J. J. *et al.* The Origin of Glucocorticoid Hormone Oscillations. *PLoS Biol.* **10**, e1001341 (2012).
28. Livadas, S. & Chrousos, G. P. Control of the onset of puberty. *Curr. Opin. Pediatr.* **28**, 551–558 (2016).
29. Chahal, H. S. & Drake, W. M. The endocrine system and ageing. *J. Pathol.* **211**, 173–180 (2007).
30. Hall, J. E. Endocrinology of the Menopause. *Endocrinol. Metab. Clin. North Am.* **44**, 485–496 (2015).
31. Liu, Y., Gold, E. B., Lasley, B. L. & Johnson, W. O. Factors affecting menstrual cycle characteristics. *Am. J. Epidemiol.* **160**, 131–140 (2004).
32. Nazni, P. Association of western diet & lifestyle with decreased fertility. *Indian J. Med. Res.* **140 Suppl**, S78-81 (2014).
33. Fernandez, R. *et al.* Fixed or Rotating Night Shift Work Undertaken by Women: Implications for Fertility and Miscarriage. *Semin. Reprod. Med.* **34**, 074–082 (2016).
34. Gamble, K. L., Resuehr, D. & Johnson, C. H. Shift Work and Circadian Dysregulation of Reproduction. *Front. Endocrinol.* **4**, (2013).
35. Plant, T. M. 60 YEARS OF NEUROENDOCRINOLOGY: The hypothalamo-pituitary-gonadal axis. *J. Endocrinol.* **226**, T41-54 (2015).
36. Ubuka, T., Parhar, I., Kriegsfeld, L. J. & Tsutsui, K. Editorial: The Roles of GnIH in Reproductive Function and Behavior. *Front. Endocrinol.* **9**, 19 (2018).

37. Angelopoulou, E., Quignon, C., Kriegsfeld, L. J. & Simonneaux, V. Functional Implications of RFRP-3 in the Central Control of Daily and Seasonal Rhythms in Reproduction. *Front. Endocrinol.* **10**, 183 (2019).
38. Christian, C. A. & Moenter, S. M. The neurobiology of preovulatory and estradiol-induced gonadotropin-releasing hormone surges. *Endocr. Rev.* **31**, 544–577 (2010).
39. Herbison, A. E. The Gonadotropin-Releasing Hormone Pulse Generator. *Endocrinology* **159**, 3723–3736 (2018).
40. Kriegsfeld, L. J. Circadian regulation of kisspeptin in female reproductive functioning. *Adv. Exp. Med. Biol.* **784**, 385–410 (2013).
41. Lehman, M. N., He, W., Coolen, L. M., Levine, J. E. & Goodman, R. L. Does the KNDy Model for the Control of Gonadotropin-Releasing Hormone Pulses Apply to Monkeys and Humans? *Semin. Reprod. Med.* **37**, 71–83 (2019).
42. Backstrom, C., McNeilly, A. S., Leask, R. & Baird, D. Pulsatile secretion of LH, FSH, Prolactin, oestradiol, and progesterone during the human menstrual cycle. *Clin. Endocrinol. (Oxf.)* **17**, 29–42 (1982).
43. Goodman, R. L., Parfitt, D. B., Evans, N. P., Dahl, G. E. & Karsch, F. J. Endogenous opioid peptides control the amplitude and shape of gonadotropin-releasing hormone pulses in the ewe. *Endocrinology* **136**, 2412–2420 (1995).
44. Moenter, S. M., Caraty, A., Locatelli, A. & Karsch, F. J. Pattern of Gonadotropin-Releasing Hormone (GnRH) Secretion Leading up to Ovulation in the Ewe: Existence of a Preovulatory GnRH Surge. *Endocrinology* **129**, 1175–1182 (1991).
45. Moenter, S. M., Brand, R. M., Midgley, A. R. & Karsch, F. J. Dynamics of gonadotropin-releasing hormone release during a pulse. *Endocrinology* **130**, 503–510 (1992).
46. Albertsson-Wikland, K. *et al.* Twenty-Four-Hour Profiles of Luteinizing Hormone, Follicle-Stimulating Hormone, Testosterone, and Estradiol Levels: A Semilongitudinal Study throughout Puberty in Healthy Boys. *J. Clin. Endocrinol. Metab.* **82**, 541–549 (1997).
47. Thompson, I. R. & Kaiser, U. B. GnRH pulse frequency-dependent differential regulation of LH and FSH gene expression. *Mol. Cell. Endocrinol.* **385**, 28–35 (2014).
48. Zavala, E. *et al.* Mathematical Modelling of Endocrine Systems. *Trends Endocrinol. Metab.* **30**, 244–257 (2019).
49. Hunjan, T. & Abbara, A. Clinical Translational Studies of Kisspeptin and Neurokinin B. *Semin. Reprod. Med.* **37**, 119–124 (2019).
50. Chaudhari, N., Dawalbhakta, M. & Nampoothiri, L. GnRH dysregulation in polycystic ovarian syndrome (PCOS) is a manifestation of an altered neurotransmitter profile. *Reprod. Biol. Endocrinol. RBE* **16**, 37 (2018).
51. Coutinho, E. A. & Kauffman, A. S. The Role of the Brain in the Pathogenesis and Physiology of Polycystic Ovary Syndrome (PCOS). *Med. Sci. Basel Switz.* **7**, E84 (2019).
52. Meczekalski, B., Katulski, K., Czyzyk, A., Podfigurna-Stopa, A. & Maciejewska-Jeske, M. Functional hypothalamic amenorrhea and its influence on women's health. *J. Endocrinol. Invest.* **37**, 1049–1056 (2014).
53. Fourman, L. T. & Fazeli, P. K. Neuroendocrine Causes of Amenorrhea—An Update. *J. Clin. Endocrinol. Metab.* **100**, 812–824 (2015).

54. Hao, M. *et al.* Efficacy and safety of pulsatile gonadotropin-releasing hormone therapy in patients with congenital hypogonadotropic hypogonadism: a multicentre clinical study. *Ann. Transl. Med.* **9**, 962 (2021).
55. Belchetz, P. E., Plant, T. M., Nakai, Y., Keogh, E. J. & Knobil, E. Hypophysial responses to continuous and intermittent delivery of hypopthalamic gonadotropin-releasing hormone. *Science* **202**, 631–633 (1978).
56. Gronier, H., Peigné, M., Catteau-Jonard, S., Dewailly, D. & Robin, G. [Ovulation induction by pulsatile GnRH therapy in 2014: literature review and synthesis of current practice]. *Gynecol. Obstet. Fertil.* **42**, 732–740 (2014).
57. Ginther, O. J., Pinaffi, F. L. V., Khan, F. A., Duarte, L. F. & Beg, M. A. Circadian influence on the preovulatory LH surge, ovulation, and prolactin concentrations in heifers. *Theriogenology* **79**, 528–533 (2013).
58. Smarr, B. L., Morris, E. & de la Iglesia, H. O. The dorsomedial suprachiasmatic nucleus times circadian expression of Kiss1 and the luteinizing hormone surge. *Endocrinology* **153**, 2839–2850 (2012).
59. Direito, A., Bailly, S., Mariani, A. & Ecochard, R. Relationships between the luteinizing hormone surge and other characteristics of the menstrual cycle in normally ovulating women. *Fertil. Steril.* **99**, 279-285.e3 (2013).
60. Goodman, R. L. & Inskeep, E. K. Control of the Ovarian Cycle of the Sheep. in *Knobil and Neill's Physiology of Reproduction* 1259–1305 (Elsevier, 2015). doi:10.1016/B978-0-12-397175-3.00027-2.
61. Prendergast, B. J. & Zucker, I. Ultradian rhythms in mammalian physiology and behavior. *Curr. Opin. Neurobiol.* **40**, 150–154 (2016).
62. Liu, X. *et al.* Highly redundant neuropeptide volume co-transmission underlying episodic activation of the GnRH neuron dendron. *eLife* **10**, e62455 (2021).
63. Clarkson, J. *et al.* Definition of the hypothalamic GnRH pulse generator in mice. *Proc. Natl. Acad. Sci. U. S. A.* **114**, E10216–E10223 (2017).
64. Han, S. Y., McLennan, T., Czieselsky, K. & Herbison, A. E. Selective optogenetic activation of arcuate kisspeptin neurons generates pulsatile luteinizing hormone secretion. *Proc. Natl. Acad. Sci.* **112**, 13109–13114 (2015).
65. Hrabovszky, E. *et al.* The kisspeptin system of the human hypothalamus: sexual dimorphism and relationship with gonadotropin-releasing hormone and neurokinin B neurons. *Eur. J. Neurosci.* **31**, 1984–1998 (2010).
66. Chan, Y.-M., Butler, J. P., Sidhoum, V. F., Pinnell, N. E. & Seminara, S. B. Kisspeptin administration to women: a window into endogenous kisspeptin secretion and GnRH responsiveness across the menstrual cycle. *J. Clin. Endocrinol. Metab.* **97**, E1458-1467 (2012).
67. Jayasena, C. N., Dhillo, W. S. & Bloom, S. R. Kisspeptins and the control of gonadotropin secretion in humans. *Peptides* **30**, 76–82 (2009).
68. Frontiers | Neuropeptide co-expression in hypothalamic kisspeptin neurons of laboratory animals and the human | Neuroscience. https://www.frontiersin.org/articles/10.3389/fnins.2015.00029/full.

69. SOPER, B. D. & WEICK, R. F. Hypothalamic and Extrahypothalamic Mediation of Pulsatile Discharges of Luteinizing Hormone in the Ovariectomized Rat*. *Endocrinology* **106**, 348–355 (1980).
70. Duittoz, A. H. & Batailler, M. Pulsatile GnRH secretion from primary cultures of sheep olfactory placode explants. *J. Reprod. Fertil.* **120**, 391–396 (2000).
71. Funabashi, T., Daikoku, S., Shinohara, K. & Kimura, F. Pulsatile gonadotropin-releasing hormone (GnRH) secretion is an inherent function of GnRH neurons, as revealed by the culture of medial olfactory placode obtained from embryonic rats. *Neuroendocrinology* **71**, 138–144 (2000).
72. Gore, A. C., Windsor-Engnell, B. M. & Terasawa, E. Menopausal increases in pulsatile gonadotropin-releasing hormone release in a nonhuman primate (Macaca mulatta). *Endocrinology* **145**, 4653–4659 (2004).
73. Moore, J. P., Shang, E. & Wray, S. In situ GABAergic modulation of synchronous gonadotropin releasing hormone-1 neuronal activity. *J. Neurosci. Off. J. Soc. Neurosci.* **22**, 8932–8941 (2002).
74. Terasawa, E., Keen, K. L., Mogi, K. & Claude, P. Pulsatile release of luteinizing hormone-releasing hormone (LHRH) in cultured LHRH neurons derived from the embryonic olfactory placode of the rhesus monkey. *Endocrinology* **140**, 1432–1441 (1999).
75. Weiner, R. I. *et al.* Gonadotropin-releasing hormone neuronal cell lines. *Front. Neuroendocrinol.* **13**, 95–119 (1992).
76. Campos, P. & Herbison, A. E. Optogenetic activation of GnRH neurons reveals minimal requirements for pulsatile luteinizing hormone secretion. *Proc. Natl. Acad. Sci.* **111**, 18387–18392 (2014).
77. Czieselsky, K. *et al.* Pulse and Surge Profiles of Luteinizing Hormone Secretion in the Mouse. *Endocrinology* **157**, 4794–4802 (2016).
78. Romanovsky, A. A. The thermoregulation system and how it works. *Handb. Clin. Neurol.* **156**, 3–43 (2018).
79. Childs, C. Body temperature and clinical thermometry. *Handb. Clin. Neurol.* **157**, 467–482 (2018).
80. Krauchi, K. *et al.* Diurnal and menstrual cycles in body temperature are regulated differently: a 28-day ambulatory study in healthy women with thermal discomfort of cold extremities and controls. *Chronobiol. Int.* **31**, 102–113 (2014).
81. Krauchi, K. & Wirz-Justice, A. Circadian rhythm of heat production, heart rate, and skin and core temperature under unmasking conditions in men. *Am. J. Physiol.* **267**, R819-829 (1994).
82. Charkoudian, N., Hart, E. C. J., Barnes, J. N. & Joyner, M. J. Autonomic control of body temperature and blood pressure: influences of female sex hormones. *Clin. Auton. Res. Off. J. Clin. Auton. Res. Soc.* **27**, 149–155 (2017).
83. Tan, C. L. & Knight, Z. A. Regulation of body temperature by the nervous system. *Neuron* **98**, 31–48 (2018).
84. van der Vinne, V. *et al.* Continuous and non-invasive thermography of mouse skin accurately describes core body temperature patterns, but not absolute core temperature. *Sci. Rep.* **10**, 20680 (2020).

85. Weiss, N., Attali, V., Bouzbib, C. & Thabut, D. Altered distal-proximal temperature gradient as a possible explanation for sleep-wake disturbances in cirrhotic patients. *Liver Int. Off. J. Int. Assoc. Study Liver* **37**, 1776–1779 (2017).
86. Reid, K. J. *et al.* Effects of manipulating body temperature on sleep in postmenopausal women. *Sleep Med.* **81**, 109–115 (2021).
87. Batinga, H. *et al.* Ontogeny and aging of the distal skin temperature rhythm in humans. *Age Dordr. Neth.* **37**, 29 (2015).
88. Morrison, S. F. & Nakamura, K. Central neural pathways for thermoregulation. *Front. Biosci. Landmark Ed.* **16**, 74–104 (2011).
89. Charkoudian, N. & Stachenfeld, N. S. Reproductive Hormone Influences on Thermoregulation in Women. in *Comprehensive Physiology* (John Wiley & Sons, Inc., 2011). doi:10.1002/cphy.c130029.
90. Tan, C. L. *et al.* Warm-sensitive neurons that control body temperature. *Cell* **167**, 47-59.e15 (2016).
91. Zhao, Z.-D. *et al.* A hypothalamic circuit that controls body temperature. *Proc. Natl. Acad. Sci. U. S. A.* **114**, 2042–2047 (2017).
92. Morrison, S. F., Nakamura, K. & Madden, C. J. Central control of thermogenesis in mammals. *Exp. Physiol.* **93**, 773–797 (2008).
93. Silva, N. L. & Boulant, J. A. Effects of testosterone, estradiol, and temperature on neurons in preoptic tissue slices. *Am. J. Physiol.* **250**, R625-632 (1986).
94. Boulant, J. A. & Hardy, J. D. The effect of spinal and skin temperatures on the firing rate and thermosensitivity of preoptic neurones. *J. Physiol.* **240**, 639–660 (1974).
95. Wit, A. & Wang, S. C. Temperature-sensitive neurons in preoptic-anterior hypothalamic region: effects of increasing ambient temperature. *Am. J. Physiol.* **215**, 1151–1159 (1968).
96. Vriens, J., Nilius, B. & Voets, T. Peripheral thermosensation in mammals. *Nat. Rev. Neurosci.* **15**, 573–589 (2014).
97. Marrone, B. L., Gentry, R. T. & Wade, G. N. Gonadal hormones and body temperature in rats: effects of estrous cycles, castration and steroid replacement. *Physiol. Behav.* **17**, 419–425 (1976).
98. Mittelman-Smith, M. A., Williams, H., Krajewski-Hall, S. J., McMullen, N. T. & Rance, N. E. Role for kisspeptin/neurokinin B/dynorphin (KNDy) neurons in cutaneous vasodilatation and the estrogen modulation of body temperature. *Proc. Natl. Acad. Sci. U. S. A.* **109**, 19846–19851 (2012).
99. Rance, N. E., Dacks, P. A., Mittelman-Smith, M. A., Romanovsky, A. A. & Krajewski-Hall, S. J. Modulation of body temperature and LH secretion by hypothalamic KNDy (kisspeptin, neurokinin B and dynorphin) neurons: a novel hypothesis on the mechanism of hot flushes. *Front. Neuroendocrinol.* **34**, 211–227 (2013).
100. Williams, H., Dacks, P. A. & Rance, N. E. An Improved Method for Recording Tail Skin Temperature in the Rat Reveals Changes During the Estrous Cycle and Effects of Ovarian Steroids. *Endocrinology* **151**, 5389–5394 (2010).
101. Ding, F. *et al.* Ovariectomy induces a shift in fuel availability and metabolism in the hippocampus of the female transgenic model of familial Alzheimer's. *PloS One* **8**, e59825 (2013).

102. Clarke, S. D., Clarke, I. J., Rao, A., Cowley, M. A. & Henry, B. A. Sex differences in the metabolic effects of testosterone in sheep. *Endocrinology* **153**, 123–131 (2012).
103. Mauvais-Jarvis, F. Estrogen and androgen receptors: regulators of fuel homeostasis and emerging targets for diabetes and obesity. *Trends Endocrinol. Metab. TEM* **22**, 24–33 (2011).
104. Sanchez-Alavez, M. *et al.* Insulin causes hyperthermia by direct inhibition of warm-sensitive neurons. *Diabetes* **59**, 43–50 (2010).
105. Shilaih, M. *et al.* Modern fertility awareness methods: Wrist wearables capture the changes of temperature associated with the menstrual cycle. *Biosci. Rep.* Epub ahead of print (2017) doi:info:doi/10.1042/BSR20171279.
106. Shilaih, M. *et al.* Modern fertility awareness methods: wrist wearables capture the changes in temperature associated with the menstrual cycle. *Biosci. Rep.* **38**, (2018).
107. Berglund Scherwitzl, E., Lindén Hirschberg, A. & Scherwitzl, R. Identification and prediction of the fertile window using NaturalCycles. *Eur. J. Contracept. Reprod. Health Care Off. J. Eur. Soc. Contracept.* **20**, 403–408 (2015).
108. Kleinschmidt, T. K. *et al.* Advantages of determining the fertile window with the individualised Natural Cycles algorithm over calendar-based methods. *Eur. J. Contracept. Reprod. Health Care Off. J. Eur. Soc. Contracept.* **24**, 457–463 (2019).
109. Krajewski-Hall, S. J., Miranda Dos Santos, F., McMullen, N. T., Blackmore, E. M. & Rance, N. E. Glutamatergic Neurokinin 3 Receptor Neurons in the Median Preoptic Nucleus Modulate Heat-Defense Pathways in Female Mice. *Endocrinology* **160**, 803–816 (2019).
110. Inagaki, K., Kihira, M., Suzuki, M. & Tomoda, Y. [Effects of iontophoretically-applied LHRH, TRH, estrogen and clomiphene on thermo-sensitive neurons in the rat hypothalamus]. *Nihon Sanka Fujinka Gakkai Zasshi* **37**, 611–618 (1985).
111. Bridge, M. W., Weller, A. S., Rayson, M. & Jones, D. A. Ambient temperature and the pituitary hormone responses to exercise in humans. *Exp. Physiol.* **88**, 627–635 (2003).
112. Tsai, C. L., Matsumura, K. & Nakayama, T. Effects of progesterone on thermosensitive neurons in preoptic slice preparations. *Neurosci. Lett.* **86**, 56–60 (1988).
113. Kimura, F. & Tsai, C. W. Ultradian rhythm of growth hormone secretion and sleep in the adult male rat. *J. Physiol.* **353**, 305–315 (1984).
114. Rusyniak, D. E., Zaretsky, D. V., Zaretskaia, M. V. & DiMicco, J. A. The role of orexin-1 receptors in physiologic responses evoked by microinjection of PgE2 or muscimol into the medial preoptic area. *Neurosci. Lett.* **498**, 162–166 (2011).
115. Pardey-Borrero, B. M., Tamasy, V. & Timiras, P. S. Circadian Pattern of Multiunit Activity of the Rat Suprachiasmatic Nucleus during the Estrous Cycle. *Neuroendocrinology* **40**, 450–456 (1985).
116. Miyamoto, H., Nakamaru-Ogiso, E., Hamada, K. & Hensch, T. K. Serotonergic integration of circadian clock and ultradian sleep-wake cycles. *J. Neurosci. Off. J. Soc. Neurosci.* **32**, 14794–14803 (2012).
117. Hori, T., Kiyohara, T., Osaka, T., Shibata, M. & Nakashima, T. Responses of preoptic thermosensitive neurons to mediobasal hypothalamic stimulation. *Brain Res. Bull.* **8**, 677–683 (1982).
118. Wang, W. *et al.* Effect of low estrogen on neurons in the preoptic area of hypothalamus of ovariectomized rats. *Acta Histochem.* **116**, 1259–1269 (2014).

119. Hui, Z. *et al.* Effects of black cohosh and estrogen on the hypothalamic nuclei of ovariectomized rats at different temperatures. *J. Ethnopharmacol.* **142**, 769–775 (2012).
120. Blum, I. D. *et al.* A highly tunable dopaminergic oscillator generates ultradian rhythms of behavioral arousal. *eLife* **3**, e05105 (2014).
121. Blessing, W. & Ootsuka, Y. Timing of activities of daily life is jaggy: How episodic ultradian changes in body and brain temperature are integrated into this process. *Temp. Austin Tex* **3**, 371–383 (2016).
122. Aransay, A., Rodríguez-López, C., García-Amado, M., Clascá, F. & Prensa, L. Long-range projection neurons of the mouse ventral tegmental area: a single-cell axon tracing analysis. *Front. Neuroanat.* **0**, (2015).
123. West, K. S. & Roseberry, A. G. Neuropeptide-Y alters VTA dopamine neuron activity through both pre- and postsynaptic mechanisms. *J. Neurophysiol.* **118**, 625–633 (2017).
124. Qu, N. *et al.* A POMC-originated circuit regulates stress-induced hypophagia, depression, and anhedonia. *Mol. Psychiatry* **25**, 1006–1021 (2020).
125. Gumbs, M. C. R. *et al.* Afferent neuropeptide Y projections to the ventral tegmental area in normal-weight male Wistar rats. *J. Comp. Neurol.* **527**, 2659–2674 (2019).
126. Stagkourakis, S., Kim, H., Lyons, D. J. & Broberger, C. Dopamine Autoreceptor Regulation of a Hypothalamic Dopaminergic Network. *Cell Rep.* **15**, 735–747 (2016).
127. Freeman, M. E., Kanyicska, B., Lerant, A. & Nagy, G. Prolactin: structure, function, and regulation of secretion. *Physiol. Rev.* **80**, 1523–1631 (2000).
128. Holt, R. I. G. & Peveler, R. C. Antipsychotics and hyperprolactinaemia: mechanisms, consequences and management. *Clin. Endocrinol. (Oxf.)* **74**, 141–147 (2011).
129. Nestor, C. C. *et al.* Regulation of GnRH Pulsatility in Ewes. *Reprod. Camb. Engl.* **156**, R83–R99 (2018).
130. Goodman, R. L. *et al.* Evidence That Dopamine Acts via Kisspeptin to Hold GnRH Pulse Frequency in Check in Anestrous Ewes. *Endocrinology* **153**, 5918–5927 (2012).
131. Lehman, M. N., Merkley, C. M., Coolen, L. M. & Goodman, R. L. Anatomy of the kisspeptin neural network in mammals. *Brain Res.* **1364**, 90–102 (2010).
132. Weems, P. *et al.* Effects of Season and Estradiol on KNDy Neuron Peptides, Colocalization With D2 Dopamine Receptors, and Dopaminergic Inputs in the Ewe. *Endocrinology* **158**, 831–841 (2017).
133. Thiéry, J. C. *et al.* Dopaminergic control of LH secretion by the A15 nucleus in anoestrous ewes. *J. Reprod. Fertil. Suppl.* **49**, 285–296 (1995).
134. Franchimont, P. *et al.* Prolactin levels during the menstrual cycle. *Clin. Endocrinol. (Oxf.)* **5**, 643–650 (1976).
135. Baker, F. C., Siboza, F. & Fuller, A. Temperature regulation in women: Effects of the menstrual cycle. *Temperature* **7**, 226–262 (2020).
136. Fuller-Jackson, J.-P., Dordevic, A. L., Clarke, I. J. & Henry, B. A. Effect of sex and sex steroids on brown adipose tissue heat production in humans. *Eur. J. Endocrinol.* **183**, 343–355 (2020).
137. Hampl, R., Stárka, L. & Janský, L. Steroids and thermogenesis. *Physiol. Res.* **55**, 123–131 (2006).

138. Ramage, L. E. *et al.* Glucocorticoids Acutely Increase Brown Adipose Tissue Activity in Humans, Revealing Species-Specific Differences in UCP-1 Regulation. *Cell Metab.* **24**, 130–141 (2016).
139. Smarr, B. L., Burnett, D. C., Mesri, S. M., Pister, K. S. J. & Kriegsfeld, L. J. A Wearable Sensor System with Circadian Rhythm Stability Estimation for Prototyping Biomedical Studies. *IEEE Trans. Affect. Comput.* **7**, 220–230 (2016).
140. McMurray, R. G. & Katz, V. L. Thermoregulation in Pregnancy: Implications for Exercise. *Sports Med.* **10**, 146–158 (1990).
141. Charkoudian, N. & Stachenfeld, N. S. Reproductive Hormone Influences on Thermoregulation in Women. in *Comprehensive Physiology* (John Wiley & Sons, Inc., 2011). doi:10.1002/cphy.c130029.
142. Boyle, J. A. *et al.* Ask PCOS: Identifying Need to Inform Evidence-Based App Development for Polycystic Ovary Syndrome. *Semin. Reprod. Med.* **36**, 59–65 (2018).
143. Katulski, K., Podfigurna, A., Czyzyk, A., Meczekalski, B. & Genazzani, A. D. Kisspeptin and LH pulsatile temporal coupling in PCOS patients. *Endocrine* **61**, 149–157 (2018).
144. Casper, R. F. & Gladanac, B. Introduction: circadian rhythm and its disruption: impact on reproductive function. *Fertil. Steril.* **102**, 319–320 (2014).
145. Culver, A. *et al.* Circadian disruption of core body temperature in trauma patients: a single-center retrospective observational study. *J. Intensive Care* **8**, 4 (2020).
146. Evans, J. A. & Davidson, A. J. Health consequences of circadian disruption in humans and animal models. *Prog. Mol. Biol. Transl. Sci.* **119**, 283–323 (2013).
147. Rutters, F. *et al.* Is social jetlag associated with an adverse endocrine, behavioral, and cardiovascular risk profile? *J. Biol. Rhythms* **29**, 377–383 (2014).
148. Wong, P. M., Hasler, B. P., Kamarck, T. W., Muldoon, M. F. & Manuck, S. B. Social Jetlag, Chronotype, and Cardiometabolic Risk. *J. Clin. Endocrinol. Metab.* **100**, 4612–4620 (2015).
149. Smarr, B. L. & Schirmer, A. E. 3.4 million real-world learning management system logins reveal the majority of students experience social jet lag correlated with decreased performance. *Sci. Rep.* **8**, 4793 (2018).
150. Giacchetti, S. *et al.* Phase III trial comparing 4-day chronomodulated therapy versus 2-day conventional delivery of fluorouracil, leucovorin, and oxaliplatin as first-line chemotherapy of metastatic colorectal cancer: the European Organisation for Research and Treatment of Cancer Chronotherapy Group. *J. Clin. Oncol. Off. J. Am. Soc. Clin. Oncol.* **24**, 3562–3569 (2006).
151. Lévi, F., Okyar, A., Dulong, S., Innominato, P. F. & Clairambault, J. Circadian Timing in Cancer Treatments. *Annu. Rev. Pharmacol. Toxicol.* **50**, 377–421 (2010).

# 2. Adolescent Development of Biological Rhythms: Estradiol Dependence and Effects of Combined Contraceptives

## 2.1 Abstract

**Purpose:** Adolescence is a period of continuous development, including the maturation of endogenous rhythms across systems and timescales. Although these dynamic changes are well recognized, their continuous structure and hormonal dependence have not been systematically characterized. Given the well-established link between core body temperature (CBT) and reproductive hormones in adults, we hypothesized that high-resolution CBT can be applied to passively monitor pubertal development and disruption with high fidelity.

**Methods:** To examine this possibility, we used signal processing to investigate the trajectory of CBT rhythms at the within-day (ultradian), daily (circadian), and ovulatory timescales, their dependence on estradiol, and the effects of hormonal contraceptives.

**Results:** Puberty onset was marked by a rise in fecal estradiol (fE2), followed by an elevation in CBT and circadian power. This time period marked the commencement of 4-day rhythmicity in fE2, CBT, and ultradian power marking the onset of the estrous cycle. The rise in circadian amplitude was accelerated by E2 treatment, indicating a role for this hormone in rhythmic development. Contraceptive administration in later adolescence reduced CBT and circadian power and resulted in disruption to 4-day cycles that persisted after discontinuation.

**Conclusions:** Our data reveal with precise temporal resolution how biological rhythms change across adolescence and demonstrate a role for E2 in the emergence and preservation of multiscale rhythmicity. These findings also demonstrate how hormones delivered exogenously in a non-rhythmic pattern can disrupt rhythmic development. These data lay the groundwork for a future in which temperature metrics provide an inexpensive, convenient method for monitoring pubertal maturation and support the development of hormone therapies that better mimic and support human chronobiology.

## 2.2 Introduction

Adolescence is a period of rhythmic reorganization during which physiology transitions from a non-reproductive juvenile state into reproductive early adulthood[1–5]. Historically, researchers have relied on self-report, tanner staging, or infrequent salivary or blood hormone samples to track milestones of pubertal development. We reasoned that a time series characterization of continuous core body temperature (CBT)[6–10] could reflect dynamic, rhythmic features of hormonal development across the pubertal trajectory. If feasible, CBT could become a highly convenient and more accurate pubertal staging tool with unprecedented temporal resolution. Its application could also improve our understanding of the range of typical pubertal trajectories and factors that drive deviation from these trajectories.

Rhythmic development occurs at multiple timescales, including within-a-day (ultradian rhythms; URs)[11], daily (circadian rhythms; CRs)[12,13], and multi-day ovulatory cycles in females (ovulatory rhythms; ORs)[14]. These rhythms occur across physiological systems, serving to increase the efficiency of signal transduction[15–17], temporally segregate incompatible processes[18], synchronize internal systems to the environment[19], and maximize reproductive success[20]. Although structure at one timescale can be modulated by changes at another[21,22], distinct mechanisms underlie each rhythmic frequency. This suggests individual rhythmic frequencies may each follow distinct developmental trajectories.

Coordinated URs are observed in hypothalamic-pituitary-peripheral axes and beyond in adult mammals, with broad manifestation in systems including cardiovascular outputs, thermoregulation, and even cognition (reviewed in[6,23–26]). Many URs, including those in reproductive and growth hormones, are present early in life[27] and increase in amplitude from pre-to-mid puberty[28–30]. Some URs increase markedly in frequency and amplitude around puberty onset (e.g., gonadotropin releasing hormone (GnRH) luteinizing hormone (LH) and estradiol (E2)[11,28,31–35,28,35]). In adults, URs are modulated by time of day[36] and phase of the ovulatory cycle[21], suggesting that pubertal modifications at the CR and OR timescales likely impact UR structure. Conversely, increases in UR amplitude increase CR amplitude *by definition*, although, it is unclear if UR structure impacts regulation of CRs. Although URs are thought to be centrally controlled, potentially via interaction of dopaminergic and hypothalamic circuits[23,37–42], relatively little is understood about mechanisms and progression of URs across adolescence.

Whereas the mechanisms and phenomenology of ultradian development require much further study, those underlying circadian rhythms and pubertal changes to CRs are well documented. Circadian rhythms are nearly ubiquitous, generated intracellularly via interlocked transcription-translation feedback loops, and are governed by a central pacemaker within the suprachiasmatic nucleus (SCN) of the hypothalamus[43–45]. Although changes in SCN output and connectivity during adolescence are not well characterized, integration of new neurons into the central clock[46] and reproductive neurocircuitry[47] alongside adolescent increases in SCN input to the GnRH system[48] may contribute to downstream CR changes. For example, circadian amplitude appears to increase across puberty in many systems (e.g., cortisol[49], activity[45], and potentially temperature[50]), while emerging for the first time in others (e.g., LH[34] and FSH[29]). Finally,

circadian activity[45] and sleep-wake[51] rhythms are phase delayed during puberty[52] and are more vulnerable to disruption by mistimed light and food cues than in adults[53].

In contrast to ultradian and circadian rhythms, which are apparent to variable degrees in juveniles, the female ovulatory, or estrous, cycle emerges for the first time in adolescence[14]. Briefly, in spontaneously-ovulating rodents, the 4 to 5 day cycle begins with rising E2 levels that maintain LH at low concentrations through negative feedback. When E2 is sufficiently high, and a pool of ovarian follicles has matured, E2 positive feedback integrates with circadian signaling and progesterone of neural origin[47,54,55] to induce a preovulatory LH surge that initiates ovulation[55–60]. Subsequent formation of the corpus luteum leads to a brief rise in circulating progesterone prior to beginning the next cycle. As with URs and CRs, ORs manifest as changes in a number of systems, including metabolic hormones, cardiac output, and thermoregulation[61–63]. Although it is clear that ORs emerge at puberty, the continuous patterns of commencement and stabilization are poorly understood. Pre-pubertal ovarian follicles typically undergo development and atresia without substantial release of sex steroids[30]. Soon after the emergence of the first cycle, at menarche in girls[20], cycles have a higher likelihood of anovulation or low post-ovulatory progesterone compared to adults[64]. Although high temporal resolution patterns are unknown, large increases in plasma E2 and FSH occur from pre to mid puberty[28,34,65]. Given these changes in hormones across puberty, one aim of the present investigation was to employ continuous, longitudinal, and high-resolution CBT monitoring alongside daily E2 measures to characterize the emergence of the ovulatory cycle in rats.

By characterizing rhythmic outputs that reflect underlying physiological change across adolescence, a greater understanding of typical progression can be garnered and the impact of exogenous hormone manipulation on temporal trajectories can be observed. Temporal disruption at all three timescales is associated with negative health outcomes in adults[66–71], and adolescence may be a sensitive period where disruptions have rapid[1] and potentially long-term health impacts[2,53,72,73]. A growing proportion of teenage girls (estimated between 22-54% across the first two decades of the 21$^{st}$ century[74,75]) receive hormonal contraceptives for a variety of purposes, including pregnancy prevention[76] or treatment of menstrual symptoms[77], and acne[78]. These hormonal contraceptives aim to prevent ovulation, sperm penetration, and implantation by maintaining elevated progestin levels akin to the post-ovulatory portion of the cycle (with or without estrogen derivatives)[79–83]. As they are delivered at static or once daily bolus concentrations that differ from the endogenous, multiscale rhythmic pattern of release[84–86], hormonal contraceptives can be considered a form of temporal endocrine disruption[87,88]. Hormonal contraceptive use is associated with elevated body temperature[89], decoupling of follicular maturation cycles within the ovary[88,90], weight change[91,92], mental health risks[93–95], lasting luteal phase deficiency[96], and a variety of other off target effects[97–100]. Furthermore, women under 21 are more likely to exhibit anovulatory cycles following birth control cessation than are older individuals[101], suggesting that contraceptives taken during late adolescence may be more disruptive than in adulthood. Although currently considered safe, discontinuation rate is high[102] and impact on the temporal progression of development is unclear.

CBT as a continuous surrogate marker for pubertal status may provide convenience and new information to longitudinal research studies on this topic and beyond. Continuous measures of

activity have been used for rhythmic monitoring[52], but this measure is not as closely tied to high-frequency changes driven by hormonal systems[9,10] and does not appear to predict individual health events with comparable specificity[9,10,103]. In contrast, CBT exhibits clear URs, CRs, and ORs that reflect underlying hormonal changes[6,61,104], including ultradian rhythmic CBT patterns that mirror LH[21,105] and estradiol[21] prior to ovulation. Likewise, CBT is a reliable phase marker for circadian rhythmicity[106,107]. Hormonal alterations across the ovulatory cycle directly influence CBT, with E2 decreasing temperatures prior to ovulation, and E2 with progesterone increasing temperature following ovulation[8,106]. As a result, we hypothesized that insight into changes in the temporal structure of underlying physiology across adolescence can be garnered via assessment of continuous CBT levels and rhythms. The present study employed continuous CBT to characterize rhythmic change across adolescent development and examine the role of pubertal onset of E2 production and ovarian status in guiding the typical developmental trajectory. Additionally, because late pubertal contraceptive use might act to disrupt the typical progression of rhythmic development, we examined the impact of a common contraceptive regimen (i.e., ethinyl estradiol and levonorgestrel) on endogenous estradiol concentrations and CBT rhythms. As the pulse amplitude of multiple hormones increases across adolescence, we hypothesized that the amplitude of CBT URs would be similarly impacted. We also hypothesized that CR amplitude and overall body temperature would increase during adolescence, and that these increases would be influenced by E2. As changes to rhythmicity have primarily been reported from early to mid-adolescence, we hypothesized that rhythmic restructuring would be most pronounced during this period. Finally, we hypothesized that rhythmic patterns of body temperature change identified during adolescent development would be disrupted during and potentially after, the cessation of contraceptive administration, and in ovariectomized individuals.

## 2.3 Materials and Methods

Animals. Female Wistar rats were purchased at 250 g from Charles River (Charles River, Wilmington, MA) and bred in the lab and weaned at p21. Weanlings were housed in standard translucent propylene (96 x 54 x 40 cm) rodent cages, and provided *ad libitum* access to food and water, wood chips for floor cover, bedding material, and chew toys for the duration of the study. To minimize social isolation stress, which is known to affect pubertal development[108,109], animals were housed with a same sex, non-experimental sibling. Animals were maintained on a 12:12 light dark (LD) cycle; light intensity during the photo- and scotophases were ~500 lux white light and <1 lux red light, respectively, with lights on at 1 AM and off at 1 PM. Animals were gently handled before weighing daily to minimize stress. To prevent mixing of feces used for hormone analysis, cage mates were separated by a flexible stainless steel lattice that permitted aural, scent, and touch interaction between siblings. A total of 64 animals were included in the study: 32 as experimental animals (Intact, Intact + Contraceptives, Ovariectomized (OVX) and OVX + E2; n=8/group), and 32 as social, littermate partners. All procedures were approved by the Institutional Animal Care and Use Committee of the University of California, Berkeley.

Core Body Temperature Data Collection. Data were gathered with G2 E-Mitter implants that chronically record CBT (Starr Life Sciences Co., Oakmont, PA). At weaning, G2 E-Mitters were implanted in the intraperitoneal cavity under isoflurane anesthesia with analgesia achieved by

subcutaneous injections of 0.03 mg/kg buprenorphine (Hospira, Lake Forest, IL) in saline (administered every 12 h for 2 days after surgery). E-Mitters were sutured to the ventral muscle wall to maintain consistent core temperature measurements. Recordings began immediately, but data collected for the first 4 days post-surgery were not included in analyses. Recordings were continuous and stored in 1-min bins.

Ovariectomy and Silastic Capsule Replacement. Ovariectomies were performed at weaning (p21) at the same time as the implantation of the E-Mitter, as previously described[10,57]. The E-Mitter surgery served as a control operation in non-OVX animals. Incisions were closed using dissolvable sutures and wound clips. At p29, OVX animals were anesthetized and implanted with silastic capsules (0.78 mm I.D., 1.25 O.D.; Dow Corning, Midland, M). Capsules were implanted subcutaneously and intrascapular. Capsules were 20mm in length with with 5mm silicone sealant at each end (Sigma Aldrich, St. Louis, MO) and contained either 112µg (180µg/mL) 17β estradiol in sesame oil, or sesame oil alone. E2 treatment results in plasma E2 concentrations averaging ~ 5µg/day, beginning in animals of 80-100g[110,111]. Capsules were primed for 24 h prior to implantation via submersion in 0.9% saline in order to avoid delivering a large initial bolus of E2. Although these doses have been tested previously, large variability in serum E2 levels following silastic implant is typically reported[110–113]. Incisions were closed using dissolvable suture and a wound clip, and buprenorphine was delivered as above for post-operative analgesia.

Contraceptive Administration. Ethinyl Estradiol (EE2, 30µg/day) and Levonorgestrel (30 µg/day), a progestin, were dissolved in in 0.01 mL of sesame oil and delivered subcutaneously at the nape of the neck daily for the duration of two estrous cycles during mid to late adolescence (p50 to p58). Although a wide range of rodent doses of EE2 and Levonorgestrel have been reported[114–116], the doses chosen here aimed to match those used consistently for suppressing ovulation and mimicking effects observed in humans, such as increased blood pressure[117], and for comparability to existing rodent literature on subcutaneous delivery of Levonorgestrel and EE2[118–120]. Many doses for orally delivered EE2 and Levonorgestrel in rats also fall in this range[82,115,121,122]. These drugs have been available as human contraceptives for decades under several brand names in widely varying doses[100,123].

Fecal Sample Collection. Fecal E2 (fE2) concentrations were assessed across puberty from feces generated over 24 h periods. Fecal samples provide hormone concentrations more representative of average daily hormone concentrations than single timepoint blood samples[124–128] and eliminates associated stress and infeasibility of high-frequency, longitudinal blood collection. Samples were collected in small, airtight bags at the end of dark phase under dim red light (<5 lux) from p25 to p37 (pre puberty and first cycle), p45 to p51 (mid-puberty), and p55 to p65 (late puberty to early adulthood) in all groups, and additionally to p75 in Intact+C and Intact groups (adulthood). Samples soiled with urine were discarded, and all other droppings generated over each 24-h segment were combined. Within 1 h of collection, samples were stored at -20°C until processed. Sample collection was rapid (~ 1 min per animal).

Before assessment of hormone concentration, samples were processed according to manufacturers' instructions[129]. Briefly, samples were placed in a tin weigh boat and heated at 65°C for 90 minutes, until completely dry. Dry samples were ground to a fine powder in a coffee grinder, which was wiped down with ethanol and dried between samples to avoid cross

contamination. Powder was weighed into 0.2 mg aliquots. For hormone extraction, 1.8mL of 100% ethanol was added to each test tube, and tubes were shaken vigorously for 30 minutes. Tubes were then centrifuged at 5,000 RPM for 15 minutes at 4°C. Supernatant was moved to a new tube and evaporated under 65°C until dry (~ 90 minutes). Sample residue was reconstituted in 100uL of 100% ethanol. 25µL of this solution was diluted for use in the assay and remaining sample was diluted and stored.

ELISA Assays. A commercially available fE2 enzyme-linked immunosorbent assay (ELISA) kit was used to quantify E2 in fecal samples (Arbor Assays, Ann Arbor, MI). These assays have been previously published in species ranging from rats and mice[130–132], to wolves[133], to humans[134]. ELISAs were conducted according to manufacturer's instructions. To ensure each sample contained ≤ 5% alcohol, 25µL of concentrate were vortexed in 475µL assay buffer. All samples were run in duplicate, and an inter-assay control was run with each plate. Sensitivity for the assay was 39.6 pg/mL and the limit of detection was 26.5 pg/mL. fE2 intra-assay coefficient of variation (COV) was 5.94% and inter-assay COV was 5.71%.

Data Availability and analysis. All code and data used in this paper are available at A.G.'s and L.J.K.'s Github Repository (https://github.com/azuredominique; https://github.com/Kriegsfeld-Lab)[135]. Code was written in MATLAB 2020b with Wavelet Transform (WT) code modified from the Jlab toolbox and from Dr. Tanya Leise[136,137]. Briefly, data were imported to MATLAB at 1-min resolution. Any data points outside ± 4 standard deviations were set to the median value of the prior hour, and any points showing near instantaneous change, as defined by local abs(derivative) > $10^5$ as an arbitrary cutoff, were also set to the median value of the previous hour. Small data gaps resulting from intermittent data collection (<10 minutes) were linearly interpolated. Continuous data from p26 to p74 were divided into three equal-length phases: early to mid-puberty (p26 to p41), mid to late puberty (p42 to p58), and late puberty to early adulthood (p59 to p74).

Wavelet Analyses and Statistics of CBT Data. Wavelet Transformation (WT) was used to generate a power estimate, representing amplitude and stability of oscillation at a given periodicity, within a signal at each moment in time. Whereas Fourier transforms allow transformation of a signal into frequency space without temporal position (i.e., using sine wave components with infinite length), wavelets are constructed with amplitude diminishing to 0 in both directions from center. This property permits frequency strength calculation at a given position. In the present analyses we use a Morse wavelet with a low number of oscillations (defined by β=5 and γ=3, the frequencies of the two waves superimposed to create the wavelet[138]), similar to wavelets used in many circadian and ultradian applications[9,10,136–139]. Additional values of β (3–8) and γ (2–5) did not alter the findings (data not shown). As WTs exhibit artifacts at the edges of the data being transformed, only the WT from p26 to p74 were analyzed further. Periods of 1 to 39 h were assessed. For quantification of spectral differences, WT spectra were isolated in bands; circadian periodicity power was defined as the max power per minute within the 23 to 25 h band; ultradian periodicity power was defined as the max power per minute in the 1 to 3 h band. The latter band was chosen because this band corresponded with the daily ultradian peak power observed in ultradian rhythms (URs) across physiological systems in rats[6,140–142].

For statistical comparisons of any two groups, Mann Whitney U (MW) rank sum tests were used to avoid assumptions of normality for any distribution. Non-parametric Kruskal-Wallis tests were used instead of ANOVAs for the same reason; for all Kruskal-Wallis (KW) tests, $\chi^2$ and p values are listed. In cases of repeated measures within an individual over adolescence, Friedman's tests were used. Data from each estrous cycle were treated as independent. We chose to treat estrous cycles as independent for 3 reasons: 1) the estrous cycle is the longest periodicity rhythm within the study, 2) the adolescent estrous cycle develops rapidly from one iteration to the next in rats , and 3) because the interventions of ovariectomy and birth control administration exert their effects by removal or modification of estrous cycles. Dunn's test was used for multiple comparisons. Mann Kendall (MK) tests were used to assess trends over time in wavelet power and linear CBT over three equally sized temporal windows described above. For short term (<3 days of data) statistical comparisons, 1 data point per hour was used; for longer term (>3 days of data) statistical comparisons, 1 data point per day was used. Continuous wavelet power data were smoothed with a 24 h window using the MATLAB function "movmean". Violin plots, which are similar to box plots with probability density of finding different values represented by width[143], were calculated using the MATLAB function "violin". Median daily circadian power was regressed against each day's fE2 for each group using a mixed effects linear regression (MATLAB function "fitlme", formula: circadian daily medians~1+E2 values + ( 1+ E2 |Individual ID)).

Analysis of fE2 Concentrations and Estrous Cyclicity. The day of fE2 rise before cycling began was defined as the first day fE2 level rose > 2 standard deviations above its starting value at p25. The initial rise in fE2 was used as an alignment point for CBT, ultradian power, and Z-Score(CBT) - Z-Score(UR power) group averages. Group differences in fE2 area under the curve by cycle were assessed using the MATLAB function "trapz" and KW tests with Dunn's post hoc correction. As estrous cycles are not all aligned in time or by age, samples were aligned with the highest value in a collection period (e.g., mid puberty) where a 'fall' was observed three days later. Fast Fourier Transforms (FFT) were used to assess the presence or absence of 4-5 day power in CBT in each individual from the period of fE2 rise until p50 (when Intact+C animals started receiving daily contraceptive injections), and from p50 to p74. In order to further assess commencement and stability of estrous cycling after first rise in fE2, as well as any potential perturbation during and after contraceptive administration, metrics were divided into 4 day blocks, with each day labelled 1,2,3, and 4: repeating for subsequent cycle lengths. Groups for statistical comparison were constructed from all data corresponding to 1's, 2's, 3's and 4's. Friedman's tests with Dunn's correction for multiple comparisons were used to determine if values associated with each day of cycle (e.g., all day 1's) varied significantly from other days of the cycle by group.

## 2.4 Results

Impact of Hormonal Status on Estradiol Concentrations and Weight Gain Across Adolescence. Frequent fecal estradiol (fE2) measurements were collected to assess if hormonal status affected the level or temporal patterning of fE2 across puberty. FE2 concentrations did not differ between groups from p25-p31, a baseline period prior to puberty onset ($\chi^2$=4.48, p=0.214; **Figure 1A**). Vaginal opening occurred between p31 and p33 in Intact rats, and fE2 rose 2 standard deviations above its p25 starting value between p31 and p36.

During this window, Intact and Intact+C animals' fE2 concentrations exceeded that of OVX animals ($\chi^2$=15.9, p=0.001; p=0.0134 and p=0.003, respectively; **Figure 1B**). This difference was maintained at mid puberty (cycles aligned from p40 to p47) ($\chi^2$=13.7, p=0.003; p=0.003 and 0.032, respectively) and early adulthood (cycles aligned from p55 to p61) ($\chi^2$=17.1, p=0.001; p=0.001 and 0.009, respectively; **Figure 1C-D**). OVX+E2 animals were not different from other groups at any timepoint, with intermediate values between Intact and OVX groups (p>0.05 in all cases). Unlike Intact animals, Intact+C animals did not exhibit days of elevated fE2 every 4$^{th}$ day (See **Supplemental Figure 1**). However, fE2 concentrations did not differ between Intact and Intact+C groups approximately 4 to 5 cycles after contraceptive administration ceased, between p69 to p75 ($\chi^2$=1.62 p=0.203). See **Methods** for details of within-cycle alignment.

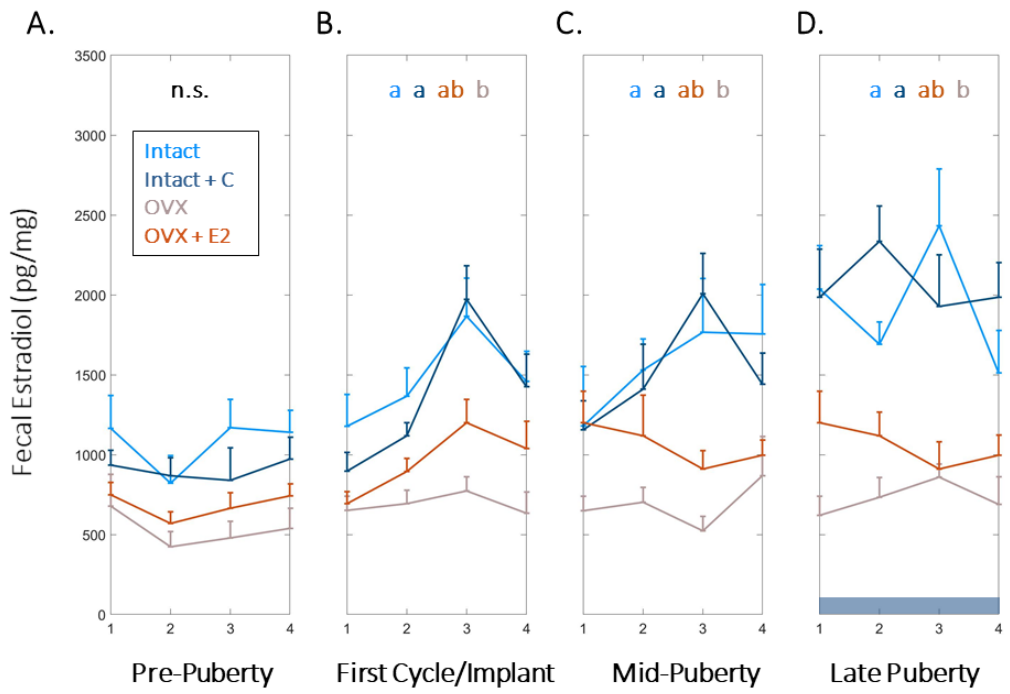


**Figure 1. High Frequency Fecal Estradiol Enables Monitoring of Estrous Cycle Emergence, Sex Steroid Manipulation, and Ovarian Status During Adolescence.** Group mean (+S.E.M.) fecal estradiol concentrations of Intact (light blue), intact + short-term pubertal contraceptives (Intact+C; dark blue), OVX (gray), and OVX+E2 (orange) groups did not significantly differ prior to puberty (p24-30) (A). Fecal estradiol in Intact and Intact+C groups increased over that of OVX animals beginning at the first cycle following vaginal opening or relative to the time of silastic implant in OVX+E2 animals (p30-37) (B) and remained significantly elevated thereafter at mid puberty (p43-p49; C) and during late puberty (p55-61; D). Dark horizontal bar in D indicates Intact+C data were gathered during contraceptive administration. Color of letters at the top of B, C, and D indicate experimental group; letters indicate statistical differences, with groups not sharing the same letter being significantly different (p<0.03).

Additionally, daily weights were measured to recapitulate known effects of E2 on pubertal growth trajectory, and to assess if contraceptive administration modulated weight gain. Intact animals gained weight consistently across puberty. Pre-pubertal OVX was associated with increased body weight at mid puberty, with OVX animals weighing more than animals from all other groups, and

OVX+E2 animals weighing more than Intact or Intact+C groups ($\chi^2$=57.9, p=1.65*$10^{-12}$; p<0.05 for all individual comparisons). By early adulthood, both OVX and OVX+E2 groups weighed significantly more than Intact or Intact+C groups and did not differ from one another ($\chi^2$=76.1, p=2.08*$10^{-16}$ ; p=0.99 for OVX vs. OVX+E2; p<0.05 for all other comparisons). Eight days of contraceptive administration did not significantly impact weight relative to Intact animals ($\chi^2$=0.28, p=0.594; See **Supplemental Figure 2**).

Circadian, but not Ultradian, Power of Body Temperature Increased Across Pre-to-Mid Adolescence. As reproductive circadian and ultradian rhythms change markedly across adolescence and may be coupled to CBT[32,49,144], we investigated the impact of estradiol status on the timing and tempo of CBT rhythmicity. All animals exhibited a significant positive trend in CR power from pre-to-mid adolescence (p26 to p41) (p=0.002, 0.007, 0.029, 0.04 for Intact, Intact+C, OVX, and OVX+E2 animals, respectively). CR power stabilized thereafter (p>0.05 in all cases; **Figure 2A-B**). To examine the relative rate of this increase across groups, we set a criterion of 2 standard deviations above the mean. CR power rose 2 standard deviations above the mean significantly faster in OVX+E2 animals compared to Intact or OVX animals ($\chi^2$ =19.0, p=3*$10^{-4}$; p=0.025 and 0.001, respectively; **Figure 2L**).

Ultradian power did not show a significant upward or downward trend across the study period in any group (p>0.05 for all groups at all time windows) (**Figure 2A-D**). Although directionality of CR power change across adolescence was similar (i.e., an early increase followed by a plateau) in all individuals, magnitude of circadian power differed among groups. Specifically, circadian power for OVX animals was depressed compared to all other groups from pre to mid adolescence ($\chi^2$ =125, p=4.02*$10^{-27}$, p<0.02 for OVX vs. all other groups; **Figure 2E**). From mid to late adolescence (p42 to p58), CR OVX power remained depressed and OVX+E2 trended toward lower power ($\chi^2$ =112, p=2.82*$10^{-24}$; p<0.01 Intact and Intact+C vs OVX; **Figure 2F**). In early adulthood (p59 to p74), following contraceptive administration, the CR power for Intact+C was depressed compared to Intact rats ($\chi^2$ =37.9, p=2.93*$10^{-08}$, p=0.04; **Figure 2G**).

Body Temperature Circadian Power was Most Correlated to Fecal Estradiol Level in Unmanipulated Animals. Temperature level, UR power, and E2 exhibited coupled patterning, and appeared to change markedly during adolescence. However, it was unclear if CBT circadian rhythmicity was coupled to estradiol, if such a relationship existed during adolescence, and if the relationship could be modified by hormonal state. FE2 and normalized circadian power were strongly correlated in Intact ($R^2$=0.226, p=2.90*$10^{-4}$) and Intact+C rats prior to p50 when contraceptive administration began ($R^2$=0.166, p=0.025), and weakly correlated in OVX+E2 animals ($R^2$=0.062, p=0.001; **Figure 2 H-K**). This positive correlation was abolished during and after hormonal contraceptive administration in the Intact+C group ($R^2$=1.06*$10^{-5}$, p=0.58; **Figure 2I, inset**). Circadian power and fE2 was not significantly correlated in OVX animals ($R^2$=0.013, p=0.06; **Figure 2J**).

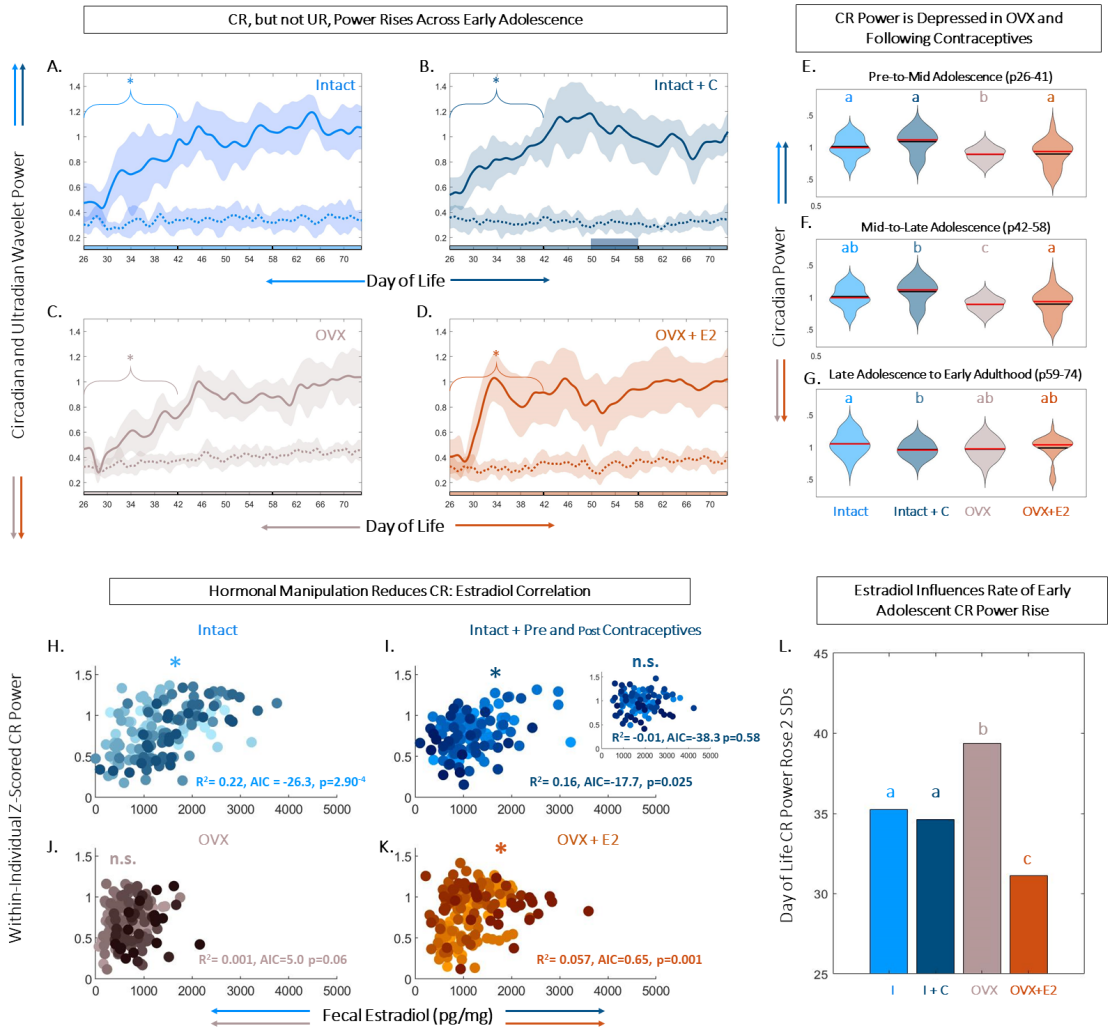


**Figure 2. Level and Rate of Early Adolescent Rise in CBT Circadian Power are Tied to Estradiol.** Circadian, but not ultradian power rises across early adolescence (A-D). Linear plots of group mean (± S.E.M.) of CBT circadian (solid) and ultradian (dashed) power in Intact (light blue, A), Intact+C (dark blue, B), OVX (gray, C) and OVX+E2 (orange, D) animals. * Indicates significant trend over time for the bracketed time region ($p<0.05$). Phase of adolescent time periods (pre to mid, mid to late, and late to adult) are indicated by black dividers in the colored x-axis at p42 and p58. Although CBT circadian power rises over early adolescence in all groups, estradiol increases the rate of this rise (L). Violin plots (E-G) of circadian power in each group analyzed by segment of life: pre to mid adolescence from p26-41 (E), mid to late adolescence from p42-57 (F), and late adolescence through early adulthood from p58-73 (G) illustrate that CR power is highest in Intact animals, with reduction following hormonal contraceptive administration and OVX, with a partial rescue in OVX+E2 animals. Black lines indicate mean and red lines indicate median of each plot. Scatters of fE2 level by CR power indicate that hormonal manipulation reduces or eliminates the correlation between CR power and fE2 concentrations (H-K). Note that each individual within a group is plotted in a unique color. CR power and fE2 are significantly correlated in Intact (light blue, H), Intact+C animals prior to contraceptive administration (dark blue, I), with inset depicting abolished correlation during and after contraceptive administration. CR power and fE2 are weakly correlated in OVX+E2 (orange, K) but not OVX animals (J). * Indicates significant positive correlation between fE2 and circadian power. AIC indicates relative performance of the mixed effects model. Color of letters at the top in E-G and L indicate experimental group; letters indicate statistical differences, with groups not sharing the same letter being significantly different ($p<0.03$).

Ovulatory Rhythms in CBT and Perturbations During and After Contraceptive Administration. We next investigated the relationship between ORs and cycles in body temperature. Our goal was to determine if interactions at this timescale a) could be observed in continuous body temperature in adolescents, b) if previously described hormonal UR modulations by phase of cycle[145,146] translates to ovulatory cycles in CBT URs, and c) if exogenous hormone administration disrupts these continuous dynamics. In intact rats, we observed a significant 4-day modulation of combined CBT and UR power corresponding to the estrous cycle (Intact $\chi^2$=59.1, p=9.26*$10^{-13}$, Intact+C group prior to BC administration $\chi^2$=13.7 p=0.003; **Figure 3A-B, 4A-B**). This 4-day pattern commenced in Intact and Intact+C rats (prior to treatment) with a significant increase in mean daily CBT following the first rise in fE2 above 2 standard deviations (p=0.03 in each case). Intact and Intact+C (prior to treatment) animals also exhibited a 4-day pattern of UR power modulation. This modulation manifested as as a significant trough of UR power within 4 days of the first rise of fE2, as previously reported in adult rodents[9,10,147,148] (p=0.04, p=0.03, respectively). The combination of UR power and linear temperature yielded a more easily separable metric which rose significantly the day after first rise of fE2 in Intact and Intact+C (p=0.01, p=0.02, respectively; **Figure 3A-B**). (For individual metric comparisons see **Supplemental Figure 3**).

We noted an absence of significant 4-day differences in combined CBT and UR power in the Intact+C group during hormonal contraceptive administration, even following 4 cycle-lengths of recovery (Intact+C group $\chi^2$=7.2, p=0.07; Intact group over same time period $\chi^2$=58.9, p=1.00*$10^{-12}$ ). A FFT of data in Intact and Intact+C animals prior to contraceptive administration revealed comparable AUCs for 4 to 5 day oscillations (no group difference; $\chi^2$ =0.54, p=0.46; **Figure 3C, Inset**). However, after hormonal contraceptive administration, AUC for Intact animals was significantly greater for 4 to 5 day oscillations than in Intact+C animals ($\chi^2$ =3.98, p =0.046; **Supplemental Figure 4**). As expected, a 4-day pattern was also absent in OVX and OVX+E2 animals (p>0.05 in both cases). Note that 5-day cycles occurred rarely in Intact rats and using 5-day bins rather than 4-day bins abolished significant differences by day of cycle for all groups (*data not shown*).

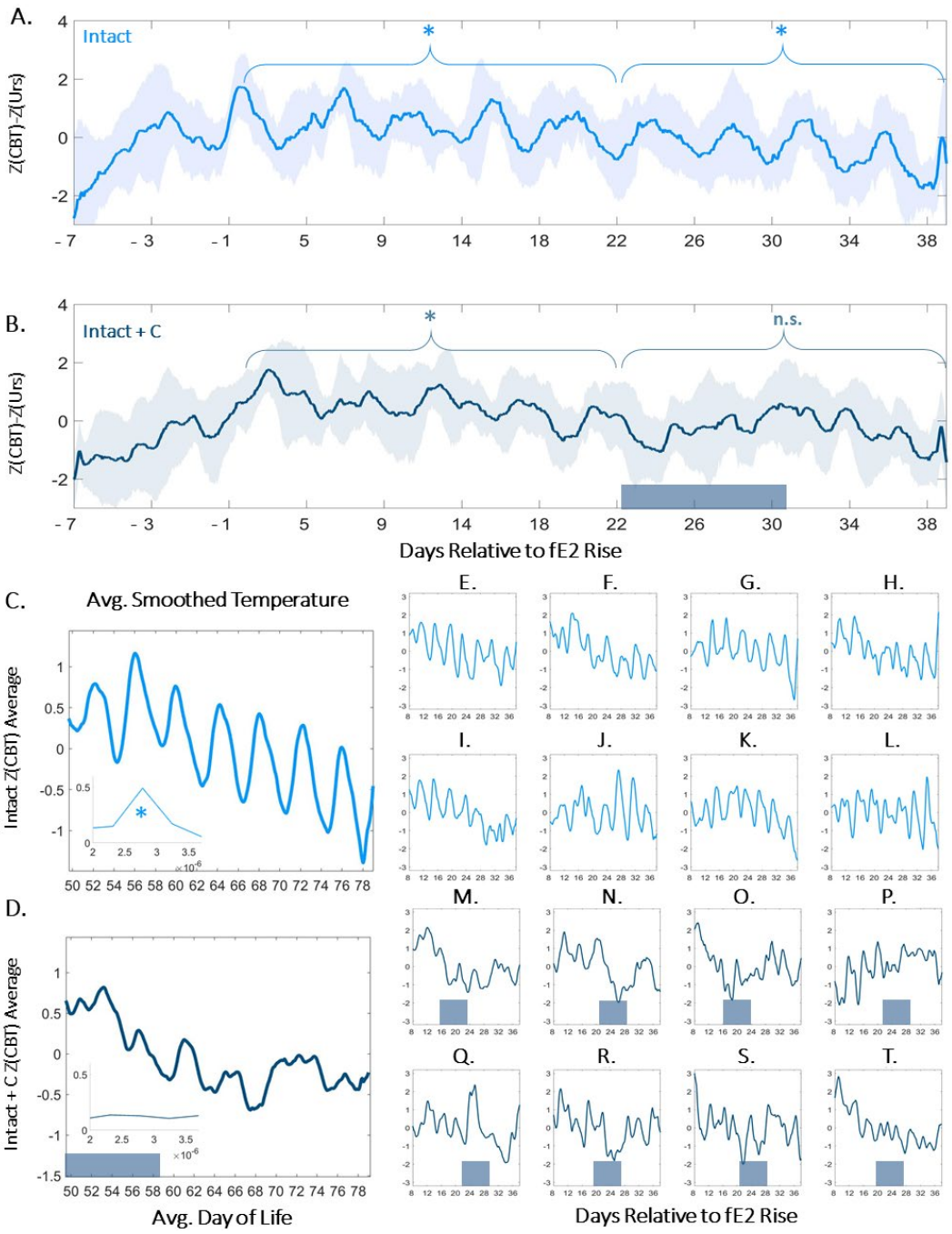


**Figure 3. Contraceptive Administration in Adolescence Persistently Perturbs 4-Day Temperature Rhythms.** Normalized CBT mean (± S.E.M.) minus UR power relative to within-individual first day of fE2 rise in Intact (A) and Intact+C (B) rats (see: Methods and Supplemental Figure 3). Dark bars along the x-axis for Intact+C animals indicate average time of contraceptive administration relative to fE2 rise. * Indicates regions of time over which every 4$^{th}$ day's CBT values are significantly elevated compared to other days of cycle ($p<0.003$). Twenty-four hour smoothed average plots of normalized linear CBT in Intact (C) and Intact+C (D) individuals from the time of contraceptive administration illustrate a reduction in regularity of oscillations. Insets show FFT centered at 4 to 5 days. * Indicates significantly higher AUCs in the 4 to 5 day range for Intact (panel C) compared to Intact+C rats (panel D). Individual animals (E-T) comprising Intact (light blue) and Intact+C (dark blue) groups prior to and following hormonal contraceptive administration. Dark bars along horizontal axes indicate time of contraceptive administration; administration days differ based on an individual's day of fE2 rise.

CBT Increased in Early to Mid-Adolescence. As growth and metabolism speed in adolescence, we hypothesized that CBT would also increase during the period of most rapid growth, pre to mid puberty. Pre to mid puberty (p26-41) was associated with a significant positive trend in CBT in Intact ($p=5.75*10^{-5}$ ) and Intact+C animals prior to contraceptive administration ($p=1.20*10^{-4}$; **Figure 4A-B**). Notably, implantation of the silastic capsule in OVX and OVX+E2 animals resulted in a transient (one day) increase in CBT (OVX p=0.01, OVX+E2 p=0.03; **Figure 4C-D, Supplemental Figure 5**). This surgical-recovery-associated rise was highly variable and did not differ between OVX and OVX+E2 animals (p=0.65; **Supplemental Figure 5**). Interestingly, the early pubertal CBT increase did not require E2, as OVX animals also exhibited a significant positive trend (p=0.034; **Figure 4C,E**). For a summary guide to CBT features that may be useful for Intact pubertal staging, see **Supplemental Figure 6**).

CBT Maintenance in Late Adolescence to Adulthood Required Estradiol. Complex interactions exist between metabolism, growth, and E2 level during adolescence. As estrogen deficiency in puberty is associated with weight gain and reduced metabolism, we investigated if maintenance of elevated temperature would be impacted by hormonal status. The maintenance of increased temperature in late puberty and adulthood was E2-dependent, with OVX animals exhibiting a significant downward trend in CBT from mid to late puberty (p58-p74; p=0.01) relative to Intact and OVX+E2 animals (p>0.05 in each case; **Figure 4C-D**). E2 treatment in the OVX+E2 group prevented intra-individual CBT decline in late puberty; correspondingly, temperatures in the OVX but not OVX + E2 groups were lower than that of Intact animals (late puberty to early adulthood $\chi^2=62.8$ $p=1.46*10^{-13}$, $p=4*10^{-4}$ for Intact vs. OVX, p=0.16 for Intact vs. OVX+ E2; **Figure 4F-G, Supplemental Figure 5**).

Contraceptive Administration Longitudinally Depressed CBT. CBT power did not exhibit a positive or negative trend from mid puberty through early adulthood (p42 to p58) in Intact animals (p=0.12), but exhibited a significant downward trend in Intact+C animals during the period of contraceptive administration (p=0.028; **Figure 4A-B**), resulting in a trend toward depressed temperatures following administration in mid to late adolescence ($\chi^2=21.84$ $p=7.04*10^{-05}$, p=0.1 for Intact vs. Intact+C) that persisted into early adulthood ($\chi^2=62.83$ $p=1.46*10^{-13}$, p=0.1 for Intact vs. Intact+C; **Figure 4B, 4F-G**).

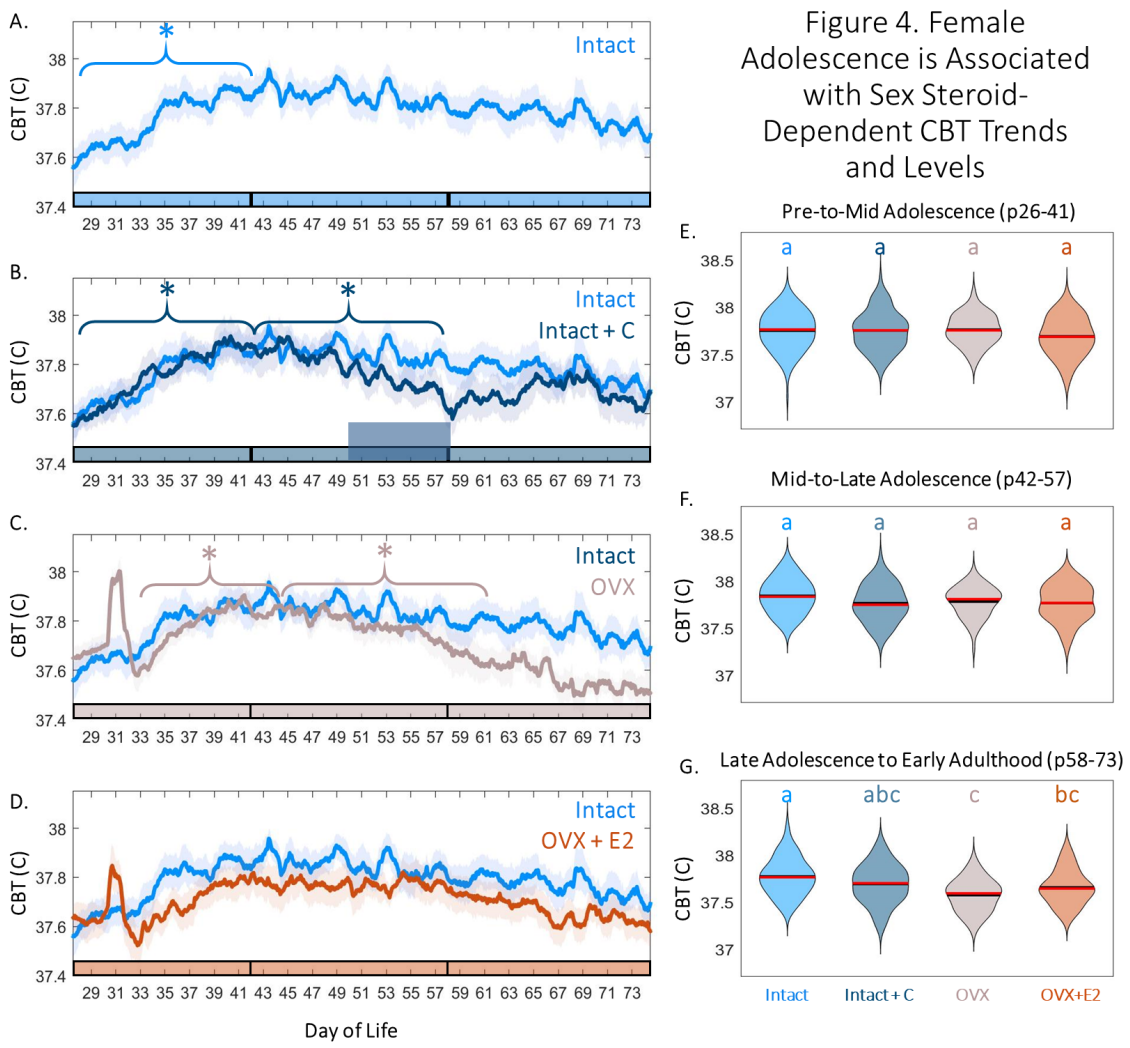


**Figure 4. Female Adolescence is Associated with Sex Steroid-Dependent CBT Levels and Trends.** CBT linear group means (± S.E.M.) in Intact (A, light blue) compared to Intact+C (B, dark blue), OVX + sham (C, gray), and OVX+E2 (D, orange) animals. * Indicates significant trend during the bracketed time period for the group matching the color of the bracket ($p<0.03$). Phase of adolescence time periods (pre to mid, mid to late, and late to adult) are indicated by breaks in the colored x-axis at p42 and p58. Time of hormonal contraceptive administration in panel B is indicated by the tall horizontal bar. Violin plots of temperature for all groups at early to mid-adolescence (E), mid to late adolescence (F), and early adulthood (G) indicate that hormonal contraceptive administration leads to reductions in CBT relative to controls after administration. Ovariectomy, even with E2 replacement, is also associated with significantly reduced temperatures by early adulthood (G). Color of letters at the top in E-G indicate experimental group. Letters indicate statistical differences, with groups of different letters being significantly different ($p<0.001$).

## 2.5 Discussion and Conclusions

Adolescent Development and Estradiol Dependence of CBT Rhythmicity. Female adolescence is characterized by stereotyped development of CBT rhythms at the ultradian, circadian, and ovulatory timescales. The present findings reveal that early adolescence in the female rat is marked by rising CBT and CBT circadian power, and commencement of 4-day cycling in CBT and CBT URs. These early circadian and ultradian changes likely reflect maturation of the reproductive axis, as 1) the rate of CR power rise was hastened by estradiol, 2) the commencement of 4-day temperature cycling was preceded by a rise in fE2, and 3) CBT CR power was correlated with fE2 concentration[65,149]. These observations confirm and extend reports of early pubertal development of ultradian-circadian-ovulatory interactions[46 47], and suggest that reproductive-thermoregulatory coupling may develop prior to, or in tandem with, pubertal onset.

Adolescent increases in UR amplitude for many endocrine outputs are well-documented, but UR structure across all of puberty is not well mapped[28,65]. However, from the time of rise in fE2 (a defining marker of pubertal onset), CBT UR power retained the same mean value but commenced a 4-day, ovulatory cycle-associated pattern. Four day cycles in URs are consistent with data collected on URs in adult rodents[10,147,148] and humans (at a longer time scale)[139]. Four-day patterning was not present in ovariectomized or E2-replaced animals, consistent with dependence on the ovarian cycle. These results support that URs in CBT achieve adult amplitude and stability early in life, prior to maturity of CRs[150–152], and that interactions among thermoregulatory and reproductive circuits permitting rapid *ultradian* coupling are established well before pubertal onset.

Additionally, the present findings suggest that some dynamics of CBT development require specific patterns of E2 rather than simply concentrations above a particular threshold. Ovariectomy eliminated ORs, increased weight, reduced CR power, rate of CR power rise, and correlation between CR power and fE2, and overall temperature[153,154]. E2 replacement partially rescued circadian metrics and reduced weight but did not recapitulate ORs. Short-term exposure to contraceptives in late adolescence longitudinally altered CBT metrics by reducing temperature and CR power, and abolishing ORs in CBT and UR power. Despite the apparently early maturation of substrate for thermoregulatory and reproductive coupling, the impact of E2 replacement and the enduring effects of short-term contraceptives suggest that these systems are sensitive to both level and patterning of reproductive hormones across the adolescent period.

Together, temperature amplitude and oscillation stability at the UR, CR, and OR timescales are modulated across the adolescent transition and are influenced by endogenous and exogenous E2. CBT URs mature to their adult amplitude and stability prior to CRs, and ORs and are rapidly modulated by ovulatory phase in intact animals (See Supplemental Figure 6). Conversely, CRs increase in magnitude and stability in early adolescence, are not significantly impacted by the phase of OR, and are impacted by ovariectomy. These results support the notion that ultradian and ovulatory systems are tightly coupled and reflected in CBT, and that circadian effects on the ovulatory cycle may be unidirectional[22,139]. Ovariectomy, E2 replacement, and pubertal contraceptive administration have a number of effects on rhythmic dynamics at each timescale,

overall indicating that 'intact' dynamics are not easily recapitulated and that exogenous sex steroids can have enduring impact.

Limitations. The ovulatory cycle of the female rat differs from that of humans, in that rats do not exhibit prolonged elevation of progesterone in the absence of pregnancy or pseudopregnancy[155]. This lack of a true luteal phase means that post-ovulatory temperature elevation in the rat follows a more compressed trajectory than in humans[156]. Therefore, exposure to estrogen and progesterone analogs in rats for prolonged periods may be associated with a different phenotype in rats than in humans[157]. Finally, the laboratory environment imposes artificially stable environmental conditions on animals; recapitulation of these patterns under naturalistic conditions in future experiments will strengthen the translational potential of this work.

Considerations of Rhythmicity Perturbation Through Adolescent Contraceptive Use. Although rats cannot fully model human biology, it was notable that contraceptive administration imposed lasting structural changes on CBT rhythmicity and its relationship with E2. Levonorgestrel and EE2 administration abolished the 4-day modulation of fE2, UR power, and temperature level, eliminated the correlation between CR power and fE2, and significantly depressed CR power. As these changes required continuous monitoring to detect and occurred in the absence of significant group changes to fE2 level, it is not unreasonable to speculate that studies of less frequently timed samples, or samples averaged across individuals, could make similar disruptions in humans difficult to detect.

Perturbation of body temperature rhythms is associated with diverse health insults across species, both reflecting perturbation in underlying systems and potentially acting as a causative agent. Circadian disruption to CBT rhythms occurs in, and is proportional to, severity of jetlag[158], depression[159], sepsis severity[160,161], post-traumatic injury[162], cognitive decline[163], and has even been proposed as a root cause of disease dubbed "Circadian Syndrome"[164] . Disruption to ovulatory temperature rhythms occurs in anovulatory and atypical luteal phase cycles[165–167], including those arising from polycystic ovarian syndrome (PCOS)[168]. The impact of ultradian rhythmic disruption of the reproductive axis requires additional study[169–171], but existing work in other hormonal systems suggests that preservation of pulsatility in drug delivery (e.g., of cortisol in Addison's disease or insulin in diabetes) can lead to better patient outcomes when compared to conventional non-rhythmic treatment[66,67,104,172,173]. It is likely that disruption of URs may result in negative impact analogous to disruption at longer timescales. It may appear counter-intuitive that thermoregulation could be both a reporter for such diverse maladies and a potential mediator for disease progression. However, temperature rhythm disruption is associated with a wide range of temporal, inflammatory, and endocrine insults, in part, because thermoregulatory circuits are directly impacted by the master clock, and modulated by inflammatory factors, autonomic status, and a variety of endocrine factors including estradiol[8,174] and progesterone[7]. Lastly, CBT itself acts as a synchronizing cue for peripheral circadian oscillators[175]. Further research is needed to disentangle if disruption of CBT rhythmicity itself causes harm, or if CBT rhythms are merely reporting perturbations in underlying systems (e.g., sex hormones or metabolic factors).

Our observations suggest that a non-physiological pattern of contraceptive administration may act as 'hormonal jetlag'. The degree of lasting impact to other systems that rely on temperature as an entraining stimulus, or disrupted systems reported indirectly by temperature (e.g., SCN, endocrine, autonomic) remain to be assessed. Furthermore, the extent to which such disruptive effects differ among species[157], contraceptive agents, administration methods, or between adolescent populations and adults requires further investigation. Encouragingly, the observation that rodents and humans exhibit similar CBT patterning during the peri-ovulatory period[10,139,140] points to potential translational relevance.

Together, despite established societal benefits of widely available hormonal contraception[176], especially in individuals experiencing hormonal irregularities[177], the present findings suggest that administration of exogenous estrogens and progestins during adolescence leads to persistent rhythmic disruption across timescales. Future research is needed to determine if rhythmic patterns of sex steroid administration more closely mimicking endogenous release, analogous to those implemented in cortisol[67] and closed loop insulin therapy[178], can minimize rhythmic disruption. Conversely, future studies that validate an "updated" symptom-thermal method using signal processing of continuous CBT data may provide feasible, non-disruptive alternatives for contraception[106,139,179–181]. Contraceptive administration to adolescent girls is on the rise[74], and there are a paucity of data on the impact of chronic hormonal perturbation on endogenous rhythmicity, or if such disruptions during the sensitive window of adolescence have lasting effects[93,94,101,182,183]. Further research is needed to characterize the impact of adolescent hormonal contraceptive use so that further improvements can be made, individuals at-risk for side effects can be identified, and informed decisions about hormonal contraceptive use can be made.

Utility of CBT for Monitoring Pubertal Development in Rodents and Potential Translational Relevance. Continuous monitoring of CBT may have great utility for passive detection of pubertal milestones in rodents in preclinical research. Existing methods for pubertal staging in rodents carry considerable downsides: frequent blood sampling and vaginal lavage[184] are repeatedly invasive, and fecal hormone analysis is time consuming and costly[124,185]. Moreover, our results indicate that individual rats do not traverse identical pubertal trajectories by day of life, and that this assumption could lead to considerable errors in staging. Conversely, signal processing of passively collected CBT can add temporal resolution, greater quantitative power, and limit repeated invasive procedures for staging puberty[186].

In human subjects, continuous temperature monitoring via wearables may similarly facilitate the study of pubertal development. The signal characteristics of rat CBT exhibit remarkable similarities to human peripheral temperature (See:[61,148,187] ). Monitoring human peripheral temperature during adolescence could serve broad purposes – from personalizing health education based on self-collected data[188,189], to adapting teaching style to an individual's developmental phase[190–193], to enabling research into the impact of teen contraceptive use[194,195] or the process of gender transition[196,197]. Together, pubertal monitoring via continuous body temperature is worthy of further investigation in both animal models and human subject populations for its potential utility to individuals, researchers, families, and clinicians.

Conclusions. In conclusion, body temperature monitoring provides a window into the development of biological rhythms in puberty over multiple timescales. These rhythms may serve

as convenient and high temporal resolution indicators of developmental stage and trajectory for application in research and clinical studies. Our study of body temperature also reveals unintended side effects of tonic hormonal manipulations. We anticipate that these findings will inform creative improvements to female reproductive research and healthcare.

2.6 Acknowledgements The authors would like to thank Andrew Ahn, Ronald Dahl, Frédéric Theunissen, and Albert Qü for their helpful feedback on study design and methods and invaluable comments and suggestions on an earlier version of this manuscript.

## 2.7 Supplemental Figures

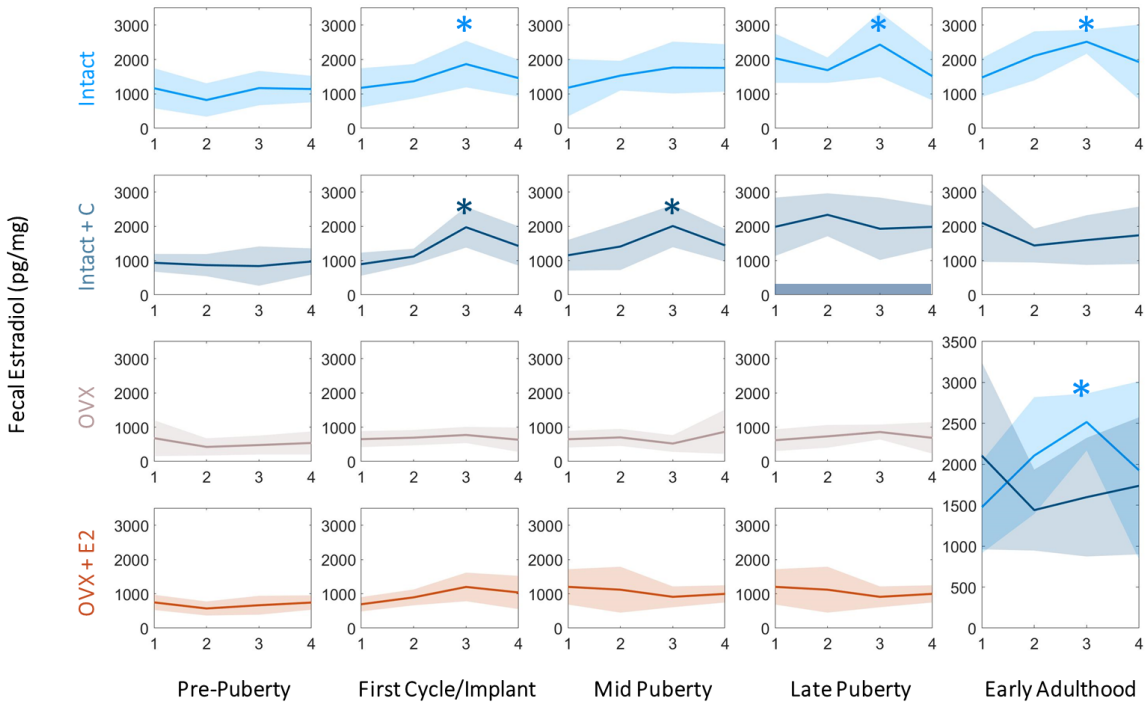


**Supplemental Figure 1. Estradiol Group Averages from Pre-Puberty to Adulthood Post-Contraception: Contraceptives Longitudinally Alter the Pattern but Not Level of Fecal Estradiol.** Pre-puberty (p24 to p30), early puberty (p30 to p37), mid puberty (p43 to p49), late puberty (p55 to p61) and early adulthood (p69 to p76) in Intact (A), Intact+C (B), OVX (C) and OVX+E2 (D). Early adulthood post-contraceptive administration, captured only in Intact and Intact+C animals, are overlaid in (E), illustrating persistent perturbation of estrous-cycle estradiol patterning. Dark bar indicates samples were collected during contraceptive administration in Intact+C animals. * Indicates significant elevation of day 3 compared to day 1 ($p<0.05$).

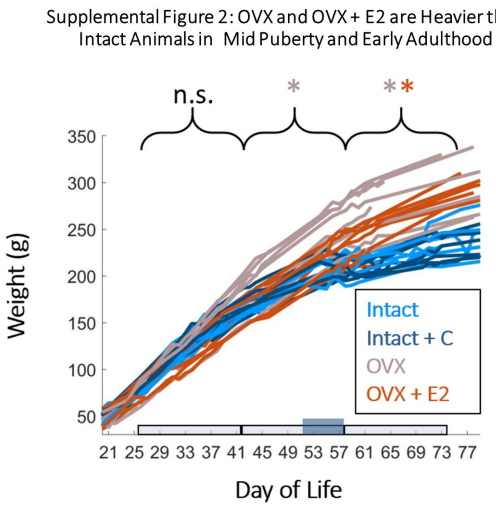


**Supplemental Figure 2. OVX and OVX + E2 are Heavier than Intact Animals in Mid Puberty and Early Adulthood.** Prepubertal OVX did not significantly impact weight gain before mid-puberty. OVX animals (gray) are significantly heavier than all other groups at mid-puberty. OVX animals remain significantly heavier into adulthood. In early adulthood, OVX+E2 animals (orange) are not different from OVX animals and are significantly heavier than either Intact (light blue) or Intact+C animals (dark blue). Colors of * Indicate groups that are significantly heavier ($p<0.05$).

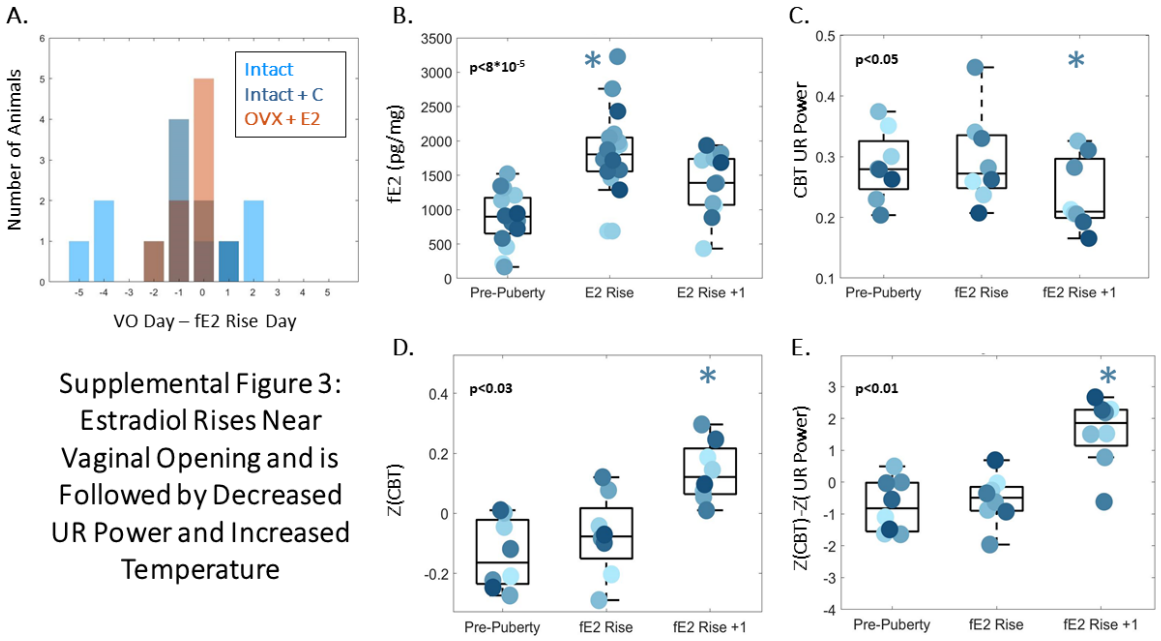


Supplemental Figure 3: Estradiol Rises Near Vaginal Opening and is Followed by Decreased UR Power and Increased Temperature

**Supplemental Figure 3. Day of First Estradiol Rise Occurs Near Vaginal Opening and Coincides with Markers of Estrus.** Subsequent Drop in UR Power and Rise in CBT. Estradiol has a unique day in proximity to, but distinct from, vaginal opening, during which fE2 rises > 2 Standard Deviations within an individual (A-B). Alignment to this day as a proxy for puberty onset provides a convenient point from which to average across animals to permit easy visualization of the estrous cycle. Daily mean UR power decreases significantly following this day (C), and daily mean CBT rises significantly following this day (D), The difference between these two metrics exaggerates the difference, and the differences across subsequent cycles (E). After this point, all three metrics commence the 4-day estrous pattern. * Indicates significant difference from all other time periods.

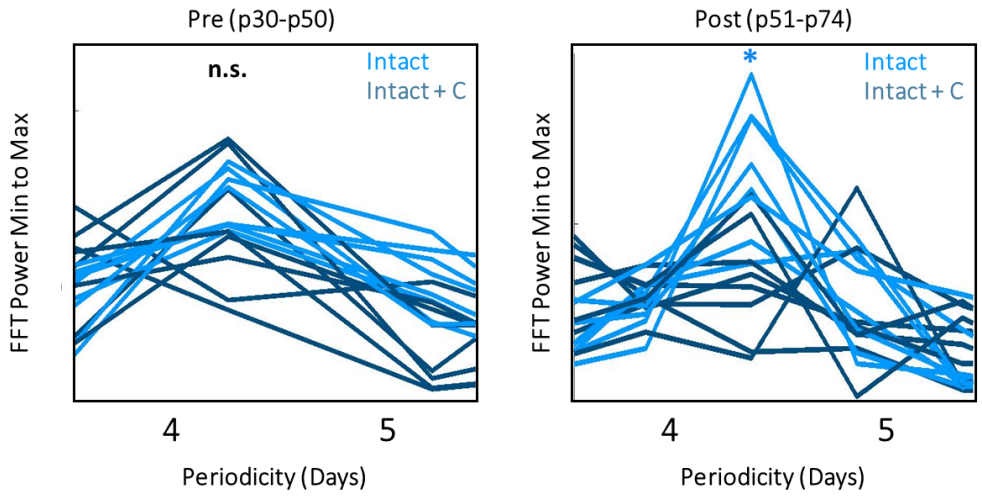


**Supplemental Figure 4. FFT Power of Intact Temperature Across Life Peaks Unique at 4 Days and is Disrupted During and After Contraceptive Administration.** Fast Fourier Transform of Each Individual's CBT Log in Intact (light blue) and Intact + BC (dark blue) prior to contraceptive administration (left), and during and after contraceptive administration (right). * Indicates significant difference for AUC between the groups in 4-5 periodicity.

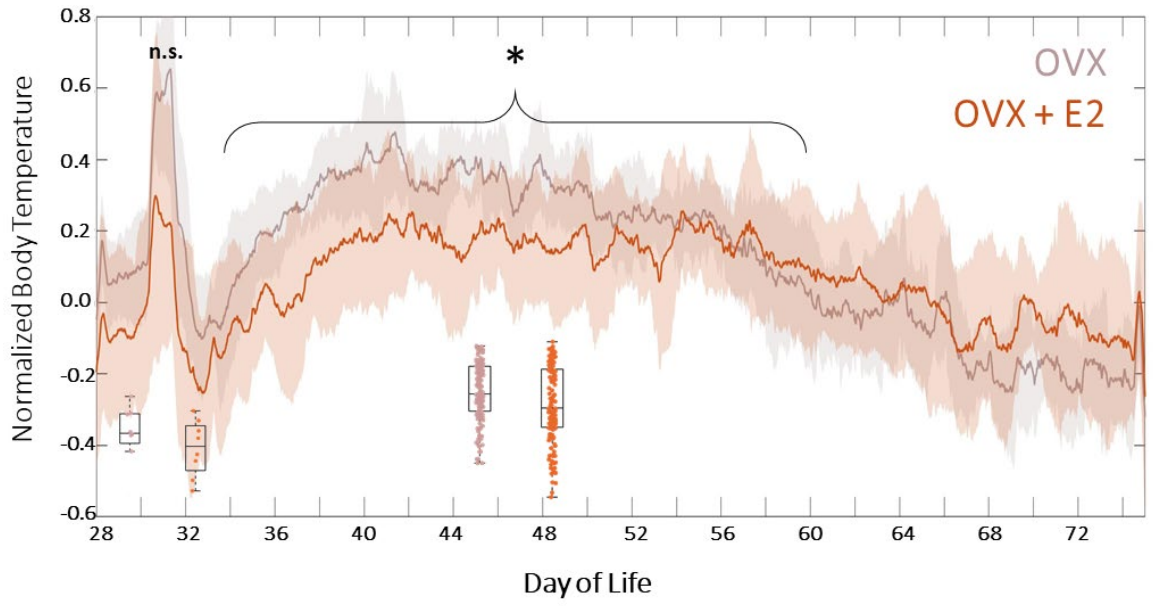


**Supplemental Figure 5. Estradiol Administration in Ovariectomized Animals is Associated with Lower Temperatures Across Adolescence.** Core CBT linear group means (± standard deviation) in OVX (gray) and OVX+E2 animals from p28-p72. Box plots indicate values used in KW comparisons between groups during silastic implant recovery (left) and across adolescence (right) with independent y-axes. * Indicates significant difference between groups during the marked time period ($p<0.03$).

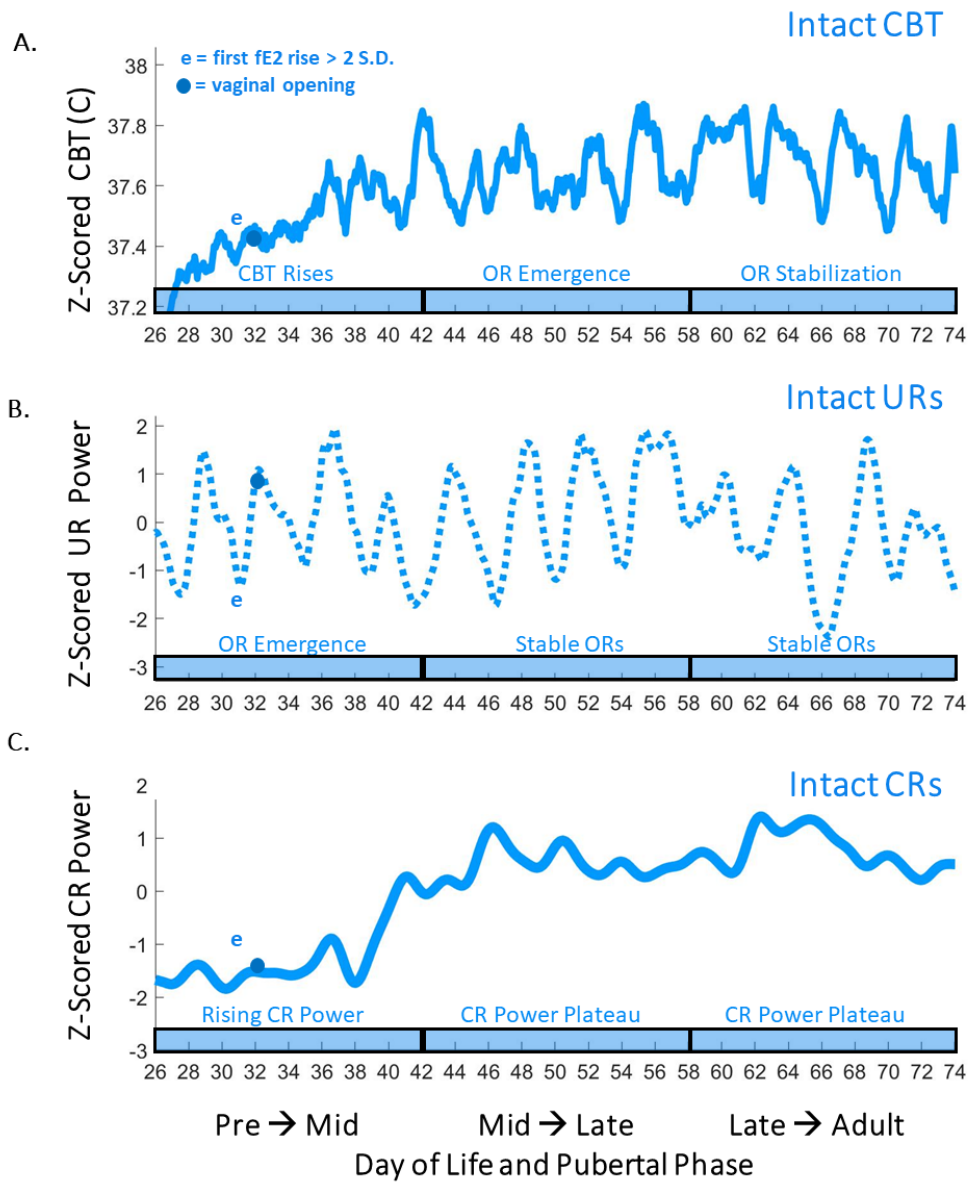


**Supplemental Figure 6: Summary of CBT Feature Use for Pubertal Staging in an Intact Female.** Features of CBT and CBT rhythmicity can be used to complement and extend hormonal and external markers of adolescence. Here, we illustrate derived features on an example Intact female from p26 to p74, with fE2 rise and vaginal opening occurring on p31 and p32, respectively. Dots indicate vaginal opening and "e" indicates first rise of fE2 > 2 standard deviations. Rising CBT, emergence of ORs in UR power, and Rising CR power can be used to characterize pubertal onset. Mid to late adolescence is characterized by a plateau of CR power, as well as the emergence of ORs in raw CBT their persistence in UR power. Post-natal day 60 did not correspond with any overt transitions in CBT or CBT metrics.

## 2.8 References


1. Jain Gupta, N. & Khare, A. Disruption in daily eating-fasting and activity-rest cycles in Indian adolescents attending school. *PloS One* **15**, e0227002 (2020).
2. Pereira, L. R. *et al.* Biological Rhythm Disruption Associated with Obesity in School Children. *Child. Obes. Print* **15**, 200–205 (2019).
3. Smarr, B. L. & Schirmer, A. E. 3.4 million real-world learning management system logins reveal the majority of students experience social jet lag correlated with decreased performance. *Sci. Rep.* **8**, 4793 (2018).
4. Mohr, M. A. & Sisk, C. L. Pubertally born neurons and glia are functionally integrated into limbic and hypothalamic circuits of the male Syrian hamster. *Proc. Natl. Acad. Sci.* **110**, 4792–4797 (2013).
5. Sisk, C. L. & Foster, D. L. The neural basis of puberty and adolescence. *Nat. Neurosci.* **7**, 1040–1047 (2004).
6. Grant, A. D., Wilsterman, K., Smarr, B. L. & Kriegsfeld, L. J. Evidence for a Coupled Oscillator Model of Endocrine Ultradian Rhythms. *J. Biol. Rhythms* **33**, 475–496 (2018).
7. Forman, R. G., Chapman, M. C. & Steptoe, P. C. The effect of endogenous progesterone on basal body temperature in stimulated ovarian cycles. *Hum. Reprod. Oxf. Engl.* **2**, 631–634 (1987).
8. Williams, H., Dacks, P. A. & Rance, N. E. An Improved Method for Recording Tail Skin Temperature in the Rat Reveals Changes During the Estrous Cycle and Effects of Ovarian Steroids. *Endocrinology* **151**, 5389–5394 (2010).
9. Smarr, B. L., Zucker, I. & Kriegsfeld, L. J. Detection of Successful and Unsuccessful Pregnancies in Mice within Hours of Pairing through Frequency Analysis of High Temporal Resolution Core Body Temperature Data. *PloS One* **11**, e0160127 (2016).
10. Smarr, B. L., Grant, A. D., Zucker, I., Prendergast, B. J. & Kriegsfeld, L. J. Sex differences in variability across timescales in BALB/c mice. *Biol. Sex Differ.* **8**, 7 (2017).
11. Bourguignon, J. P. Time-related neuroendocrine manifestations of puberty: a combined clinical and experimental approach extracted from the 4th Belgian Endocrine Society lecture. *Horm. Res.* **30**, 224–234 (1988).
12. MacKinnon, P. C. B., Puig-Duran, E. & Laynes, R. Reflections on the attainment of puberty in the rat: have circadian signals a role to play in its onset? *Reproduction* **52**, 401–412 (1978).
13. Garcia, J., Rosen, G. & Mahowald, M. Circadian rhythms and circadian rhythm disorders in children and adolescents. *Semin. Pediatr. Neurol.* **8**, 229–240 (2001).
14. Vidal, J. D. The Impact of Age on the Female Reproductive System. *Toxicol. Pathol.* **45**, 206–215 (2017).
15. Brodsky, V. Y. & Lloyd, D. Self-Organized Intracellular Ultradian Rhythms Provide Direct Cell-Cell Communication. in *Ultradian Rhythms from Molecules to Mind: A New Vision of Life* (eds. Lloyd, D. & Rossi, E. L.) 85–104 (Springer Netherlands, 2008). doi:10.1007/978-1-4020-8352-5_3.
16. Lloyd, D. & Stupfel, M. The occurrence and functions of ultradian rhythms. *Biol. Rev. Camb. Philos. Soc.* **66**, 275–299 (1991).
17. Walker, J. J. *et al.* Encoding and Decoding Mechanisms of Pulsatile Hormone Secretion. *J. Neuroendocrinol.* **22**, 1226–1238 (2010).

18. Panda, S. Circadian physiology of metabolism. *Science* **354**, 1008–1015 (2016).
19. The Mammalian Circadian Timing System: Organization and Coordination of Central and Peripheral Clocks. *Annu. Rev. Physiol.* **72**, 517–549 (2010).
20. Carlson, L. J. & Shaw, N. D. Development of Ovulatory Menstrual Cycles in Adolescent Girls. *J. Pediatr. Adolesc. Gynecol.* **32**, 249–253 (2019).
21. Backstrom, C., McNeilly, A. S., Leask, R. & Baird, D. Pulsatile secretion of LH, FSH, Prolactin, oestradiol, and progesterone during the human menstrual cycle. *Clin. Endocrinol. (Oxf.)* **17**, 29–42 (1982).
22. Shechter, A. & Boivin, D. B. Sleep, Hormones, and Circadian Rhythms throughout the Menstrual Cycle in Healthy Women and Women with Premenstrual Dysphoric Disorder. *Int. J. Endocrinol.* **2010**, e259345 (2010).
23. Goh, G. H., Maloney, S. K., Mark, P. J. & Blache, D. Episodic Ultradian Events—Ultradian Rhythms. *Biology* **8**, 15 (2019).
24. Shannahoff-Khalsa, D. S., Kennedy, B., Yates, F. E. & Ziegler, M. G. Ultradian rhythms of autonomic, cardiovascular, and neuroendocrine systems are related in humans. *Am. J. Physiol.* **270**, R873-887 (1996).
25. Brodsky, V. Y. Circahoralian (Ultradian) metabolic rhythms. *Biochem. Mosc.* **79**, 483–495 (2014).
26. Brandenberger, G., Simon, C. & Follenius, M. Ultradian endocrine rhythms: A multioscillatory system. *J. Interdiscip. Cycle Res.* **18**, 307–315 (1987).
27. Ojeda, S. R., Urbanski, H. F. & Ahmed, C. E. The Onset of Female Puberty: Studies in the Rat. in *Proceedings of the 1985 Laurentian Hormone Conference* (ed. Greep, R. O.) vol. 42 385–442 (Academic Press, 1986).
28. Dunger, D. B., Matthews, D. R., Edge, J. A., Jones, J. & Preece, M. A. Evidence for temporal coupling of growth hormone, prolactin, LH and FSH pulsatility overnight during normal puberty. *J. Endocrinol.* **130**, 141–149 (1991).
29. Albertsson-Wikland, K. *et al.* Twenty-Four-Hour Profiles of Luteinizing Hormone, Follicle-Stimulating Hormone, Testosterone, and Estradiol Levels: A Semilongitudinal Study throughout Puberty in Healthy Boys. *J. Clin. Endocrinol. Metab.* **82**, 541–549 (1997).
30. Apter, D. Development of the hypothalamic-pituitary-ovarian axis. *Ann. N. Y. Acad. Sci.* **816**, 9–21 (1997).
31. Jenner, M. R., Kelch, R. P., Kaplan, S. L. & Grumbach, M. M. Hormonal Changes in Puberty: IV. Plasma Estradiol, LH, and FSH in Prepubertal Children, Pubertal Females, and in Precocious Puberty, Premature Thelarche, Hypogonadism, and in a Child with a Feminizing Ovarian Tumor. *J. Clin. Endocrinol. Metab.* **34**, 521–530 (1972).
32. Shaw, N. D. *et al.* Insights into Puberty: The Relationship between Sleep Stages and Pulsatile LH Secretion. *J. Clin. Endocrinol. Metab.* **97**, E2055–E2062 (2012).
33. Apter, D., Bützow, T., Laughlin, G. A. & Yen, S. S. Accelerated 24-hour luteinizing hormone pulsatile activity in adolescent girls with ovarian hyperandrogenism: relevance to the developmental phase of polycystic ovarian syndrome. *J. Clin. Endocrinol. Metab.* **79**, 119–125 (1994).
34. Ojeda, S. R. & Skinner, M. K. Puberty in the rat. *Knobil Neills Physiol. Reprod.* 2061–2126 (2006) doi:10.1016/B978-012515400-0/50043-9.

35. Dunger, D. B. *et al.* Pattern of secretion of bioactive and immunoreactive gonadotrophins in normal pubertal children. *Clin. Endocrinol. (Oxf.)* **35**, 267–275 (1991).
36. Refinetti, R. Circadian modulation of ultradian oscillation in the body temperature of the golden hamster. *J. Therm. Biol.* **19**, 269–275 (1994).
37. Ootsuka, Y. *et al.* Brown adipose tissue thermogenesis heats brain and body as part of the brain-coordinated ultradian basic rest-activity cycle. *Neuroscience* **164**, 849–861 (2009).
38. Prendergast, B. J. & Zucker, I. Ultradian rhythms in mammalian physiology and behavior. *Curr. Opin. Neurobiol.* **40**, 150–154 (2016).
39. Blum, I. D. *et al.* A highly tunable dopaminergic oscillator generates ultradian rhythms of behavioral arousal. *eLife* **3**, e05105 (2014).
40. Lehman, M. N., He, W., Coolen, L. M., Levine, J. E. & Goodman, R. L. Does the KNDy Model for the Control of Gonadotropin-Releasing Hormone Pulses Apply to Monkeys and Humans? *Semin. Reprod. Med.* **37**, 71–83 (2019).
41. Merkley, C. M. *et al.* KNDy (kisspeptin/neurokinin B/dynorphin) neurons are activated during both pulsatile and surge secretion of LH in the ewe. *Endocrinology* **153**, 5406–5414 (2012).
42. Merkley, C. M., Coolen, L. M., Goodman, R. L. & Lehman, M. N. Evidence for Changes in Numbers of Synaptic Inputs onto KNDy and GnRH Neurones during the Preovulatory LH Surge in the Ewe. *J. Neuroendocrinol.* **27**, 624–635 (2015).
43. Takahashi, J. S. Transcriptional architecture of the mammalian circadian clock. *Nat. Rev. Genet.* **18**, 164–179 (2017).
44. Hastings, M. H., Maywood, E. S. & Brancaccio, M. Generation of circadian rhythms in the suprachiasmatic nucleus. *Nat. Rev. Neurosci.* **19**, 453–469 (2018).
45. Hagenauer, M. H. *et al.* Changes in circadian rhythms during puberty in Rattus norvegicus: developmental time course and gonadal dependency. *Horm. Behav.* **60**, 46–57 (2011).
46. Mohr, M. A., DonCarlos, L. L. & Sisk, C. L. Inhibiting Production of New Brain Cells during Puberty or Adulthood Blunts the Hormonally Induced Surge of Luteinizing Hormone in Female Rats. *eNeuro* **4**, (2017).
47. Mohr, M. A., Wong, A. M., Tomm, R. J., Soma, K. K. & Micevych, P. E. Pubertal development of estradiol-induced hypothalamic progesterone synthesis. *Horm. Behav.* **111**, 110–113 (2019).
48. Kriegsfeld, L. J., Silver, R., Gore, A. C. & Crews, D. Vasoactive intestinal polypeptide contacts on gonadotropin-releasing hormone neurones increase following puberty in female rats. *J. Neuroendocrinol.* **14**, 685–690 (2002).
49. Duan, X. N. *et al.* [Developmental characteristics of circadian rhythms in hypothalamic-pituitary-adrenal axis during puberty]. *Zhonghua Liu Xing Bing Xue Za Zhi Zhonghua Liuxingbingxue Zazhi* **39**, 1086–1090 (2018).
50. Pronina, T. S., Orlova, N. I. & Rybakov, V. P. [Circadian rhythm of skin temperature of children during puberty]. *Fiziol. Cheloveka* **41**, 74–84 (2015).
51. Hummer, D. L. & Lee, T. M. Daily timing of the adolescent sleep phase: Insights from a cross-species comparison. *Neurosci. Biobehav. Rev.* **70**, 171–181 (2016).
52. Hagenauer, M. H. & Lee, T. M. The neuroendocrine control of the circadian system: adolescent chronotype. *Front. Neuroendocrinol.* **33**, 211–229 (2012).

53. Crowley, S. J., Cain, S. W., Burns, A. C., Acebo, C. & Carskadon, M. A. Increased Sensitivity of the Circadian System to Light in Early/Mid-Puberty. *J. Clin. Endocrinol. Metab.* **100**, 4067–4073 (2015).
54. Kim, S. H. *et al.* Progesterone-Mediated Inhibition of the GnRH Pulse Generator: Differential Sensitivity as a Function of Sleep Status. *J. Clin. Endocrinol. Metab.* **103**, 1112–1121 (2018).
55. Angelopoulou, E., Quignon, C., Kriegsfeld, L. J. & Simonneaux, V. Functional Implications of RFRP-3 in the Central Control of Daily and Seasonal Rhythms in Reproduction. *Front. Endocrinol.* **10**, (2019).
56. Ginther, O. J., Pinaffi, F. L. V., Khan, F. A., Duarte, L. F. & Beg, M. A. Circadian influence on the preovulatory LH surge, ovulation, and prolactin concentrations in heifers. *Theriogenology* **79**, 528–533 (2013).
57. Russo, K. A. *et al.* Circadian Control of the Female Reproductive Axis Through Gated Responsiveness of the RFRP-3 System to VIP Signaling. *Endocrinology* **156**, 2608–2618 (2015).
58. Piet, R., Fraissenon, A., Boehm, U. & Herbison, A. E. Estrogen Permits Vasopressin Signaling in Preoptic Kisspeptin Neurons in the Female Mouse. *J. Neurosci.* **35**, 6881–6892 (2015).
59. Gibson, E. M. *et al.* Alterations in RFamide-related peptide expression are coordinated with the preovulatory luteinizing hormone surge. *Endocrinology* **149**, 4958–4969 (2008).
60. Williams, W. P., Jarjisian, S. G., Mikkelsen, J. D. & Kriegsfeld, L. J. Circadian control of kisspeptin and a gated GnRH response mediate the preovulatory luteinizing hormone surge. *Endocrinology* **152**, 595–606 (2011).
61. Grant, A. D., Newman, M. & Kriegsfeld, L. J. Ultradian Rhythms in Heart Rate Variability and Distal Body Temperature Anticipate the Luteinizing Hormone Surge Onset. *bioRxiv* 2020.07.15.205450 (2020) doi:10.1101/2020.07.15.205450.
62. Brar, T. K., Singh, K. D. & Kumar, A. Effect of Different Phases of Menstrual Cycle on Heart Rate Variability (HRV). *J. Clin. Diagn. Res. JCDR* **9**, CC01-04 (2015).
63. Buxton, C. L. & Atkinson, W. B. Hormonal factors involved in the regulation of basal body temperature during the menstrual cycle and pregnancy. *J. Clin. Endocrinol. Metab.* **8**, 544–549 (1948).
64. Peña, A. S. *et al.* The majority of irregular menstrual cycles in adolescence are ovulatory: results of a prospective study. *Arch. Dis. Child.* **103**, 235–239 (2018).
65. Delemarre-Van De Waal, H. A., Wennink, J. M. & Odink, R. J. Gonadotrophin and growth hormone secretion throughout puberty. *Acta Paediatr. Scand. Suppl.* **372**, 26–31; discussion 32 (1991).
66. Lightman, S. L., Birnie, M. T. & Conway-Campbell, B. L. Dynamics of ACTH and Cortisol Secretion and Implications for Disease. *Endocr. Rev.* **41**, (2020).
67. Kalafatakis, K. *et al.* Ultradian rhythmicity of plasma cortisol is necessary for normal emotional and cognitive responses in man. *Proc. Natl. Acad. Sci. U. S. A.* **115**, E4091–E4100 (2018).
68. Casper, R. F. & Gladanac, B. Introduction: circadian rhythm and its disruption: impact on reproductive function. *Fertil. Steril.* **102**, 319–320 (2014).
69. Wang, F. *et al.* Association between circadian rhythm disruption and polycystic ovary syndrome. *Fertil. Steril.* (2020) doi:10.1016/j.fertnstert.2020.08.1425.

70. Gibson, E. M., Wang, C., Tjho, S., Khattar, N. & Kriegsfeld, L. J. Experimental 'jet lag' inhibits adult neurogenesis and produces long-term cognitive deficits in female hamsters. *PloS One* **5**, e15267 (2010).
71. Gotlieb, N., Moeller, J. & Kriegsfeld, L. J. Circadian Control of Neuroendocrine Function: Implications for Health and Disease. *Curr. Opin. Physiol.* **5**, 133–140 (2018).
72. Logan, R. W. *et al.* Impact of Sleep and Circadian Rhythms on Addiction Vulnerability in Adolescents. *Biol. Psychiatry* **83**, 987–996 (2018).
73. Carskadon, M. A. *et al.* Pubertal changes in daytime sleepiness. 1980. *Sleep* **25**, 453–460 (2002).
74. Birth Control Pill Use - Child Trends. https://www.childtrends.org/indicators/birth-control-pill-use.
75. Products - Data Briefs - Number 327 - December 2018. https://www.cdc.gov/nchs/products/databriefs/db327.htm (2019).
76. Apter, D. Contraception options: Aspects unique to adolescent and young adult. *Best Pract. Res. Clin. Obstet. Gynaecol.* **48**, 115–127 (2018).
77. Adeyemi-Fowode, O. A., Santos, X. M., Dietrich, J. E. & Srivaths, L. Levonorgestrel-Releasing Intrauterine Device Use in Female Adolescents with Heavy Menstrual Bleeding and Bleeding Disorders: Single Institution Review. *J. Pediatr. Adolesc. Gynecol.* **30**, 479–483 (2017).
78. Mwanthi, M. & Zaenglein, A. L. Update in the management of acne in adolescence. *Curr. Opin. Pediatr.* **30**, 492–498 (2018).
79. Knobil and Neill's Physiology of Reproduction - 4th Edition. https://www.elsevier.com/books/knobil-and-neills-physiology-of-reproduction/plant/978-0-12-397175-3.
80. Gemzell-Danielsson, K. Mechanism of action of emergency contraception. *Contraception* **82**, 404–409 (2010).
81. Li, C. *et al.* Effects of Levonorgestrel and progesterone on Oviductal physiology in mammals. *Reprod. Biol. Endocrinol. RBE* **16**, 59 (2018).
82. Nowaczyk-Dura, G. & Czekaj, P. Effects of ethinylestradiol and levonorgestrel on morphology, ultrastructure and histoenzymatic activity of rat kidney. *Physiol. Res.* **47**, 241–251 (1998).
83. Krishnan, S. & Kiley, J. The lowest-dose, extended-cycle combined oral contraceptive pill with continuous ethinyl estradiol in the United States: a review of the literature on ethinyl estradiol 20 μg/levonorgestrel 100 μg + ethinyl estradiol 10 μg. *Int. J. Womens Health* **2**, 235–239 (2010).
84. Strom, J. O., Theodorsson, E., Holm, L. & Theodorsson, A. Different methods for administering 17β-estradiol to ovariectomized rats result in opposite effects on ischemic brain damage. *BMC Neurosci.* **11**, 39 (2010).
85. Zhou, X., Shao, Q., Han, X., Weng, L. & Sang, G. Pharmacokinetics of medroxyprogesterone acetate after single and multiple injection of cyclofem® in Chinese women. *Contraception* **57**, 405–411 (1998).
86. Naqvi, R. H., Mitra, S. B., Saksena, I. F. & Lindberg, M. C. Pharmacokinetics of levonorgestrel in the rat. *Contraception* **30**, 81–88 (1984).
87. Lucaccioni, L. *et al.* Endocrine-Disrupting Chemicals and Their Effects during Female Puberty: A Review of Current Evidence. *Int. J. Mol. Sci.* **21**, (2020).

88. Landersoe, S. K. *et al.* Ovarian reserve markers in women using various hormonal contraceptives. *Eur. J. Contracept. Reprod. Health Care* **25**, 65–71 (2020).
89. Baker, F. C., Mitchell, D. & Driver, H. S. Oral contraceptives alter sleep and raise body temperature in young women. *Pflugers Arch.* **442**, 729–737 (2001).
90. Obruca, A. *et al.* Ovarian function during and after treatment with the new progestagen Org 30659. *Fertil. Steril.* **76**, 108–115 (2001).
91. Lopez, L. M. *et al.* Progestin-only contraceptives: effects on weight. *Cochrane Database Syst. Rev.* CD008815 (2016) doi:10.1002/14651858.CD008815.pub4.
92. Okunola, T. O., Bola-Oyebamiji, S. B. & Sowemimo, O. Comparison of weight gain between levonorgestrel and etonogestrel implants after 12 months of insertion. *Int. J. Gynaecol. Obstet. Off. Organ Int. Fed. Gynaecol. Obstet.* **147**, 54–58 (2019).
93. Skovlund, C. W., Mørch, L. S., Kessing, L. V., Lange, T. & Lidegaard, Ø. Association of Hormonal Contraception With Suicide Attempts and Suicides. *Am. J. Psychiatry* **175**, 336–342 (2018).
94. Skovlund, C. W., Mørch, L. S., Kessing, L. V. & Lidegaard, Ø. Association of Hormonal Contraception With Depression. *JAMA Psychiatry* **73**, 1154–1162 (2016).
95. Fruzzetti, F. & Fidecicchi, T. Hormonal Contraception and Depression: Updated Evidence and Implications in Clinical Practice. *Clin. Drug Investig.* **40**, 1097–1106 (2020).
96. Gnoth, C., Frank-Herrmann, P., Schmoll, A., Godehardt, E. & Freundl, G. Cycle characteristics after discontinuation of oral contraceptives. *Gynecol. Endocrinol. Off. J. Int. Soc. Gynecol. Endocrinol.* **16**, 307–317 (2002).
97. Benagiano, G., Benagiano, M., Bianchi, P., D'Elios, M. M. & Brosens, I. Contraception in autoimmune diseases. *Best Pract. Res. Clin. Obstet. Gynaecol.* **60**, 111–123 (2019).
98. Combination birth control pills - Mayo Clinic. https://www.mayoclinic.org/tests-procedures/combination-birth-control-pills/about/pac-20385282.
99. Barr, N. G. Managing Adverse Effects of Hormonal Contraceptives. *Am. Fam. Physician* **82**, 1499–1506 (2010).
100. Levonorgestrel And Ethinyl Estradiol (Oral Route) Description and Brand Names - Mayo Clinic. https://www.mayoclinic.org/drugs-supplements/levonorgestrel-and-ethinyl-estradiol-oral-route/description/drg-20406441.
101. Pinkerton, G. D. & Carey, H. M. Post-pill anovulation. *Med. J. Aust.* **1**, 220–222 (1976).
102. Coukell, A. J. & Balfour, J. A. Levonorgestrel subdermal implants. A review of contraceptive efficacy and acceptability. *Drugs* **55**, 861–887 (1998).
103. Smarr, B. L. *et al.* Feasibility of continuous fever monitoring using wearable devices. *Sci. Rep.* **10**, (2020).
104. Smarr, B. L., Burnett, D. C., Mesri, S. M., Pister, K. S. J. & Kriegsfeld, L. J. A Wearable Sensor System with Circadian Rhythm Stability Estimation for Prototyping Biomedical Studies. *IEEE Trans. Affect. Comput.* **7**, 220–230 (2016).
105. Moenter, S. M., Caraty, A., Locatelli, A. & Karsch, F. J. Pattern of Gonadotropin-Releasing Hormone (GnRH) Secretion Leading up to Ovulation in the Ewe: Existence of a Preovulatory GnRH Surge. *Endocrinology* **129**, 1175–1182 (1991).
106. Webster, W. W. & Smarr, B. Using Circadian Rhythm Patterns of Continuous Core Body Temperature to Improve Fertility and Pregnancy Planning. *J. Circadian Rhythms* **18**, 5 (2020).

107. Refinetti, R. & Menaker, M. The circadian rhythm of body temperature. *Physiol. Behav.* **51**, 613–637 (1992).
108. Bakshi, V. P. & Geyer, M. A. Ontogeny of isolation rearing-induced deficits in sensorimotor gating in rats. *Physiol. Behav.* **67**, 385–392 (1999).
109. Boggiano, M. M. *et al.* Effect of a cage divider permitting social stimuli on stress and food intake in rats. *Physiol. Behav.* **95**, 222–228 (2008).
110. Ojeda & Andrews. The maturation of estradiol-negative feedback in female rats: evidence that the resetting of the hypothalamic 'gonadostat' does not precede the fir... - PubMed - NCBI. https://www.ncbi.nlm.nih.gov/pubmed/6796387.
111. Ström, J. O., Theodorsson, A., Ingberg, E., Isaksson, I.-M. & Theodorsson, E. Ovariectomy and 17β-estradiol Replacement in Rats and Mice: A Visual Demonstration. *J. Vis. Exp. JoVE* (2012) doi:10.3791/4013.
112. Clark, R. G. & Tarttelin, M. F. Some effects of ovariectomy and estrogen replacement on body composition in the rat. *Physiol. Behav.* **28**, 963–969 (1982).
113. day & kinder. Influence of prepubertal ovariectomy and estradiol replacement therapy on secretion of luteinizing hormone before and after pubertal age in heifers. (1986).
114. Prakapenka, A. V. *et al.* Contrasting effects of individual versus combined estrogen and progestogen regimens as working memory load increases in middle-aged ovariectomized rats: one plus one does not equal two. *Neurobiol. Aging* **64**, 1–14 (2018).
115. Olaniyi, K. S. & Olatunji, L. A. Oral ethinylestradiol-levonorgestrel attenuates cardiac glycogen and triglyceride accumulation in high fructose female rats by suppressing pyruvate dehydrogenase kinase-4. *Naunyn. Schmiedebergs Arch. Pharmacol.* **392**, 89–101 (2019).
116. Santoru, F., Berretti, R., Locci, A., Porcu, P. & Concas, A. Decreased allopregnanolone induced by hormonal contraceptives is associated with a reduction in social behavior and sexual motivation in female rats. *Psychopharmacology (Berl.)* **231**, 3351–3364 (2014).
117. Geraghty, D. P., Byrne, K. B., McPherson, G. A. & Burcher, E. Renal and myocardial adrenoceptors in steroid contraceptive-induced hypertension in rats. *Clin. Exp. Pharmacol. Physiol.* **17**, 567–578 (1990).
118. Simone, J. *et al.* Ethinyl estradiol and levonorgestrel alter cognition and anxiety in rats concurrent with a decrease in tyrosine hydroxylase expression in the locus coeruleus and brain-derived neurotrophic factor expression in the hippocampus. *Psychoneuroendocrinology* **62**, 265–278 (2015).
119. Follesa, P. *et al.* Changes in GABAA receptor gamma 2 subunit gene expression induced by long-term administration of oral contraceptives in rats. *Neuropharmacology* **42**, 325–336 (2002).
120. Dehghan, M. *et al.* Associations of fats and carbohydrate intake with cardiovascular disease and mortality in 18 countries from five continents (PURE): a prospective cohort study. *The Lancet* **0**, (2017).
121. Olatunji, L. A. *et al.* Combined oral contraceptive and nitric oxide synthesis inhibition synergistically causes cardiac hypertrophy and exacerbates insulin resistance in female rats. *Environ. Toxicol. Pharmacol.* **52**, 54–61 (2017).
122. Guerra, M. D. O., Souza, E. R. D. & Peters, V. M. Reproductive performance of female wistar rat, descendent of mothers treated with levonorgestrel during the lactation. *Rev. Assoc. Médica Bras.* **48**, 135–139 (2002).

123. JADELLE (levonorgestrel implants) for subdermal use. 35.
124. Woodruff, J. A., Lacey, E. A. & Bentley, G. Contrasting fecal corticosterone metabolite levels in captive and free-living colonial tuco-tucos (Ctenomys sociabilis). *J. Exp. Zool. Part Ecol. Genet. Physiol.* **313A**, 498–507 (2010).
125. Touma, C., Palme, R. & Sachser, N. Analyzing corticosterone metabolites in fecal samples of mice: a noninvasive technique to monitor stress hormones. *Horm. Behav.* **45**, 10–22 (2004).
126. Millspaugh, J. J. & Washburn, B. E. Within-sample variation of fecal glucocorticoid measurements. *Gen. Comp. Endocrinol.* **132**, 21–26 (2003).
127. Harper, J. M. & Austad, S. N. Fecal glucocorticoids: a noninvasive method of measuring adrenal activity in wild and captive rodents. *Physiol. Biochem. Zool. PBZ* **73**, 12–22 (2000).
128. Auer, K. E. *et al.* Measurement of Fecal Testosterone Metabolites in Mice: Replacement of Invasive Techniques. *Anim. Open Access J. MDPI* **10**, (2020).
129. Place, 1514 Eisenhower & Ann Arbor, M. 48108-3284. Steroid Solid Extraction. *Arbor Assays* https://www.arborassays.com/resource/steroid-solid-extraction/.
130. Neurodevelopmental Consequences of Maternal Omega-3 Fatty Acid Deficiency - ProQuest. https://search.proquest.com/openview/2b9eaffc7b3f492b60daf6e1fababebd/1?pq-origsite=gscholar&cbl=2026366&diss=y.
131. Lv, X. *et al.* Reprogramming of ovarian granulosa cells by YAP1 leads to development of high-grade cancer with mesenchymal lineage and serous features. *Sci. Bull.* **65**, 1281–1296 (2020).
132. Mathew, L., Gaikwad, A., Gonzalez, A., Nugent, E. K. & Smith, J. A. Evaluation of Active Hexose Correlated Compound (AHCC) in Combination With Anticancer Hormones in Orthotopic Breast Cancer Models. *Integr. Cancer Ther.* **16**, 300–307 (2017).
133. Franklin, A. D., Waddell, W. T., Behrns, S. & Goodrowe, K. L. Estrous cyclicity and reproductive success are unaffected by translocation for the formation of new reproductive pairs in captive red wolves (Canis rufus). *Zoo Biol.* **39**, 230–238 (2020).
134. Righetti, F. *et al.* How reproductive hormonal changes affect relationship dynamics for women and men: A 15-day diary study. *Biol. Psychol.* **149**, 107784 (2020).
135. azuredominique. *azuredominique/Rat-Puberty-Lab-Conditions*. (2021).
136. Leise, T. L. Wavelet analysis of circadian and ultradian behavioral rhythms. *J. Circadian Rhythms* **11**, 5 (2013).
137. Leise, T. L. Chapter Five - Wavelet-Based Analysis of Circadian Behavioral Rhythms. in *Methods in Enzymology* (ed. Sehgal, A.) vol. 551 95–119 (Academic Press, 2015).
138. Lilly, J. M. & Olhede, S. C. Generalized Morse Wavelets as a Superfamily of Analytic Wavelets. *IEEE Trans. Signal Process.* **60**, 6036–6041 (2012).
139. Grant, A. D., Newman, M. & Kriegsfeld, L. J. Ultradian rhythms in heart rate variability and distal body temperature anticipate onset of the luteinizing hormone surge. *Sci. Rep.* **10**, 20378 (2020).
140. Sanchez-Alavez, M. *et al.* Insulin causes hyperthermia by direct inhibition of warm-sensitive neurons. *Diabetes* **59**, 43–50 (2010).

141. Kottler, M. L., Coussieu, C., Valensi, P., Levi, F. & Degrelle, H. Ultradian, circadian and seasonal variations of plasma progesterone and LH concentrations during the luteal phase. *Chronobiol. Int.* **6**, 267–277 (1989).
142. de Kloet, E. R. & Sarabdjitsingh, R. A. Everything has rhythm: focus on glucocorticoid pulsatility. *Endocrinology* **149**, 3241–3243 (2008).
143. Violin Plots 101: Visualizing Distribution and Probability Density. https://mode.com/blog/violin-plot-examples/.
144. Wu, F. C., Butler, G. E., Kelnar, C. J., Huhtaniemi, I. & Veldhuis, J. D. Ontogeny of pulsatile gonadotropin releasing hormone secretion from midchildhood, through puberty, to adulthood in the human male: a study using deconvolution analysis and an ultrasensitive immunofluorometric assay. *J. Clin. Endocrinol. Metab.* **81**, 1798–1805 (1996).
145. Gabriel, S. M., Roncancio, J. R. & Ruiz, N. S. Growth hormone pulsatility and the endocrine milieu during sexual maturation in male and female rats. *Neuroendocrinology* **56**, 619–625 (1992).
146. Hoeger, K. M., Kolp, L. A., Strobl, F. J. & Veldhuis, J. D. Evaluation of LH secretory dynamics during the rat proestrous LH surge. *Am. J. Physiol.* **276**, R219-225 (1999).
147. Prendergast, B. J., Beery, A. K., Paul, M. J. & Zucker, I. Enhancement and Suppression of Ultradian and Circadian Rhythms across the Female Hamster Reproductive Cycle. *J. Biol. Rhythms* **27**, 246–256 (2012).
148. Sanchez-Alavez, M., Alboni, S. & Conti, B. Sex- and age-specific differences in core body temperature of C57Bl/6 mice. *Age Dordr. Neth.* **33**, 89–99 (2011).
149. Apter, D., Bützow, T. L., Laughlin, G. A. & Yen, S. S. Gonadotropin-releasing hormone pulse generator activity during pubertal transition in girls: pulsatile and diurnal patterns of circulating gonadotropins. *J. Clin. Endocrinol. Metab.* **76**, 940–949 (1993).
150. Tenreiro, S. *et al.* The development of ultradian and circadian rhythms in premature babies maintained in constant conditions. *Early Hum. Dev.* **27**, 33–52 (1991).
151. Menna-Barreto, L., Benedito-Silva, A. A., Marques, N., de Andrade, M. M. & Louzada, F. Ultradian components of the sleep-wake cycle in babies. *Chronobiol. Int.* **10**, 103–108 (1993).
152. Bueno, C. & Menna-Barreto, L. Development of sleep/wake, activity and temperature rhythms in newborns maintained in a neonatal intensive care unit and the impact of feeding schedules. *Infant Behav. Dev.* **44**, 21–28 (2016).
153. Curtis, K. S. *et al.* Temporal and Site-Specific Changes in Central Neuroimmune Factors During Rapid Weight Gain After Ovariectomy in Rats. *Neurochem. Res.* **43**, 1802–1813 (2018).
154. Wegorzewska, I. N. *et al.* Postovariectomy weight gain in female rats is reversed by estrogen receptor α agonist, propylpyrazoletriol. *Am. J. Obstet. Gynecol.* **199**, 67.e1-67.e5 (2008).
155. Paccola, C. C., Resende, C. G., Stumpp, T., Miraglia, S. M. & Cipriano, I. The rat estrous cycle revisited: a quantitative and qualitative analysis. 7 (2013).
156. Marrone, B. L., Gentry, R. T. & Wade, G. N. Gonadal hormones and body temperature in rats: effects of estrous cycles, castration and steroid replacement. *Physiol. Behav.* **17**, 419–425 (1976).
157. Liechty, E. R., Bergin, I. L. & Bell, J. D. Animal models of contraception: utility and limitations. *Open Access J. Contracept.* **6**, 27–35 (2015).

158. Ariznavarreta, C. *et al.* Circadian rhythms in airline pilots submitted to long-haul transmeridian flights. *Aviat. Space Environ. Med.* **73**, 445–455 (2002).
159. Polugrudov, A. S. *et al.* Wrist temperature and cortisol awakening response in humans with social jetlag in the North. *Chronobiol. Int.* **33**, 802–809 (2016).
160. Drewry, A. M., Fuller, B. M., Bailey, T. C. & Hotchkiss, R. S. Body temperature patterns as a predictor of hospital-acquired sepsis in afebrile adult intensive care unit patients: a case-control study. *Crit. Care Lond. Engl.* **17**, R200 (2013).
161. Granger, J. I., Ratti, P.-L., Datta, S. C., Raymond, R. M. & Opp, M. R. Sepsis-induced morbidity in mice: effects on body temperature, body weight, cage activity, social behavior and cytokines in brain. *Psychoneuroendocrinology* **38**, 1047–1057 (2013).
162. Culver, A. *et al.* Circadian disruption of core body temperature in trauma patients: a single-center retrospective observational study. *J. Intensive Care* **8**, 4 (2020).
163. Sharma, A. *et al.* Circadian Rhythm Disruption and Alzheimer's Disease: The Dynamics of a Vicious Cycle. *Curr. Neuropharmacol.* **19**, 248–264 (2021).
164. Zimmet, P. *et al.* The Circadian Syndrome: is the Metabolic Syndrome and much more! *J. Intern. Med.* **286**, 181–191 (2019).
165. Akin, A. & Elstein, M. The value of the basal temperature chart in the management of infertility. *Int. J. Fertil.* **20**, 122–124 (1975).
166. He, H. [Diagnosis of basal body temperature, serum progesterone and endometrial biopsy for luteal phase defect]. *Zhonghua Fu Chan Ke Za Zhi* **28**, 82–84, 122–123 (1993).
167. Bopp, B. & Shoupe, D. Luteal phase defects. *J. Reprod. Med.* **38**, 348–356 (1993).
168. Mitwally, M. F., Kuscu, N. K. & Yalcinkaya, T. M. High ovulatory rates with use of troglitazone in clomiphene-resistant women with polycystic ovary syndrome. *Hum. Reprod. Oxf. Engl.* **14**, 2700–2703 (1999).
169. Veldhuis, J. D. *et al.* Physiological Profiles of Episodic Progesterone Release During the Midluteal Phase of the Human Menstrual Cycle: Analysis of Circadian and Ultradian Rhythms, Discrete Pulse Properties, and Correlations With Simultaneous Luteinizing Hormone Release. *J. Clin. Endocrinol. Metab.* **66**, 414–421 (1988).
170. Sir-Petermann, T. *et al.* Are circulating leptin and luteinizing hormone synchronized in patients with polycystic ovary syndrome? *Hum. Reprod. Oxf. Engl.* **14**, 1435–1439 (1999).
171. Herbison, A. E. The Gonadotropin-Releasing Hormone Pulse Generator. *Endocrinology* **159**, 3723–3736 (2018).
172. Lightman, S. & Terry, J. R. The importance of dynamic signalling for endocrine regulation and drug development: relevance for glucocorticoid hormones. *Lancet Diabetes Endocrinol.* **2**, 593–599 (2014).
173. Bong Choi, S., Shil Hong, E. & Hee Noh, Y. Open Artificial Pancreas System Reduced Hypoglycemia and Improved Glycemic Control in Patients with Type 1 Diabetes | Diabetes. https://diabetes.diabetesjournals.org/content/67/Supplement_1/964-P (2018).
174. Marui, S., Uchida, Y. & Nagashima, K. Daily Changes of Body Temperature and Heart Rate are Modulated after Estradiol Depletion in Female Rats. in (2016). doi:10.4172/2161-0940.1000197.
175. Brown, S. A., Zumbrunn, G., Fleury-Olela, F., Preitner, N. & Schibler, U. Rhythms of mammalian body temperature can sustain peripheral circadian clocks. *Curr. Biol. CB* **12**, 1574–1583 (2002).

176. Peachman, R. R. Weighing the Risks and Benefits of Hormonal Contraception. *JAMA* **319**, 1083–1084 (2018).
177. Bahamondes, L., Valeria Bahamondes, M. & Shulman, L. P. Non-contraceptive benefits of hormonal and intrauterine reversible contraceptive methods. *Hum. Reprod. Update* **21**, 640–651 (2015).
178. Lewis, D. M. *Automated Insulin Delivery*. (2019).
179. Webster, W., Godfrey, E. M., Costantini, L. & Katilius, J. Passive fertility prediction using a novel vaginal ring and smartphone application. *Fertil. Steril.* **104**, e98 (2015).
180. Aptekar, D., Costantini, L., Katilius, J. & Webster, W. Continuous, Passive Personal Wearable Sensor to Predict Ovulation [21G]. *Obstet. Gynecol.* **127**, 64S (2016).
181. Shilaih, M. *et al.* Modern fertility awareness methods: Wrist wearables capture the changes of temperature associated with the menstrual cycle. *Biosci. Rep.* Epub ahead of print (2017) doi:info:doi/10.1042/BSR20171279.
182. Mørch, L. S. *et al.* Contemporary Hormonal Contraception and the Risk of Breast Cancer. *N. Engl. J. Med.* **377**, 2228–2239 (2017).
183. Westhoff, C. L. & Pike, M. C. Hormonal contraception and breast cancer. *Contraception* **98**, 171–173 (2018).
184. McLean, A. C., Valenzuela, N., Fai, S. & Bennett, S. A. L. Performing vaginal lavage, crystal violet staining, and vaginal cytological evaluation for mouse estrous cycle staging identification. *J. Vis. Exp. JoVE* e4389 (2012) doi:10.3791/4389.
185. Chelini, M. O. M., Souza, N. L., Rocha, A. M., Felippe, E. C. G. & Oliveira, C. A. Quantification of fecal estradiol and progesterone metabolites in Syrian hamsters (Mesocricetus auratus). *Braz. J. Med. Biol. Res.* **38**, 1711–1717 (2005).
186. van der Vinne, V. *et al.* Continuous and non-invasive thermography of mouse skin accurately describes core body temperature patterns, but not absolute core temperature. *Sci. Rep.* **10**, 20680 (2020).
187. Shechter, A., Boudreau, P., Varin, F. & Boivin, D. B. Predominance of distal skin temperature changes at sleep onset across menstrual and circadian phases. *J. Biol. Rhythms* **26**, 260–270 (2011).
188. Fowler, L. R., Gillard, C. & Morain, S. Teenage Use of Smartphone Applications for Menstrual Cycle Tracking. *Pediatrics* **145**, (2020).
189. Eschler, J., Menking, A., Fox, S. & Backonja, U. Defining Menstrual Literacy With the Aim of Evaluating Mobile Menstrual Tracking Applications. *Comput. Inform. Nurs. CIN* **37**, 638–646 (2019).
190. Master, S. L. *et al.* Distentangling the systems contributing to changes in learning during adolescence. *Dev. Cogn. Neurosci.* **41**, 100732 (2020).
191. Piekarski, D. J. *et al.* Does puberty mark a transition in sensitive periods for plasticity in the associative neocortex? *Brain Res.* **1654**, 123–144 (2017).
192. Davidow, J. Y., Foerde, K., Galván, A. & Shohamy, D. An Upside to Reward Sensitivity: The Hippocampus Supports Enhanced Reinforcement Learning in Adolescence. *Neuron* **92**, 93–99 (2016).
193. DePasque, S. & Galván, A. Frontostriatal development and probabilistic reinforcement learning during adolescence. *Neurobiol. Learn. Mem.* **143**, 1–7 (2017).

194. Martinez, G. M. Sexual Activity, Contraceptive Use, and Childbearing of Teenagers Aged 15–19 in the United States. 8 (2015).
195. Patseadou, M. & Michala, L. Usage of the levonorgestrel-releasing intrauterine system (LNG-IUS) in adolescence: what is the evidence so far? *Arch. Gynecol. Obstet.* **295**, 529–541 (2017).
196. Strittmatter, E. & Holtmann, M. [Gender identities in transition]. *Z. Kinder. Jugendpsychiatr. Psychother.* **48**, 93–102 (2020).
197. Castilla-Peón, M. F. Medical management of transgender children and adolescents. *Bol. Med. Hosp. Infant. Mex.* **75**, 7–14 (2018).

# 3. Sex Differences in Pubertal Circadian and Ultradian Rhythm Development Under Naturalistic Conditions

## 3.1 Abstract

Biological rhythms in core body temperature (CBT) provide informative markers of adolescent development under controlled laboratory conditions. However, it is unknown if the approach is practical under more variable naturalistic conditions, and if it may therefore prove useful in a real-world setting. To evaluate this possibility, we examined fecal steroid concentrations and CBT rhythms from pre-adolescence (p26) through early adulthood (p76) in intact male and female Wistar rats under natural light and temperatures at the University of California, Berkeley Field Station. Despite greater environmental variability, CBT markers of pubertal onset and its rhythmic progression were comparable to those previously reported in laboratory conditions in female rats. Specifically, sex differences emerged in circadian rhythm (CR) power and temperature amplitude prior to pubertal onset and persisted into early adulthood, with females exhibiting elevated CBT and decreased CR power. Within-day (ultradian rhythm; UR) patterns also exhibited a pronounced sex difference associated with estrous cyclicity. Pubertal onset occurred later than previously reported under lab conditions for both sexes, with vaginal opening and increased fecal estradiol closely tied to the commencement of 4 day oscillations in CBT and UR power. In contrast, preputial separation and the first rise in testosterone concentration was not associated with adolescent changes to CBT rhythms in male rats. Together, males and females exhibited unique temporal patterning of CBT and sex steroids across pubertal development, with tractable associations between hormonal concentrations, external development, and temporal structure in females. The preservation of these features outside the laboratory supports CBT as a strong candidate for translational pubertal monitoring under naturalistic conditions in females.

## 3.2 Introduction

Clinical or self-assessment[1] of pubertal status is typically conducted via observation of external characteristics (e.g., Tanner Scale, developed in the late 1960's)[2], manual ovulatory cycle tracking in girls[3], or costly hormone measurement[4]. Today, relatively inexpensive wearable sensors that capture metrics influenced by reproductive hormones and metabolism, such as body temperature[5,6], are widely available. These sensors provide a unique opportunity to automatically generate markers of pubertal events in real-world settings. Such sensors, along with a database of normative changes, could provide non-invasive information about pubertal development to teens, families, or clinicians[7]. These investigations require years of future study, wider adoption of wearables by preteens and teens, and further development of regulatory standards for wearable companies and clinicians[7–10]. Although the value of identifying these features for pre-clinical and translational studies is evident, whether real-world environmental variability masks patterns identified under controlled laboratory conditions requires empirical investigation.

Biological rhythms in core body temperature (CBT) change markedly across adolescent development in rodents, enabling unobtrusive monitoring of this trajectory in a laboratory setting[11–13]. These rhythms are coupled across physiological systems[5,14–16] and at multiple timescales, including within-a-day (ultradian rhythms; URs)[17], daily (circadian rhythms; CRs)[18,19], and multi-day ovulatory cycles in females (ovulatory rhythms; ORs)[20]. Rhythmicity serves numerous functions, including coordination of reproductive development[11,21–23] and synchronization of internal systems to variation in the environment[24–27], and can provide clinically-relevant diagnostic information[5,6,28,29]. We recently applied this approach to monitor female adolescent development in rats under controlled laboratory conditions[13]. This strategy revealed predictable features of CBT across adolescent development, with CR power and CBT amplitude rising from early to mid-adolescence and stabilizing by early adulthood. Such outputs were coordinated with changes in reproductive hormones, consistent with well-established temperature modulating effects of estrogen[30] and progesterone[31].

In addition to introducing more 'noise', exposure to the greater spectro-temporal variability of natural light, temperature, humidity, and enriched sensory complexity of such environments[32,33] may affect pubertal timing and tempo. Although a great deal of research has focused on extreme environments (e.g., polar[34]), temperate environments may reveal differences from laboratory-derived features. Mice and rats exposed to longer or variable day lengths, for example, exhibit delayed external markers of pubertal onset[35], more variable activity rhythms[36,37], and have altered weight gain trajectories[38]. In contrast, male Siberian hamsters (*Phodopus sungorus*) advance puberty in long day lengths[39] to maximize reproductive success prior to winter. These changes suggest species-specific decoupling of maturation mechanisms that are coordinated under laboratory conditions and may decouple temperature features from sexual maturation under natural conditions[40]. Additionally, animals raised in naturalistic environments exhibit elevated steroid hormone concentrations[41,42], suggesting that the hormonal milieu influencing the adolescent trajectory may alter temperature rhythms relative to laboratory-based studies.

To assess the potential impact of these factors on CBT rhythmicity during adolescence, we examined reproductive hormones and CBT patterns in a naturalistic setting. As humans face a

complex environment of combined artificial and natural stimuli, we chose to investigate rhythmic features of adolescence in animals housed at the Field Station (FS) in Berkeley, CA, which is an intermediate between laboratory and field conditions. This environment provides shelters open to natural changes in light, humidity, and temperature while providing a social partner and standard laboratory housing and food. We hypothesized that the FS environment would result in higher and more variable sex steroid concentrations[41,42] and pubertal timing onset compared to previous reports in the laboratory environment[13]. We also speculated that these changes would be mirrored in CR and UR patterns and temperature amplitude. Finally, we anticipated that reported features of adolescence would occur in males as well as females, with the exception of the emergence of patterns associated with the ovulatory cycle, and that males may exhibit sex difference of elevated ultradian power and decreased temperature, as previously reported [12], compared to females.

## 3.3 Materials and Methods

*Animals.* Male and female Wistar rats were purchased at 250 g from Charles River (Charles River, Wilmington, MA). Animals were bred at the FS and weaned at postnatal day 21 (p21). Weanlings were housed in same-sex pairs to minimize social isolation stress known to affect pubertal development[43,44] in standard translucent propylene (96 x 54 x 40 cm) rodent cages, and provided *ad libitum* access to food and water, wood chips for floor cover, bedding material, and chew toys during the study. Animals were gently handled daily before weighing to minimize stress. To prevent mixing of feces collected, cage mates were separated by a flexible stainless-steel lattice that permitted aural, scent, and touch interaction between siblings. A total of 16 animals were included in the study (n=8 per sex), with 16 same-sex individuals as social, littermate partners. The experiment was conducted in rooms with natural light (light intensity during the mean photo- and scotophases were 677 ± 254 and 2.65 ± 0.40 lux, respectively), outdoor ambient temperatures averaging 22.6 ± 0.34° C , and air circulation from August 9$^{th}$ to September 29$^{th}$, 2019, at the field station at the University of California, Berkeley. All procedures were approved by the Institutional Animal Care and Use Committee of the University of California, Berkeley and conformed to the principles in the Guide for the Care and Use of Laboratory Animals, 8$^{th}$ ed.

Core Body Temperature Data Collection. Data were gathered with G2 E-Mitter implants that chronically record CBT (Starr Life Sciences Co., Oakmont, PA). At weaning, G2 E-Mitters were implanted in the intraperitoneal cavity under isoflurane anesthesia, with analgesia achieved by subcutaneous injections of 0.03 mg/kg buprenorphine (Hospira, Lake Forest, IL) in saline. Buprenorphine was administered every 12 h for 2 days following surgery. E-Mitters were sutured to the ventral muscle wall to maintain consistent core temperature measurements. Recordings began immediately, but data collected for the first 5 days post-surgery were not included in analyses to allow for post-surgical recovery. Recordings were continuous and stored in 1-min bins.

*Fecal Sample Collection.* Fecal E2 (fE2) concentrations in females, and fecal testosterone (fT) concentrations in males, were assessed across puberty from feces generated over 24 h periods. Feces provide a more representative sample of average daily hormone concentrations than do blood samples[41,45–48] and are non-invasively generated, thereby reducing stress associated with high-frequency, longitudinal blood collection. Samples were collected in small, airtight bags in the

early mornings from p25 to p37 (pre puberty and first estrous cycle), p45 to p51 (mid puberty), and p55 to p65 (late puberty to early adulthood) in females, and every 3 days in males from p25 to p74. Samples soiled with urine were discarded and all other boli generated over each 24-h segment were combined. Within 1 h of collection samples were stored at -20° C until preprocessing for ELISA assay. Sample collection took ~ 1 min per animal. One female's samples were frequently soiled with urine and were therefore not to be included in analyses of 12 out of 24 of collected timepoints.

Samples were processed according to manufacturer's instructions[49]. Briefly, samples were placed in a tin weigh boat and heated at 65°C for 90 minutes, until completely dry. Dry samples were ground to a fine powder in a coffee grinder, which was wiped down with ethanol and dried between samples to avoid cross contamination. Powder was weighed into 0.2 mg aliquots and added to 2 mL test tubes. For hormone extraction, 1.8mL of 100% ethanol was added to each test tube, and tubes were shaken vigorously for 30 minutes. Tubes were then centrifuged at 5,000 RPM for 15 minutes at 4°C. Supernatant was moved to a new tube and evaporated under 65°C until dry (~ 90 minutes). Sample residue was reconstituted in 100µL of 100% ethanol. 25µL of this solution was diluted for use in the assay and remaining sample was diluted and stored.

*Hormone Assessment.* A commercially available fE2 enzyme-linked immunosorbent assay (ELISA) kit was used to quantify E2 in fecal samples (Arbor Assays, Ann Arbor, MI). These assays have been previously published in species ranging from rats and mice[48,50–56], to wolves[57], to humans[58]. ELISAs were conducted according to the manufacturer's instructions. To ensure each sample contained ≤ 5% alcohol, 25µL of concentrate were vortexed in 475µL Assay Buffer. All samples were run in duplicate, and an inter-assay control was run with each plate. Sensitivity for the estradiol assay was 39.6 pg/mL and the limit of detection was 26.5 pg/mL. Sensitivity for the testosterone assay was 9.92 pg/mL and the limit of detection was 30.6 pg/mL. Fecal testosterone intra-assay coefficient of variation (C.V.) was 9.35% and inter-assay C.V. was 10.5%. Fecal estradiol intra-assay CV was 5.0% and inter-assay CV was 5.54%.

*Data Availability and Analysis.* All code and data used in this paper are available at A.G.'s and L.K.'s Github[59,60]. Code was written in MATLAB 2020b and 2021a with Wavelet Transform (WT) code modified from the Jlab toolbox and from Dr. Tanya Leise[61,62]. Briefly, data were imported to MATLAB at 1-minute resolution. Any data points outside ± 3 standard deviations were set to the median value of the prior hour, and any points showing near instantaneous change, as defined by local abs(derivative) > $10^5$ as an arbitrary cutoff, were also set to the median value of the previous hour. Small data interrupts resulting from intermittent data pulls (<10 minutes) were linearly interpolated. Continuous data from p26 to p74 were divided into three equal-length phases: pre to mid puberty (p26 to p41), mid to late puberty (p42 to p58), and late puberty to early adulthood (p59 to p74).

*Wavelet Analyses and Statistics of CBT Data.* Briefly, Wavelet Transformation (WT) was used to generate a power estimate, representing amplitude and stability of oscillation at a given periodicity, within a signal at each moment in time. Whereas Fourier transforms allow transformation of a signal into frequency space without temporal position (i.e., using sine wave components with infinite length), wavelets are constructed with amplitude diminishing to 0 in both directions from center. This property permits frequency strength calculation at a given

position. In the present analyses we use a Morse wavelet with a low number of oscillations (defined by *β=5* and *γ=3, the frequencies of the two waves superimposed to create the wavelet*[63]), similar to wavelets used in many circadian and ultradian applications[5,61–65]. Additional values of *β* (3–8) and *γ* (2–5) did not alter the findings. As WTs exhibit artifacts at the edges of the data being transformed, only the WT of the second through the second to last days of data were analyzed further, from p26 to p74. Periods of 1 to 39 h were assessed. For quantification of spectral differences, WT spectra were isolated in bands; circadian periodicity power was defined as the max power per minute within the 23 to 25 h band; ultradian periodicity power was defined as the max power per minute in the 1 to 3 h band. The latter band was chosen because this band corresponded with the daily ultradian peak power observed in ultradian rhythms across physiological systems in rats[14,66–68].

For statistical comparisons of any two groups, Mann Whitney U (MW) rank sum tests were used to avoid assumptions of normality for any distribution. Non-parametric Kruskal-Wallis tests were used instead of ANOVAs for the same reason; for all Kruskal-Wallis tests, $\chi^2$ and *p* values are listed in the text. All relevant comparisons have the same *n*/group, and thus the same degrees of freedom. Mann Kendall (MK) tests were used to assess trends over time in wavelet power (**Figure 2**) and linear CBT (**Figure 4**) over three equally sized temporal windows, described above. For short term (< 3 days of data) statistical comparisons, 1 data point per 4 hours was used (approximately once per ultradian cycle); for longer term (>3 days of data) statistical comparisons, 1 data point per day was used. Dunn's test was used for multiple comparisons, and Friedman's tests were utilized in cases of multiple measurements per individual. Circadian power, visualized in **Figure 2A-D** was smoothed with a 24 h window using the MATLAB function "movmean". Violin plots, which are similar to box plots with probability density of finding different values represented by width[69], were calculated using the MATLAB function "violin" and used to visualize both circadian power (**Figure 2J**) and linear CBT (**Figure 4E-G**). Median daily circadian power regressed against each day's fE2 for each individual using a mixed effects linear regression (MATLAB function "fitlme"). Individuals were treated as random effects, and fE2/fT and median daily CR power treated as fixed effects (**Figure 2G-H**).

*Estradiol and Testosterone Analysis and Statistics.* Fecal estradiol and testosterone concentrations by day of life were averaged across animals by group and plotted with shaded mean ± S.E.M (**Figure 1A,C**). Additionally, in females, data were plotted using a 4-day window for each cycle of life over which fecal samples were collected. As individual estrous cycles are not all aligned in time (e.g., one animal may begin puberty on p33, another on p35), samples were aligned with the highest value in a collection period (e.g., mid puberty) falling on the third day displayed (**Figure 1B**). Day of fE2 or fT rise was defined as the first day fE2 or fT concentration rose > 2 standard deviations above its starting prepubertal value. Relationship to vaginal opening, and preputial separation, are described in **Figure 1D**. Group differences in fE2 area under the curve by cycle were assessed using the MATLAB function "trapz" and Kruskal Wallis (KW) tests with Dunn's *post hoc* correction. Hormone differences by day of life were assessed using Friedman's test. In order to further assess commencement and stability of estrous cycling after first rise in fE2, metrics were divided into 4 day blocks, with each day labelled 1,2,3, and 4: repeating for subsequent cycle lengths. Groups for statistical comparison were constructed from all data corresponding to 1's, 2's, 3's and 4's.

Friedman's tests with Dunn's corrections were used to determine if values associated with each day of cycle (e.g., all day 1's) varied statistically from other days of the cycle by group.

## 3.4 Results

*High Frequency Fecal Estradiol and Testosterone Enable Monitoring of Pubertal Progression Under Naturalistic Conditions.* In females, fecal estradiol (fE2) increased after p35 ($\chi^2$= 9.80, p=0.001), and exhibited periodic days exhibited elevated fE2 thereafter (p=0.03 for days 3 versus day 1 after pubertal onset; **Figure 1A,C-F**). In males, fecal testosterone (fT) increased after p45 ($\chi^2$= 9.60, p=0.002; **Figure 1B**). The relationship between canonical external signs of pubertal onset and fE2/ fT rise was dependent on sex: fE2 rose 2 standard deviations prior to vaginal opening in most females (**Figure 1D**, top), whereas fT rose 2 standard deviations 1 to 2 weeks after preputial separation in males (**Figure 1D**, bottom).

*Sex Differences in Circadian Power are Present from Pre-Adolescence through Adulthood.* CR, but not UR power rose across early adolescence in both sexes (CR power upward trend p=0.009, 0.0012 for females and males, respectively; UR power p>0.05 for both sexes; **Figure 2A-C**). Males maintained statistically significantly higher CR power from pre adolescence to mid adolescence and in early adulthood ($\chi^2$= 8.00, 3.78, 16.53; p=0.005, 0.052, $4.79*10^{-5}$ for pre to mid adolescence, mid to late adolescence, and late adolescence to early adulthood, respectively; **Figure 2D-F**). CR power exhibited a non-significant trend toward a 4-day periodic depression after pubertal onset in females (p=0.050; **Figure 2E**). CR power was positively correlated with fE2 in adolescent females (p=0.04, $r^2$=0.08, AIC = -264; **Figure 2G**), whereas adolescent males exhibited a trend toward a negative correlation between CR power and fE2 (p=0.07, $r^2$=0.09, AIC = -132; **Figure 2H**). This pattern was not present prior to pubertal onset, defined by vaginal opening or preputial separation, in either sex (p=0.54, p=0.89 for females and males, respectively; **Figure 2G-H, insets**).

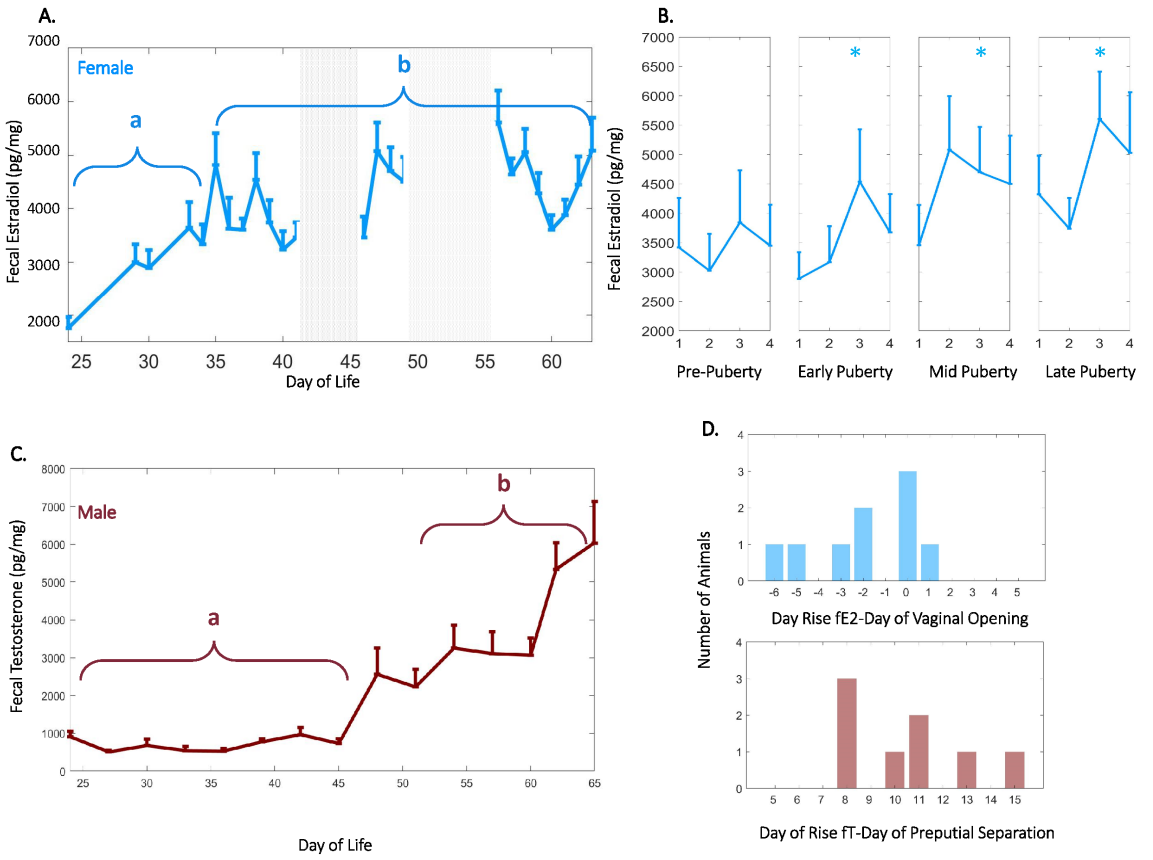


**Figure 1. High Frequency Measurement of Fecal Estradiol and Testosterone Enables Monitoring of Estrous Cycle Emergence and Pubertal Progression in Naturalistic Conditions.** Group mean ± S.E.M. of female fecal estradiol (blue, A) and male (red, C) fecal testosterone. Fecal testosterone by day of life differed significantly after p45 (C), whereas the adoption of the ovulatory cycle contributed to the variance of female fecal estradiol (A,B). * Letters signify Kruskal Wallis group differences of fT values over the bracketed time region. Group mean and S.E.M. of female (light blue, B) fecal estradiol (fE2) adopts a four-day cycle that stabilizes from early to late puberty, with levels elevated significantly by late adolescence. * Indicates significantly elevated fE2 levels in cycle as compared to pre-pubertal state. Fecal estradiol rose 2 standard deviations prior to vaginal opening in most females (D, top), but fecal testosterone rose ~1 to 2 weeks after preputial separation in males (D, bottom).

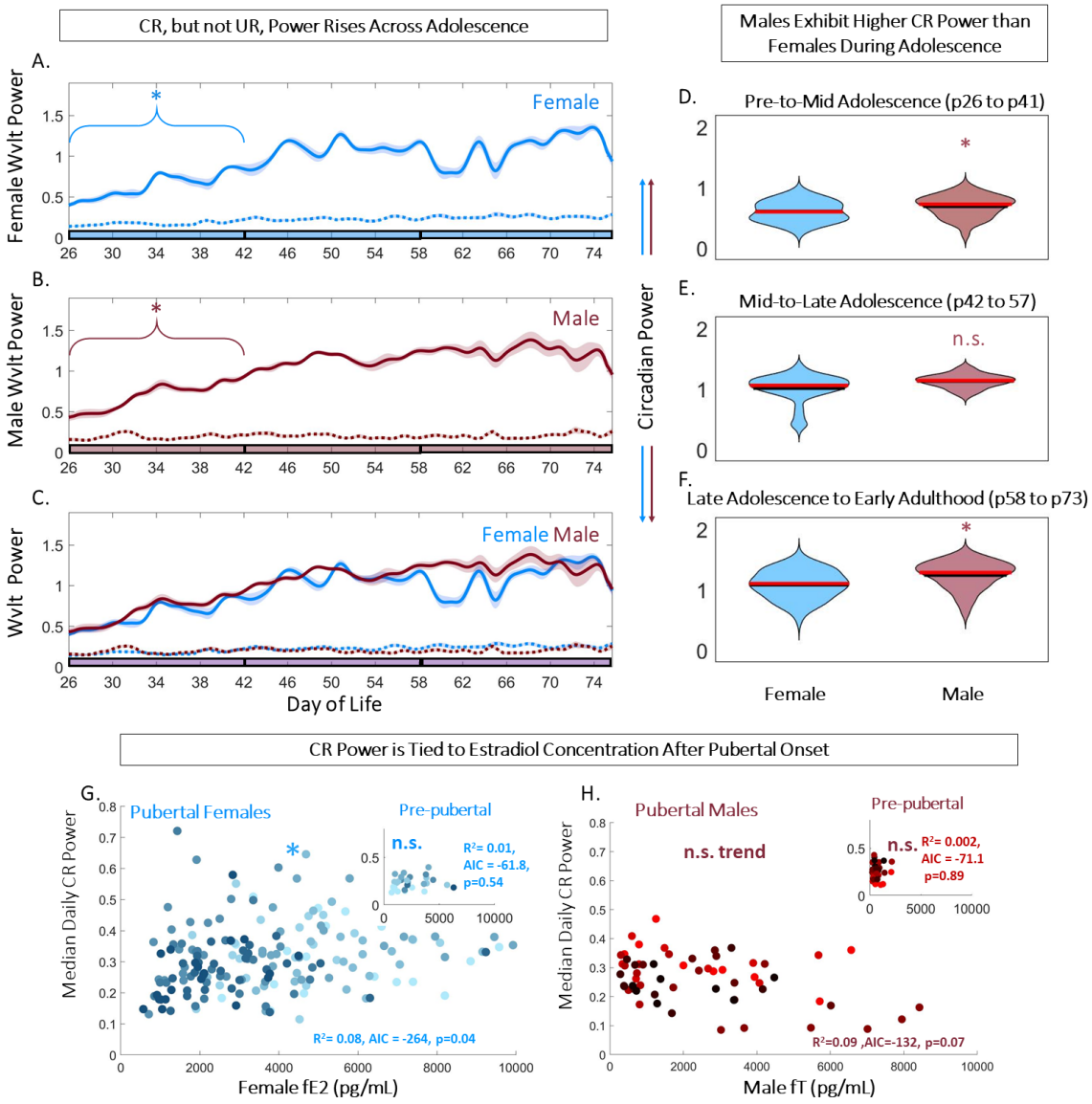


**Figure 2. Adolescence Exaggerates Sex Differences in Circadian Power and its Correlation to Sex Steroids.** Circadian, but not ultradian power rises across early adolescence in both sexes (A-C). Linear plots of group mean ± S.E.M. of CBT circadian (solid) and ultradian (dashed) power in females (blue, A), and males (red, B), overlaid in 2C. * Indicates significant trend over time for the bracketed time region. Phase of adolescence cutoffs (early to mid, mid to late, and late to adult) are indicated by breaks in the colored x-axis at p42 and p58. Violin plots of circadian power illustrate that males maintain significantly (letter indicates group difference) higher CR power than females from early in life (D-F). Scatters plots of fE2 (G) and fT (H) by median daily circadian power in females and males, respectively, illustrate a female-specific positive correlation. This correlation is not present prior to pubertal onset (G,H, insets).

*CBT and Ultradian Power Exhibited Sex-Specific Changes.* CBT exhibited an approximately 4 day periodic fluctuation in females, but not males, commencing with the rise in fE2 and vaginal opening ($\chi^2$=11.5, 1.3, p=0.003 and p>0.05 for females and males, respectively; **Figure 3A-B**). UR power exhibited a comparable 4 day pattern in females ($\chi^2$=8.75, 3.25, p=0.005) but not males (p>0.05) (**Figure 3A-B**). An FFT of male and female CBT and UR power corroborated these observations; females exhibited statistically greater A.U.C. for 4 to 5 day periodicity of CBT modulation ($\chi^2$=11.29, p=8*$10^{-4}$ for sex difference in A.U.C. of 4-5 day temperature FFT; **Figure 3C**) and UR modulation ($\chi^2$=9.28, p=0.002 for sex difference in A.U.C. of 4-5 day UR Power FFT ; UR alignment shown in **Figure 3D**). Additionally, females exhibited a statistically significant upward trend in temperature from pre to mid adolescence (p=1*$10^{-5}$ to p=0.02; mean p=0.004), and a significant downward trend in body temperature from mid to late adolescence (p=0.019) (**Figure 4A, 4C**). Conversely, males did not exhibit a statistical trend in temperature from early to mid (p=0.07) or from mid to late adolescence (p=0.12) (**Figure 4B-C**). Violin plots of temperatures across adolescence indicated that females exhibited elevated temperatures compared to males for the entire period of study ($\chi^2$= 25.37, 33.84, 25.52; p=9.75*$10^{-7}$, 5.97*$10^{-9}$, 4.37*$10^{-7}$ for pre to mid adolescence, mid to late adolescence, and late adolescence to early adulthood, respectively; **Figure 3A-B, Figure 4D-F**).

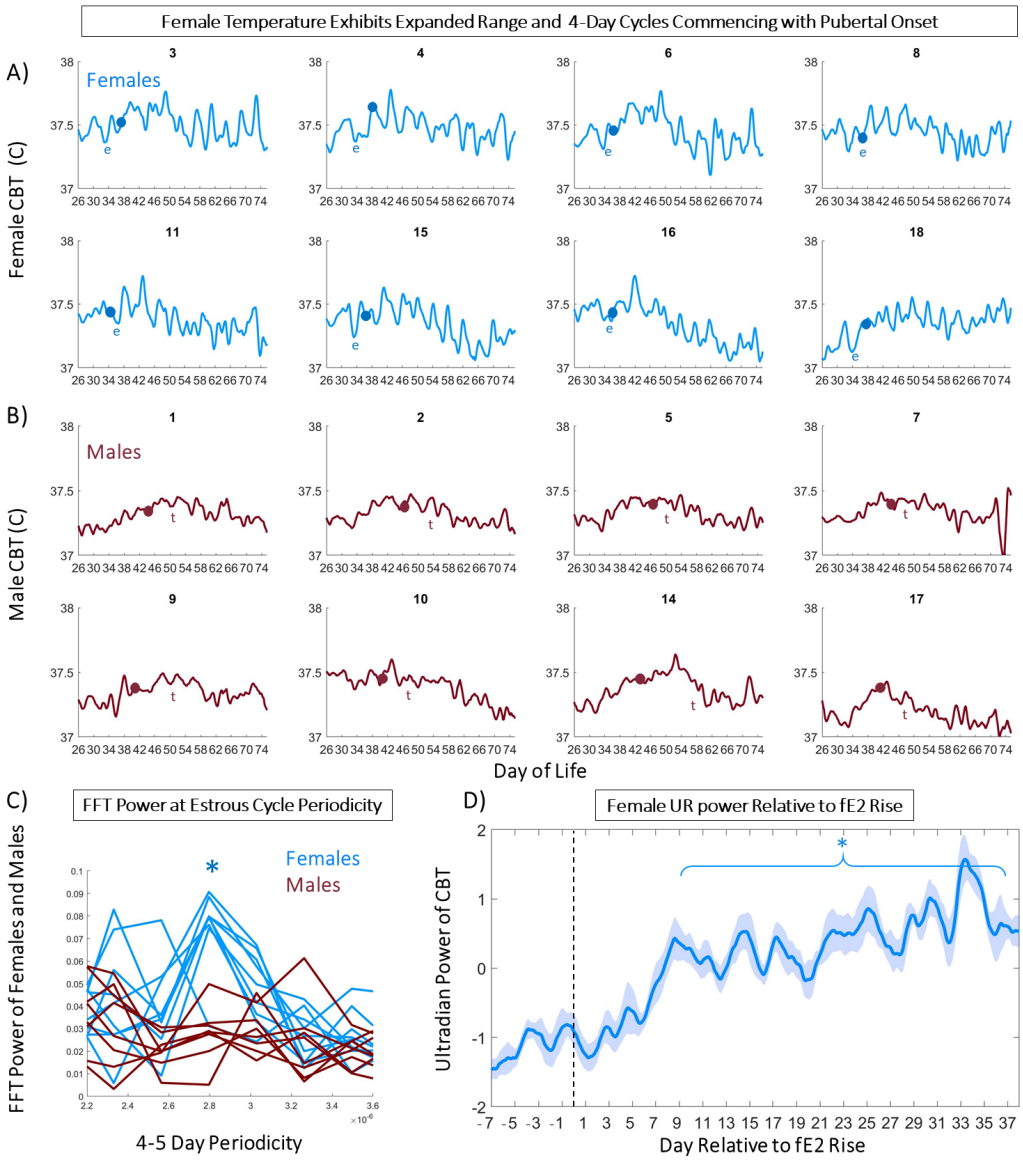


**Figure 3. 4-Day Patterns of Temperature and Ultradian Power Track Ovulatory Cycles of After Pubertal Onset.** Linear plots of smoothed temperature illustrate estrous cycles which onset in time with markers of puberty, vaginal opening and rise in fE2 in all individual females (A); and preputial separation and rise in fT in males (B). Dots indicate day of vaginal opening (blue) or preputial separation (red). Letter "e" indicates day of first rise in fE2> 2 S.D.s, whereas letter "t" indicates day of first rise in fT> 2 S.D.s. Fast Fourier Transform (FFT) of temperatures of females and males centered on 4 to 5 day periodicities indicate females (blue) exhibit a significant peak compared to males (red) (C). CBT UR power aligned among individuals with reference to first fE2 exhibits onset of 4 to 5 day modulation among females approximately 1 week after fE2 rise (D).

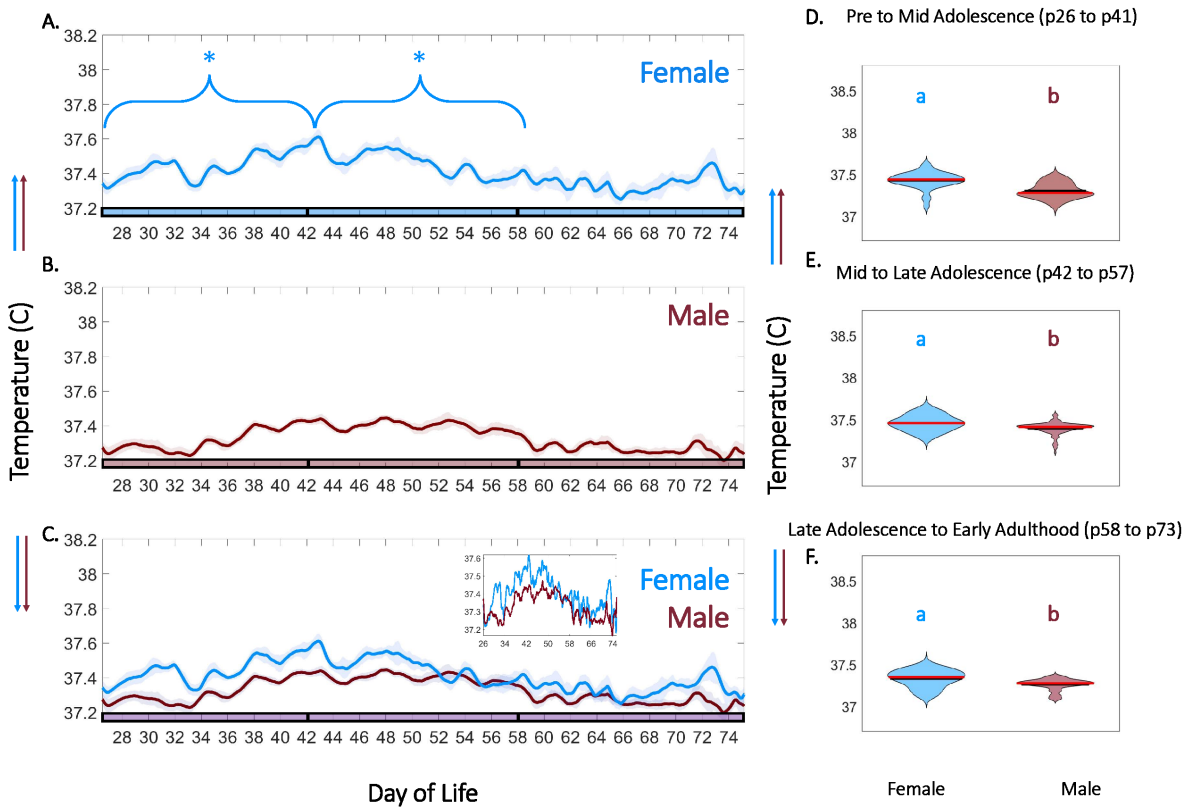


**Figure 4. Adolescence is Associated with Sex-Dependent CBT Trends and Levels.** CBT Linear group means ± S.E.M. in females (blue, **A**), and males (red, B). * Indicates statistically significant MK trend during the bracketed time period. Phase of adolescence cutoffs (early to mid, mid to late, and late to adult) are indicated by breaks in the colored x-axis at p42 and p58. Females exhibit a statistically significant upward trend in body temperature from pre to mid adolescence (A-C), and a downward trend in body temperature from mid to late adolescence (A). Violin plots of female and male temperatures across adolescence indicate that females exhibit wider ranging (a,b indicate significant difference) and elevated temperatures compared to males (C, zoomed inset; D-F).

## 3.5 Discussion and Conclusions

The present findings that CBT features gathered in a naturalistic environment can be used to monitor adolescence, despite the additional variability in sex steroid concentrations and environmental factors compared to a traditional laboratory environment. Adolescent trends in CBT and CBT rhythmicity observed in the present study were akin to those of females examined in the laboratory, with notable sex differences. Males and females exhibited differential trends and amplitude in CR and UR power, with the most notable being the rapid onset of CBT rhythms associated with ovulatory cycling in females following the rise in fE2 and vaginal opening. CR power increased from pre to mid puberty in both sexes, with females exhibiting higher CBT and lower CR power than males. Despite the observation of higher and more variable fE2 compared to lab-reported values, females retained a statistically significant correlation between fE2 and CR power after pubertal onset[13]. In contrast to the coordinated patterns in fE2 and CBT in females, coordinated changes in CBT structure and testosterone were not observed in males. Together, these findings affirm that CBT and CBT rhythmicity remain informative in variable environments, particularly in females, and support the potential for using CBT for monitoring in humans in despite greater environmental variability.

The similarity among the trajectories of circadian power in males and females is intriguing given that fT rose much later in males than fE2 in females[11,18,70]. Because rise in fT was temporally decoupled from rhythmic metrics and preputial separation, a sex-steroid-independent physiological change might drive early changes in male CBT rhythmicity (e.g., such as melatonin[71,72] or growth hormone[14,73]). Despite gross similarities in adolescent circadian, ultradian, and CBT trajectories between the sexes, the elevated CBT (which persists into adulthood[12]) and the persistent depression of circadian power in females relative to males, suggest that continuous-temperature-based diagnostic algorithms may perform more accurately if sex is taken into consideration.

If the features described here have analogous counterparts in human populations, as has recently been shown for continuous temperature for female LH surge anticipation[5,74], pregnancy[13], and fever[6]; then this approach can be applied to develop powerful tools to further understand key developmental events. At present, children in developed nations begin puberty at an earlier age[75–79], are subject to widely varying temporal disruptions in the form of light at night[80–82], late meals[81], and female hormonal contraceptives[83] and clinicians are equipped with relatively low temporal resolution tools for pubertal staging and diagnosis[1,4,84]. Likewise, the importance of rhythmic stability throughout adolescent development is often not considered by families or pediatricians[85].

Peripheral measurements of temperature, such as those from the iButton[86] or Oura Ring[5,87], could be sufficient for peripubertal detection of temperature and ultradian power rises[5], and could be used to develop a population-wide database characterizing features associated with pubertal onset and development. Indeed, rhythmic features of body temperature have already formed the basis of methods for monitoring reproductive health, including pubertal onset[13] and contraceptive use in a laboratory setting[13], adult fertility in controlled and real world conditions[5,65,88,89], and pregnancy in the laboratory[64,90]. Such tools could be informative and empowering to young people during puberty, potentially anticipating first onset of menses[3,7], impending growth spurts,

or for identifying adverse reactions to disruptive behavior[53,91] and medication[83]. If adopted and studied in teen populations, these metrics could be used to generate the first high-temporal-resolution images of healthy adolescent development and to aid early diagnosis via detection of deviations from a personalized healthy trajectory.

Together, non-invasive sex steroid measurement and chronic observation of CBT rhythms and amplitude represent promising metrics for the detection of pubertal onset and monitoring of the developmental trajectory in both sexes under naturalistic conditions, particularly in females. Future work is needed to determine the extent to which such features are extant and coordinated with markers of puberty in humans, but the present findings in rats suggest the feasibility of such an approach.

## 3.6 Acknowledgements

The authors would like to thank Andrew Ahn, Ronald Dahl, Frédéric Theunissen, and Albert Qü for their helpful feedback on methods.

## 3.7 Supplemental Figures

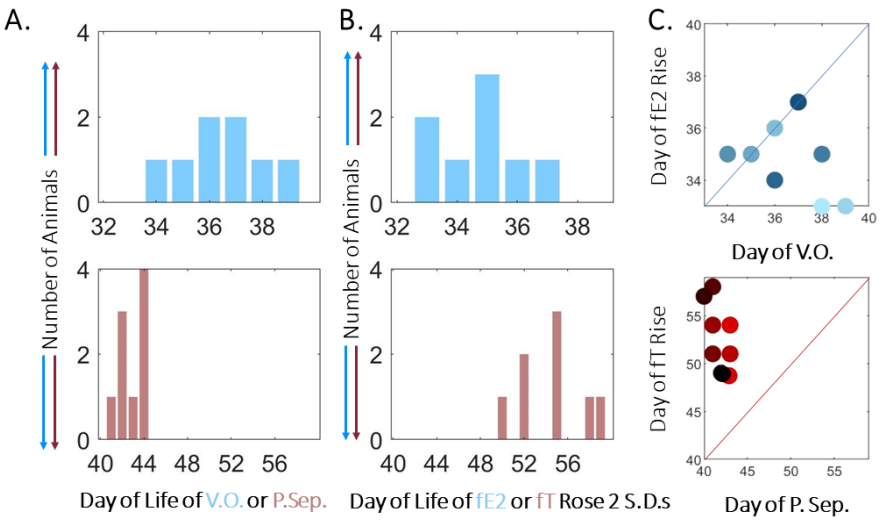


**Supplemental Figure 1: External Pubertal Signs Differ in Time from Sex Steroid Rise.** Distribution of the day of life on which vaginal opening (top) or preputial separation (bottom) (A) versus rise in fE2 (top) and rise in fT (bottom) (B) illustrate that females' external and hormonal pubertal onset markers are more tightly coupled than in males. Scatter (C) of day of external marker versus day of hormonal rise >2 S.D.

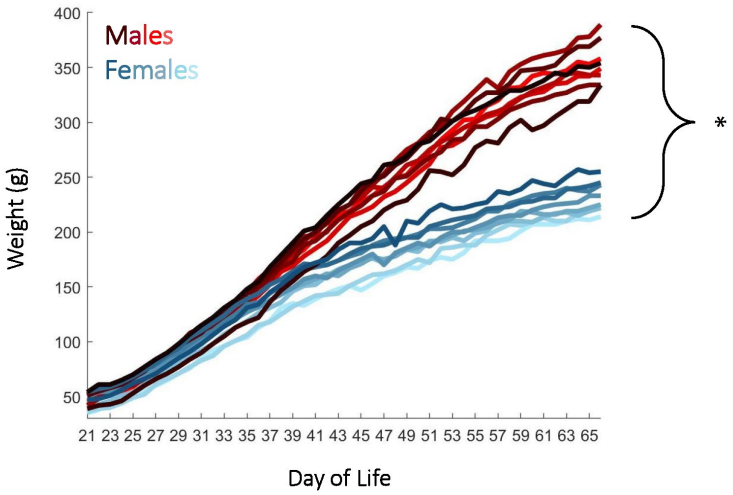


**Supplemental Figure 2: Male and Female Pubertal Weight Trajectory.** Plot of day of life and weight for females (blue gradient) and males (red gradient). Male and female weights differ statistically by the approximate time of female pubertal onset, p39.

## 3.8 References


1. Elchuri, S. V. & Momen, J. J. Disorders of Pubertal Onset. *Prim. Care Clin. Off. Pract.* **47**, 189–216 (2020).
2. Rueda-Quijano, S. M. *et al.* [Concordance of the assessment of pubertal development with the Tanner scale between adolescents and a trained physician]. *Rev. Peru. Med. Exp. Salud Publica* **36**, 408–413 (2019).
3. Fowler, L. R., Gillard, C. & Morain, S. Teenage Use of Smartphone Applications for Menstrual Cycle Tracking. *Pediatrics* **145**, (2020).
4. Klein, D. A., Emerick, J. E., Sylvester, J. E. & Vogt, K. S. Disorders of Puberty: An Approach to Diagnosis and Management. *Am. Fam. Physician* **96**, 590–599 (2017).
5. Grant, A. D., Newman, M. & Kriegsfeld, L. J. Ultradian rhythms in heart rate variability and distal body temperature anticipate onset of the luteinizing hormone surge. *Sci. Rep.* **10**, 20378 (2020).
6. Smarr, B. L. *et al.* Feasibility of continuous fever monitoring using wearable devices. *Sci. Rep.* **10**, (2020).
7. Wartella, E., Rideout, V., Montague, H., Beaudoin-Ryan, L. & Lauricella, A. Teens, health and technology: A national survey. *Media Commun.* **4**, 13–23 (2016).
8. Gear, A. J. C. H. J. C. H. Wearables Are Totally Failing the People Who Need Them Most. *WIRED* https://www.wired.com/2014/11/where-fitness-trackers-fail/ (2014).
9. Campbell-Page, R. M. & Shaw-Ridley, M. Managing Ethical Dilemmas in Community-Based Participatory Research With Vulnerable Populations. *Health Promot. Pract.* **14**, 485–490 (2013).
10. Grant, A. D., Wolf, G. I. & Nebeker, C. Approaches to governance of participant-led research: a qualitative case study. *BMJ Open* **9**, e025633 (2019).
11. Hagenauer, M. H. *et al.* Changes in circadian rhythms during puberty in Rattus norvegicus: developmental time course and gonadal dependency. *Horm. Behav.* **60**, 46–57 (2011).
12. Zuloaga, D. G., McGivern, R. F. & Handa, R. J. Organizational influence of the postnatal testosterone surge on the circadian rhythm of core body temperature of adult male rats. *Brain Res.* **1268**, 68–75 (2009).
13. Grant, A. D., Wilbrecht, L. & Kriegsfeld, L. J. Adolescent Development of Biological Rhythms: Estradiol Dependence and Effects of Combined Contraceptives. *bioRxiv* 2021.07.20.453145 (2021) doi:10.1101/2021.07.20.453145.
14. Grant, A. D., Wilsterman, K., Smarr, B. L. & Kriegsfeld, L. J. Evidence for a Coupled Oscillator Model of Endocrine Ultradian Rhythms. *J. Biol. Rhythms* **33**, 475–496 (2018).
15. Goh, G. H., Maloney, S. K., Mark, P. J. & Blache, D. Episodic Ultradian Events—Ultradian Rhythms. *Biology* **8**, 15 (2019).
16. Mohawk, J. A., Green, C. B. & Takahashi, J. S. Central and peripheral circadian clocks in mammals. *Annu. Rev. Neurosci.* **35**, 445–462 (2012).
17. Bourguignon, J. P. Time-related neuroendocrine manifestations of puberty: a combined clinical and experimental approach extracted from the 4th Belgian Endocrine Society lecture. *Horm. Res.* **30**, 224–234 (1988).
18. MacKinnon, P. C. B., Puig-Duran, E. & Laynes, R. Reflections on the attainment of puberty in the rat: have circadian signals a role to play in its onset? *Reproduction* **52**, 401–412 (1978).

19. Garcia, J., Rosen, G. & Mahowald, M. Circadian rhythms and circadian rhythm disorders in children and adolescents. *Semin. Pediatr. Neurol.* **8**, 229–240 (2001).
20. Vidal, J. D. The Impact of Age on the Female Reproductive System. *Toxicol. Pathol.* **45**, 206–215 (2017).
21. Norjavaara, E., Ankarberg, C. & Albertsson-Wikland, K. Diurnal rhythm of 17 beta-estradiol secretion throughout pubertal development in healthy girls: evaluation by a sensitive radioimmunoassay. *J. Clin. Endocrinol. Metab.* **81**, 4095–4102 (1996).
22. Albertsson-Wikland, K. *et al.* Twenty-Four-Hour Profiles of Luteinizing Hormone, Follicle-Stimulating Hormone, Testosterone, and Estradiol Levels: A Semilongitudinal Study throughout Puberty in Healthy Boys. *J. Clin. Endocrinol. Metab.* **82**, 541–549 (1997).
23. Ankarberg, C. & Norjavaara, E. Diurnal rhythm of testosterone secretion before and throughout puberty in healthy girls: correlation with 17beta-estradiol and dehydroepiandrosterone sulfate. *J. Clin. Endocrinol. Metab.* **84**, 975–984 (1999).
24. The Mammalian Circadian Timing System: Organization and Coordination of Central and Peripheral Clocks. *Annu. Rev. Physiol.* **72**, 517–549 (2010).
25. Daan, S. & Slopsema, S. Short-term rhythms in foraging behaviour of the common vole,Microtus arvalis. *J. Comp. Physiol.* **127**, 215–227 (1978).
26. Hoogenboom, I., Daan, S., Dallinga, J. H. & Schoenmakers, M. Seasonal Change in the Daily Timing of Behaviour of the Common Vole, Microtus arvalis. *Oecologia* **61**, 18–31 (1984).
27. Lewis, R. & Curtis, J. T. Male prairie voles display cardiovascular dipping associated with an ultradian activity cycle. *Physiol. Behav.* **156**, 106–116 (2016).
28. Bhavani, S. V. *et al.* Identifying Novel Sepsis Subphenotypes Using Temperature Trajectories. *Am. J. Respir. Crit. Care Med.* **200**, 327–335 (2019).
29. Akin, A. & Elstein, M. The value of the basal temperature chart in the management of infertility. *Int. J. Fertil.* **20**, 122–124 (1975).
30. Williams, H., Dacks, P. A. & Rance, N. E. An Improved Method for Recording Tail Skin Temperature in the Rat Reveals Changes During the Estrous Cycle and Effects of Ovarian Steroids. *Endocrinology* **151**, 5389–5394 (2010).
31. Buxton, C. L. & Atkinson, W. B. Hormonal factors involved in the regulation of basal body temperature during the menstrual cycle and pregnancy. *J. Clin. Endocrinol. Metab.* **8**, 544–549 (1948).
32. Joyce, D. S., Zele, A. J., Feigl, B. & Adhikari, P. The accuracy of artificial and natural light measurements by actigraphs. *J. Sleep Res.* **29**, e12963 (2020).
33. Stothard, E. R. *et al.* Circadian Entrainment to the Natural Light-Dark Cycle across Seasons and the Weekend. *Curr. Biol.* **27**, 508–513 (2017).
34. Steiger, S. S. *et al.* When the sun never sets: diverse activity rhythms under continuous daylight in free-living arctic-breeding birds. *Proc. Biol. Sci.* **280**, 20131016 (2013).
35. Lafaille, M., Gouat, P. & Féron, C. Efficiency of delayed reproduction in Mus spicilegus. *Reprod. Fertil. Dev.* **27**, 491–496 (2015).
36. Kim, H. J. & Harrington, M. E. Neuropeptide Y-deficient mice show altered circadian response to simulated natural photoperiod. *Brain Res.* **1246**, 96–100 (2008).
37. Meijer, J. H., Michel, S., Vanderleest, H. T. & Rohling, J. H. T. Daily and seasonal adaptation of the circadian clock requires plasticity of the SCN neuronal network. *Eur. J. Neurosci.* **32**, 2143–2151 (2010).

38. Brown-Douglas, C. G., Firth, E. C., Parkinson, T. J. & Fennessy, P. F. Onset of puberty in pasture-raised Thoroughbreds born in southern hemisphere spring and autumn. *Equine Vet. J.* **36**, 499–504 (2004).
39. Park, J. H., Spencer, E. M., Place, N. J., Jordan, C. L. & Zucker, I. Seasonal control of penile development of Siberian hamsters (Phodopus sungorus) by daylength and testicular hormones. *Reprod. Camb. Engl.* **125**, 397–407 (2003).
40. Silva, C.-C. & Domínguez, R. Clock control of mammalian reproductive cycles: Looking beyond the pre-ovulatory surge of gonadotropins. *Rev. Endocr. Metab. Disord.* **21**, 149–163 (2020).
41. Woodruff, J. A., Lacey, E. A. & Bentley, G. Contrasting fecal corticosterone metabolite levels in captive and free-living colonial tuco-tucos (Ctenomys sociabilis). *J. Exp. Zool. Part Ecol. Genet. Physiol.* **313A**, 498–507 (2010).
42. Woodruff, J. A., Lacey, E. A., Bentley, G. E. & Kriegsfeld, L. J. Effects of social environment on baseline glucocorticoid levels in a communally breeding rodent, the colonial tuco-tuco (Ctenomys sociabilis). *Horm. Behav.* **64**, 566–572 (2013).
43. Bakshi, V. P. & Geyer, M. A. Ontogeny of isolation rearing-induced deficits in sensorimotor gating in rats. *Physiol. Behav.* **67**, 385–392 (1999).
44. Boggiano, M. M. *et al.* Effect of a cage divider permitting social stimuli on stress and food intake in rats. *Physiol. Behav.* **95**, 222–228 (2008).
45. Touma, C., Palme, R. & Sachser, N. Analyzing corticosterone metabolites in fecal samples of mice: a noninvasive technique to monitor stress hormones. *Horm. Behav.* **45**, 10–22 (2004).
46. Millspaugh, J. J. & Washburn, B. E. Within-sample variation of fecal glucocorticoid measurements. *Gen. Comp. Endocrinol.* **132**, 21–26 (2003).
47. Harper, J. M. & Austad, S. N. Fecal glucocorticoids: a noninvasive method of measuring adrenal activity in wild and captive rodents. *Physiol. Biochem. Zool. PBZ* **73**, 12–22 (2000).
48. Auer, K. E. *et al.* Measurement of Fecal Testosterone Metabolites in Mice: Replacement of Invasive Techniques. *Anim. Open Access J. MDPI* **10**, (2020).
49. Place, 1514 Eisenhower & Ann Arbor, M. 48108-3284. Steroid Solid Extraction. *Arbor Assays* https://www.arborassays.com/resource/steroid-solid-extraction/.
50. Neurodevelopmental Consequences of Maternal Omega-3 Fatty Acid Deficiency - ProQuest. https://search.proquest.com/openview/2b9eaffc7b3f492b60daf6e1fababebd/1?pq-origsite=gscholar&cbl=2026366&diss=y.
51. Lv, X. *et al.* Reprogramming of ovarian granulosa cells by YAP1 leads to development of high-grade cancer with mesenchymal lineage and serous features. *Sci. Bull.* **65**, 1281–1296 (2020).
52. Mathew, L., Gaikwad, A., Gonzalez, A., Nugent, E. K. & Smith, J. A. Evaluation of Active Hexose Correlated Compound (AHCC) in Combination With Anticancer Hormones in Orthotopic Breast Cancer Models. *Integr. Cancer Ther.* **16**, 300–307 (2017).
53. Asimes, A., Kim, C. K., Cuarenta, A., Auger, A. P. & Pak, T. R. Binge Drinking and Intergenerational Implications: Parental Preconception Alcohol Impacts Offspring Development in Rats. *J. Endocr. Soc.* **2**, 672–686 (2018).
54. Kalliokoski, O., Teilmann, A. C., Abelson, K. S. P. & Hau, J. The distorting effect of varying diets on fecal glucocorticoid measurements as indicators of stress: A cautionary demonstration using laboratory mice. *Gen. Comp. Endocrinol.* **211**, 147–153 (2015).

55. Steadman, C. The effect of spinal cord injury on sexual function. (University of Louisville, 2019). doi:10.18297/etd/3283.
56. Steadman, C. J., Hoey, R. F., Montgomery, L. R. & Hubscher, C. H. Activity-Based Training Alters Penile Reflex Responses in a Rat Model of Spinal Cord Injury. *J. Sex. Med.* **16**, 1143–1154 (2019).
57. Franklin, A. D., Waddell, W. T., Behrns, S. & Goodrowe, K. L. Estrous cyclicity and reproductive success are unaffected by translocation for the formation of new reproductive pairs in captive red wolves (Canis rufus). *Zoo Biol.* **39**, 230–238 (2020).
58. Righetti, F. *et al.* How reproductive hormonal changes affect relationship dynamics for women and men: A 15-day diary study. *Biol. Psychol.* **149**, 107784 (2020).
59. azuredominique. *azuredominique/Rat-Puberty-Lab-Conditions*. (2021).
60. Kriegsfeld-Lab - Overview. *GitHub* https://github.com/Kriegsfeld-Lab.
61. Leise, T. L. Wavelet analysis of circadian and ultradian behavioral rhythms. *J. Circadian Rhythms* **11**, 5 (2013).
62. Leise, T. L. Chapter Five - Wavelet-Based Analysis of Circadian Behavioral Rhythms. in *Methods in Enzymology* (ed. Sehgal, A.) vol. 551 95–119 (Academic Press, 2015).
63. Lilly, J. M. & Olhede, S. C. Generalized Morse Wavelets as a Superfamily of Analytic Wavelets. *IEEE Trans. Signal Process.* **60**, 6036–6041 (2012).
64. Smarr, B. L., Zucker, I. & Kriegsfeld, L. J. Detection of Successful and Unsuccessful Pregnancies in Mice within Hours of Pairing through Frequency Analysis of High Temporal Resolution Core Body Temperature Data. *PloS One* **11**, e0160127 (2016).
65. Smarr, B. L., Grant, A. D., Zucker, I., Prendergast, B. J. & Kriegsfeld, L. J. Sex differences in variability across timescales in BALB/c mice. *Biol. Sex Differ.* **8**, 7 (2017).
66. Sanchez-Alavez, M. *et al.* Insulin causes hyperthermia by direct inhibition of warm-sensitive neurons. *Diabetes* **59**, 43–50 (2010).
67. Kottler, M. L., Coussieu, C., Valensi, P., Levi, F. & Degrelle, H. Ultradian, circadian and seasonal variations of plasma progesterone and LH concentrations during the luteal phase. *Chronobiol. Int.* **6**, 267–277 (1989).
68. de Kloet, E. R. & Sarabdjitsingh, R. A. Everything has rhythm: focus on glucocorticoid pulsatility. *Endocrinology* **149**, 3241–3243 (2008).
69. Violin Plots 101: Visualizing Distribution and Probability Density. https://mode.com/blog/violin-plot-examples/.
70. Sengupta, P. The Laboratory Rat: Relating Its Age With Human's. *Int. J. Prev. Med.* **4**, 624–630 (2013).
71. Rivest, R. W., Aubert, M. L., Lang, U. & Sizonenko, P. C. Puberty in the rat: modulation by melatonin and light. *J. Neural Transm. Suppl.* **21**, 81–108 (1986).
72. Cavallo, A. Melatonin and human puberty: current perspectives. *J. Pineal Res.* **15**, 115–121 (1993).
73. Dunger, D. B., Matthews, D. R., Edge, J. A., Jones, J. & Preece, M. A. Evidence for temporal coupling of growth hormone, prolactin, LH and FSH pulsatility overnight during normal puberty. *J. Endocrinol.* **130**, 141–149 (1991).
74. Webster, W. W. & Smarr, B. Using Circadian Rhythm Patterns of Continuous Core Body Temperature to Improve Fertility and Pregnancy Planning. *J. Circadian Rhythms* **18**, 5 (2020).

75. Delemarre-van de Waal, H. A., van Coeverden, S. C. C. M. & Engelbregt, M. T. J. Factors affecting onset of puberty. *Horm. Res.* 57 Suppl 2, 15–18 (2002).
76. Herbison, A. E. Control of puberty onset and fertility by gonadotropin-releasing hormone neurons. *Nat. Rev. Endocrinol.* 12, 452–466 (2016).
77. Chittwar, S., Shivprakash & Ammini, A. C. Precocious puberty in girls. *Indian J. Endocrinol. Metab.* 16, S188–S191 (2012).
78. Parent, A.-S. *et al.* The Timing of Normal Puberty and the Age Limits of Sexual Precocity: Variations around the World, Secular Trends, and Changes after Migration. *Endocr. Rev.* 24, 668–693 (2003).
79. Bellis, M. A., Downing, J. & Ashton, J. R. Adults at 12? Trends in puberty and their public health consequences. *J. Epidemiol. Community Health* 60, 910–911 (2006).
80. Casper, R. F. & Gladanac, B. Introduction: circadian rhythm and its disruption: impact on reproductive function. *Fertil. Steril.* 102, 319–320 (2014).
81. Jain Gupta, N. & Khare, A. Disruption in daily eating-fasting and activity-rest cycles in Indian adolescents attending school. *PloS One* 15, e0227002 (2020).
82. Smarr, B. L. & Schirmer, A. E. 3.4 million real-world learning management system logins reveal the majority of students experience social jet lag correlated with decreased performance. *Sci. Rep.* 8, 4793 (2018).
83. Apter, D. Contraception options: Aspects unique to adolescent and young adult. *Best Pract. Res. Clin. Obstet. Gynaecol.* 48, 115–127 (2018).
84. Lauffer, P., Mooij, C. F., Zwaveling-Soonawala, N. & Trotsenburg, A. S. P. van. Reforming the male Tanner genital scale. *J. Pediatr. Endocrinol. Metab.* 33, 425–426 (2020).
85. Owens, J. A. & Weiss, M. R. Insufficient sleep in adolescents: causes and consequences. *Minerva Pediatr.* 69, 326–336 (2017).
86. Hasselberg, M. J., McMahon, J. & Parker, K. The validity, reliability, and utility of the iButton® for measurement of body temperature circadian rhythms in sleep/wake research. *Sleep Med.* 14, 5–11 (2013).
87. Maijala, A., Kinnunen, H., Koskimäki, H., Jämsä, T. & Kangas, M. Nocturnal finger skin temperature in menstrual cycle tracking: ambulatory pilot study using a wearable Oura ring. *BMC Womens Health* 19, 150 (2019).
88. Sanchez-Alavez, M., Alboni, S. & Conti, B. Sex- and age-specific differences in core body temperature of C57Bl/6 mice. *Age Dordr. Neth.* 33, 89–99 (2011).
89. Prendergast, B. J., Beery, A. K., Paul, M. J. & Zucker, I. Enhancement and Suppression of Ultradian and Circadian Rhythms across the Female Hamster Reproductive Cycle. *J. Biol. Rhythms* 27, 246–256 (2012).
90. Wang, Z. Y., Cable, E. J., Zucker, I. & Prendergast, B. J. Pregnancy-induced changes in ultradian rhythms persist in circadian arrhythmic Siberian hamsters. *Horm. Behav.* 66, 228–237 (2014).
91. Logan, R. W. *et al.* Impact of Sleep and Circadian Rhythms on Addiction Vulnerability in Adolescents. *Biol. Psychiatry* 83, 987–996 (2018).

# 4. Ultradian Rhythms of Heart Rate Variability and Distal Body Temperature Anticipate Onset of the Luteinizing Hormone Surge

## 4.1 Abstract

The menstrual cycle is characterized by predictable patterns of physiological change across timescales. Although patterns of reproductive hormones across the menstrual cycle, particularly ultradian rhythms, are well described, monitoring these measures repeatedly to predict the preovulatory luteinizing hormone (LH) surge is not practical. In the present study, we explored whether non-invasive measures coupled to the reproductive system: high frequency distal body temperature (DBT), sleeping heart rate (HR), sleeping heart rate variability (HRV), and sleep timing, could be used to anticipate the preovulatory LH surge in women. To test this possibility, we used signal processing to examine these measures in 45 premenopausal and 10 perimenopausal cycles alongside dates of supra-surge threshold LH and menstruation. Additionally, urinary estradiol and progesterone metabolites were measured daily surrounding the LH surge in 20 cycles. Wavelet analysis revealed a consistent pattern of DBT and HRV ultradian rhythm (2–5 h) power that uniquely enabled anticipation of the LH surge at least 2 days prior to its onset in 100% of individuals. Together, the present findings reveal fluctuations in distal body temperature and heart rate variability that consistently anticipate the LH surge, suggesting that automated ultradian rhythm monitoring may provide a novel and convenient method for non-invasive fertility assessment.

## 4.2 Introduction

The fertility-awareness-method (FAM), a set of practices used to estimate the fertile and infertile days of the menstrual cycle, is challenging to implement and to study, and existing studies of its effectiveness are inconclusive[1]. However, an observation-based method of family planning or contraception has several potential benefits, including a lack of hormonal disruption, personalization, and relatively low cost. One challenge inherent to current FAM practices is the reliance on historical basal body temperature and symptom trends (e.g., breast tenderness, libido, cervical fluid) that can vary substantially by individual, within-individual from cycle-to-cycle[2], and that provide predominantly retrospective information. The challenges of FAM have led the majority of those seeking to avoid pregnancy to adopt another form of contraception. Unfortunately, the most widely used method, female hormonal contraception, has short and long term risks for many users, including increased breast cancer rate[3,4], luteal phase deficiency[5], dysmenorrhea[5,6], altered cognition[7,8], and depressed mood[9,10]. These risks, combined with increasing recognition that many physiological systems vary in a structured manner across the menstrual cycle11–14, provide the impetus to develop FAM approaches that employ high-temporal-resolution, non-invasive measures of physiology.

The menstrual cycle is a continuous, rhythmic succession of endocrine, ovarian, and uterine events. Briefly, the cycle begins with onset of menstruation, followed by rising levels of estradiol, follicular maturation, and proliferation of the uterine lining[15,16]. Ovulation, which is triggered by numerous factors including estradiol, a surge of luteinizing hormone (LH), the presence of a mature Graafian follicle, and likely time of day[17], frequently occurs between 1/2 and 3/4 of the way through the cycle in humans[18]. Other physiological systems, including metabolism[19, 20] and autonomic balance[21], fluctuate with the menstrual cycle. An individual is mostly likely to become pregnant during the time leading up to, and shortly past, the ovulation event, making identification of this peri-ovulatory period central for the successful use of the FAM. Although high-frequency hormone.

measurements (e.g., daily estradiol from blood or urine) and ultrasound can provide information on when an LH surge and subsequent ovulation are likely to occur, such measurements are both laborious and expensive, limiting their widespread utility. Furthermore, at home tests available for measuring supra-threshold LH concentrations provide retrospective rather than prospective information about this event. Ideally, new methods of fertility awareness would accurately indicate the approaching peri-ovulatory period via relatively inexpensive and non- invasive means[22]. This study aimed to develop such a preliminary indicator for future, larger scale investigation. The premise of the present investigation is that the presence of structured changes to peripheral biological rhythms across the menstrual cycle may allow for anticipation of the LH surge. Such a finding would further support the notion that the state of one system (e.g., reproductive) can be inferred via measurements of another (e.g., autonomic or metabolic)[14,23,56]. Perhaps the most consistent biological rhythmic changes across the

menstrual cycle occur at the few hour (ultradian rhythm, UR) timescale[14,23–26]. Most elements of the hypothalamic- pituitary-ovarian axis, including gonadotropin releasing hormone (GnRH)[27–29], LH [30–32], FSH[33–36], estradiol[30,37], progesterone[30,31,38–41], and testosterone[42] show URs that are coordinated with menstrual phase[14]. Across species, timeseries of these neuropeptides and hormones exhibit an increase in ultradian frequency and inter-hormone coupling strength leading up to ovulation[29,31] and a decrease in ultradian frequency and stability in the luteal phase[29–32,37,40,41,43]. Additionally, peripheral measures of distal body temperature (DBT) and heart rate variability (HRV) reflect the activity of reproductive[44–46], autonomic[21,23, 47–52], and metabolic systems[23,53–55] and show both URs and menstrual rhythms[44]. These peripheral and endocrine measures are proposed to operate as coupled oscillators at the ultradian timescale. Assessment of these peripheral measures could, therefore, potentially enable endocrine status assessment via timeseries analysis[14,23,56].

Recent animal work supports the idea that non-reproductive measures can be used to anticipate reproductive status. In rodents, the wavelet power of core body temperature URs exhibits a trough on the day of ovulation[12,13]. The translational capability of this method is supported by the association of gross timescale changes in DBT, heart rate (HR), and HRV by menstrual phase[11,19,44,45,53,57–61]. However, it is unknown if human ovulatory cycle phase is associated with patterns of rhythmic change in non-reproductive outputs. Although the specific factors responsible for the changes in frequency of reproductive URs across non-human mammalian ovulatory cycles are not well understood, their consistency of change across species of widely varying cycle lengths suggests a concerted role in ovulatory cycle function[14]. Finally, although the structure of some circadian rhythms (~ 24 h; CRs) is altered in the luteal phase, with estradiol acrophase advancing, and REM sleep exhibiting a modest decrease; structured sleep and circadian changes are not generally observed during the peri-ovulatory period[62]. As both URs and CRs are tightly regulated across systems, monitoring their structure may enable more accurate assessment of reproductive state than is possible using infrequently collected data (e.g., 1 temperature time point per day)[26,63,64]. Wearable devices offer unprecedented ease of collecting the continuous, longitudinal data needed to assess URs and CRs across the menstrual cycle[65–68]. To determine if rhythmic structure exhibits reliable changes leading up to the LH surge, we used a wearable device (the Oura Ring) to monitor DBT, sleeping HR, sleeping HRV (root mean square of successive differences; RMSSD), sleep timing, and duration. If endocrine, metabolic, and autonomic rhythms are sufficiently coupled at the ultradian and circadian timescales, then coordinated patterns should be observed across measures and potentially across the menstrual cycle. Such patterns would contribute to a growing body of work in "network physiology"[69,70], which proposes that changes among endocrine, metabolic, and autonomic outputs are coupled under real world conditions. As mentioned above, implicit in this hypothesis is that one could infer the state of one system via measurements of another. Anticipation of female reproductive events is a test of the network physiology framework with potential for rapid translation.

## 4.3 Materials and Methods

**Ethical approval.** This study and all procedures were approved by the Office for the Protection of Human Subjects at the University of California, Berkeley. All participants gave informed consent. All research was per- formed in accordance with relevant guidelines and regulations.

**Participants and recruitment.** Participants were recruited from the Quantified Self community, a global group of individuals interested in learning through self-measurement[95,96]. Individuals attended a prospective discussion about the project at the 2018 Quantified Self meeting in Portland, Oregon and contacted the experimenter via email if interested in participating. Prospective participants were contacted to discuss study structure, risks and benefits, and to review the informed consent form. Once informed consent was obtained, participants were instructed to complete an introductory questionnaire with their age, cycling status (regular, irregular, recovering from hormone/IUD use, perimenopausal, menopausal), and historical LH surge day(s), if known. Contact information was collected for the purposes of communication and delivery of study materials. Data from pregnancies ($n$ = 3) that overlapped with the study were excluded from these analyses. Participants had not taken hormonal contraception within the prior year and did not have any known reproductive medical concerns. There were no age or parity restrictions, consistent with the principles of participatory research[96,97]. See Table 1 for participant demographics.

**Study design.** Each of the 28 ($n$ = 20 premenopausal, $n$ = 5 perimenopausal, $n$ = 3 premenopausal and became pregnant) participants collected 2 to 3 cycles of data for analysis. For all cycles, the Oura Ring, a DBT, HRV (RMSSD), HR, and sleep sensor, was worn continuously on the finger, as previously described[65,98]. For all cycles, LH was monitored via urinary test strips (Wondfo Biotech Co., Guangzhou, China) from day 10 (with first day of menstruation considered day 1) until a positive reading was detected, and subsequently until 2 days after LH fell below the limit of detection (see below for details on the *Urinary Hormone Assay, Luteinizing Hormone*). Of the 55 total cycles collected (45 = premenopausal, 10 = perimenopausal), 20 were paired with daily, morning urine tests for E2, αPg and βPg, the major urinary progesterone metabolites (Precision Analytical, McMinnville, OR). This study was designed using the principles of participatory research[96,99] in which individual participants maintain control of their own data prior to anonymization and came to the project with personal questions that could be answered with the data to be collected. All participants received a copy of their Oura Ring data.

**Data collection and management.** HR, HRV (RMSSD), DBT, sleep onset, sleep offset, sleep duration, breathing rate, and nightly temperature deviation (described briefly below) were collected using the Oura Ring (Oura Inc., San Francisco, CA; Oura Health Oy, Ltd., Oulu, Finland). The Oura Ring is a small, wireless sensor worn on the finger. By using an LED light source and LED sensor to measure reflection off the skin above the radial artery of the finger, the Oura Ring calculates HR, HRV (RMSSD), and breathing rate. The ring also contains 3 thermistors for detection of DBT. DBT is measured 24 h a day (binned in 1-min intervals). To avoid artifacts associated with activity, HR, and HRV (RMSSD) are only measured during sleep (binned in 5-min intervals), limiting our analyses of HR and HRV (RMSSD) to the sleeping period. All other metrics

are calculated once per night. Briefly, the body temperature deviation for each night is the moving mean of nightly temperature between 10:00 pm and 8:00 am, minus the mean temperature of the previous 20 days. Oura Rings were loaned to the group by Oura Inc.

The Oura Ring can be connected to a mobile phone application, Oura, via Bluetooth. At the start of the study, each participant downloaded the Oura application from either the Google Play Store (Google Inc., Mountain View, CA) or the Apple App Store (Apple Inc, Cupertino, CA) to their mobile phones and created an Oura account. Participants were able to view their own data provided by the application throughout the study. Par- ticipants were asked to synchronize data from the ring to the application each morning. Uploaded data was automatically transferred via the internet to the study database in the Oura cloud service. In order to access data from the cloud, data were imported into the Open Humans[100] framework, which provides encrypted, password protected data access to researchers, with the participants' revocable consent. In addition to data collected by the Oura Ring, participants uploaded personal spreadsheets that tracked days of menstruation, days of LH tests and results, days of urine collection, and notes (e.g., forgot to wear the Oura Ring) to Open Humans. Participants could opt out of the study and remove their data at any time. Data were anonymized by the researchers for analysis. Data, once anonymized at the end of the study, remained in the data set.

Hormone assays. For the assessment of E2, αPg and βPg, participants collected daily, first-morning urine samples across a cycle according to manufacturer's instructions (Precision Analytical, Willamette, OR). Briefly, a standardized piece of filter paper with an attached label was submerged in the urine sample and dried for 24 h. Filter paper was then frozen at ~ -18 C in participants' home freezers until analysis. E2, αPg, and βPg were analyzed using proprietary in-house assays referred to as Dried Urine Testing for Comprehensive Hormones (DUTCH) on the Agilent 7890/7000B GC–MS/MS (Agilent Technologies, Santa Clara, CA, USA). The equivalent of approximately 600 µl of urine was extracted from the filter paper using acetate buffer. In the first week of the cycle, and from 3 days after LH surge completion until the end of the luteal phase, samples were pooled every 2 days (a third day was pooled at the end of cycles in instances where the total number of remaining days after the surge was odd). Urine samples were extracted and analyzed as previously described, with previously established ranges of hormone concentrations expected in urine by phase of cycle and during menopause[90,101]. Briefly, creatinine was measured in duplicate using a conventional colorimetric (Jaffe) assay. Conjugated hormones were extracted (C18 solid phase extraction), hydrolyzed by Helix pomatia and derivatized prior to injection (GC–MS/ MS) and analysis. The mean inter-assay coefficients of variation were 8% for E2, 12% for αPg, and 13% for βPg. The mean intra-assay coefficients of variation were 7% for E2, 12% for αPg and 12% for βPg. Sensitivities of the assays were as follows: E2 and αPg, 0.2 ng/mL; βPg, 10 ng/ mL.

Luteinizing hormone was measured using the commercially available WondFo (Wondfo Biotech Co., Guangzhou, China) Luteinizing Hormone Urinary Test[102], a validated at-home urine assay. Briefly, the strip was sub- merged by participants for 5 s in a fresh urine sample and laid horizontally for 5 min before reading. When samples were collected for E2, αPg and βPg, those same samples were used for LH testing. Each strip contains a positive control and a "test" line,

indicating if LH is present in the urine at, or over a concentration of 25 MIU/ mL[102]. Test results were depicted as either + or – (no quantitative information provided) and were recorded in a personal spreadsheet by the participant. A photograph of each test was taken by participants to ensure accurate reading of the results.

Inclusion and exclusion criteria for collected cycles. Cycles were included in the premenopausal data set as likely ovulatory by four criteria a) one or more localized days of supra-threshold LH concentration, b) the presence of a rise in E2 (if collected) within typical range prior to or coincident with supra threshold LH, c) a subsequent rise in αPg and βPg (if collected), and d) positive values of DBT deviation, as previously described[98], within 2 days of surge onset until the end of the cycle (See Supplemental Fig. 1). Cycles without E2, αPg, and βPg data were included by meeting criteria a and d only. Cycles with missing data within sixteen days of the of the LH surge (defined as no HR/HRV/DBT data for a given night) were omitted in order to avoid erroneous estimation of rhythmic power (see *Data Analysis* below). Cycles were defined as "perimenopausal" by the presence of positive LH measured at least every other day across the cycle and age > 45 years. Four such cycles were paired with daily urinary hormone analysis for E2, αPg, and βPg, as described above.

Data analysis. All code and data used in this paper are available at Open Science Framework (https://osf. io/wzf47/). Code was written in MATLAB 2019b, MATLAB 2020a and Python 3. Wavelet Transform (WT) code was modified from the Jlab toolbox and from Dr. Tanya Leise[103]. Briefly, data were imported from the Open Humans framework to Python 3, where HR, HRV (RMSSD), and DBT data were extracted. Data were cleaned in MATLAB, with any data points outside ± 4 standard deviations set to the median value of the prior hour, and any points showing near instantaneous change, as defined by local abs(derivative) > $10^5$ as an arbitrary cutoff, also set to the median value of the previous hour.

Wavelet transformation (WT) was used to assess the structure of ultradian rhythms of DBT, HR, HRV (RMSSD), and circadian rhythms in DBT. As DBT shows high plateaus during the sleeping period, and URs during the day, DBT analyses here were used on data collected during the waking hours (see Supplemental Fig. 2). Conversely, as indicated previously, because the Oura Ring only collects HR and HRV (RMSSD) during sleep, wavelet analyses were restricted to the sleeping window for these metrics. In either case, the excerpted data were compiled from all days of the cycle resulting in one continuous signal representing all days (DBT) or all nights (HR, HRV (RMSSD)). In contrast to Fourier transforms that transform a signal into frequency space without temporal position (i.e., using sine wave components with infinite length), wavelets are constructed with amplitude diminishing to 0 in both directions from center. This property permits frequency strength calculation at a given position. Wavelets can assume many functions (e.g., Mexican hat, square wave, Morse); the present analyses use a Morse wavelet with a low number of oscillations (defined by $\beta$ and $\gamma$), analogous to wavelets used in previous circadian applications[103]. Morse Wavelet parameters of $\beta = 5$ and $\gamma = 3$ describe the frequencies of the two waves superimposed to create the wavelet; Additional values of $\beta$ (3–8) and $\gamma$ (2–5) did not alter the findings (data not shown)[104]. This low number of oscillations enhances detection of contrast and transitions. The band of the wavelet matrix corresponding to 2–5 h rhythms were

averaged in order to create a linear representation of UR WT power over time. This band corresponded to the timescale of ultradian rhythmicity observed across physiological systems[14,25,56]. Potential changes to circadian power of DBT (mean power per minute within the 23–25 h band) were additionally assessed prior to extracting days for ultradian-only analyses, but no significant changes across the cycle were detected (see Supplemental Fig. 3). Because WTs exhibit artifacts at the edges of the data being transformed, only the WT of the second through the second to last days of data were analyzed further. To enable comparisons across cycles of different durations, premenopausal cycles were displayed from LH surge onset minus 7 days to LH onset plus 7 days. As perimenopausal individuals had tonically high LH, and therefore no surge onset to which all individuals could be aligned, each cycle's midpoint was chosen for alignment.

LH surge anticipation features. Wavelet power in the 2 to 5 h band was calculated as described above. Extracted bands were smoothed using a daily moving average using the MATLAB function "movmean". The MATLAB function "findpeaks" was used to identify peaks as points at which either adjacent point had a lower UR power. This function was run on the negative of the signal to identify troughs. Points at which the derivative of the signal crossed zero, indicating a change in direction of UR power (i.e., either increasing to decreasing or vice versa), were found using the MATLAB function "diff ". The first time the derivative crossed zero in the cycle (i.e., the first inflection point), excluding the first five days of the cycle, during which LH is very unlikely to rise, was marked as the presence of the first feature for either HRV (RMSSD), DBT, or HR. Following this inflection point, the next peak identified by "findpeaks" was marked as the second feature. These methods of identifying peaks, troughs, and direction changes were used to ensure the diff function was identifying all visually identified peaks.

Statistical analyses. Descriptive values are reported as means ± daily standard deviations (SD) unless otherwise stated. For statistical comparisons of average ultradian power in premenopausal and perimenopausal cycles, Kruskal Wallis (KW) tests were used instead of ANOVAS to avoid assumptions of normality for any distribution to assess the trend in average UR power leading up to the surge as compared to after the surge. For KW tests, $\chi^2$ and $p$ values are listed in the text. One-way repeated measures analysis of variance (rmANOVA) tests were used to compare peak average E2 to other days surrounding the surge, and baseline αPg and βPg (7 days prior to the surge) to other days surrounding the surge. For rmANOVAs, $p$ values are listed in the text. Because the dominant trend was an inflection point in UR power followed by a peak, slopes of individual signals were compared rather than raw values at each timepoint. The same tests were applied to individuals, in addition to tests for significance of raw power differences on peak and trough days, using 25 min centered on peaks and troughs, respectively. To avoid multiple comparisons and chance of a type I error, differences between individually-determined peak and trough values of UR WT power found using "findpeaks" were assessed using a KW test, such that each cycle contributed only 1 peak value and 1 trough value (N = 45 data points per group). Figures were formatted in Microsoft PowerPoint 2019 (Microsoft Inc., Redmond, WA) and Adobe Photoshop CS8 (Adobe Inc, San Jose, CA).

## 4.4 Results

**Demographics.** Findings are reported for individuals with premenopausal cycles ($n$ = 20, $n$ = 45 cycles, 2–3 cycles per individual) or perimenopausal cycles as ($n$ = 5, $n$ = 10 cycles, 2 cycles per individual) as defined in the Methods. Individuals who became pregnant ($n$ = 3) during the study were excluded from the analyses. All premenopausal participants experienced menses, 1 or more supra-threshold LH readings per cycle, and a sub- sequent, sustained rise in temperature deviation during all cycles. See Table 1 for participant age, ethnicity, cycle length, LH surge length, LH surge onset timing, LH surge onset relative to estradiol (E2) peak and progesterone rise, and percent of individuals with regular cycles. Some variability was observed in the day of LH surge onset relative to day of E2 peak(s), as previously reported[71].

**Premenopausal and perimenopausal estradiol, luteinizing hormone, and progesterone metabolites.** Participants monitored LH for all 55 cycles, whereas daily urine samples were collected by 20 women ($n$ = 16 premenopausal, $n$ = 4 perimenopausal) for the measurement of E2, α-Pregnanediol (αPg) and β-Pregnanediol (βPg). E2, αPg and βPg were collected to confirm that hormone concentrations were within healthy ranges for pre-menopausal women and that LH surges were followed by a rise in progesterone metabolites. For all 16 cycles, estradiol, αPg and βPg fell within normal ranges, with a pre-LH rise in E2 (2 days prior to LH onset through LH onset day were significantly greater than all other days, $p < 0.01$ in all cases). Likewise, LH surge onset was concomitant with a significant rise in αPg ($p < 0.05$ on LH onset, and < 0.01 6 days after LH onset and thereafter) (Fig. 1A–C) and βPg ($p < 0.005$ on LH onset, and < 0.001 3 days after LH onset; data not shown for βPg). These hormonal changes were associated with a rise in temperature deviation above zero and a non-significant elevation of breathing rate around LH surge onset (Supplemental Fig. 1E–F). Consistent with previous findings[71], LH surge length was variable, with 42% of individuals exhibiting supra-threshold LH concentrations 2 days following surge onset, falling to 26% of individuals 3 days after surge onset (Fig. 1A). LH was tonically supra-threshold in perimenopausal women ($n$ = 10 cycles, Fig. 1D). Perimenopausal individuals exhibited a significant increase in αPg and βPg only 6 days after midcycle ($p < 0.05$; data not shown for βPg), and a trend toward elevation of E2 prior to mid cycle ($p = 0.176$) (Fig. 1D–F).

| Factor | Premenopausal | Perimenopausal |
|---|---|---|
| Number of participants | 20 | 6 |
| Number of cycles | 45 | 10 |
| Age range, mean (STDEV) *years* | 21–38, 32 (4) | 48–60, 55 (5) |
| Ethnicity (%) | Caucasian: 94;<br>African American 6 | Caucasian: 100% |
| Cycle length | 25–36, 27.78 (4.16) | 22–50, 28.7 (8.87) |
| LH surge length range, mean (STDEV) *days* | 1–5,1.95 (1.2) | N/A; LH tonically high |
| LH surge onset day | 10–29, 15.75 (3.4) | N/A; LH tonically high |
| LH surge onset relative to E2 peak in *days* | 0–4, 1.67, (1.38) | N/A ; LH tonically high |
| LH surge day relative to progesterone rise *day*($n$ = 21) | 0–5, 1.14, (1.95) | N/A; LH tonically high |
| Regular cyclers (%) | 88 | 0 |

**Table 1.** Demographics of the QCycle cohort, including $n$ values, age, ethnicity, and hormonal cyclecharacteristics.

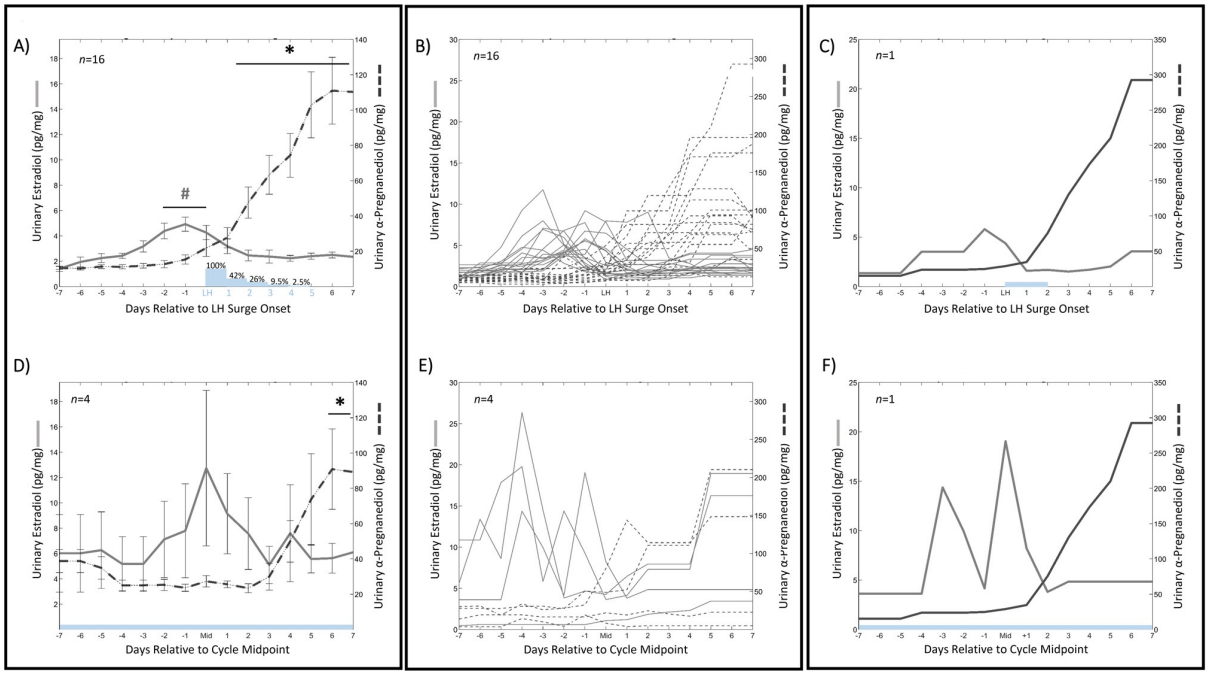


**Figure 1. Ovulatory & Perimenopausal E2 and αPg. Linear plots of premenopausal (A–C) and perimenopausal (D–F) E2 and αPg.** Mean ± standard deviation E2 (solid) and αPg (dashed) concentrations for premenopausal (**A**) and perimenopausal cycles (**D**) within one week of LH surge onset (N = 16 out of 45 premenopausal cycles, and N = 4 out of 10 perimenopausal cycles). # Indicates significantly elevated pre-LH E2 concentrations (premenopausal $p = 5.5 \times 10^{-5}$; perimenopausal non-significant $p = 0.391$), and * indicates significantly elevated αPg after LH surge onset (premenopausal $p = 4.71 \times 10^{-31}$; perimenopausal, $p = 0.028$). Blue bars and text and indicate percent of cycles showing an LH surge a given number of days after onset, beginning on the day marked "LH" (e.g., 26% indicates that 26% of individuals were still surging on the 3rd day after LH surge onset). Representative E2 (gray) and αPg (black) from premenopausal (**C**) and perimenopausal (**F**) individuals relative to LH surge onset, and cycle mid-point, respectively.

**Ultradian power of DBT, HRV, and LH surge onset.** Ultradian (2–5 h) power of daytime DBT exhibited a stereotyped pattern preceding LH surge onset in premenopausal (Fig. 2A,B), but not perimenopausal (Fig. 2C,D), cycles. Ultradian DBT power exhibited an inflection point a mean of 5.82 (± 1.82) days prior to LH surge onset and a subsequent peak a mean of 2.58 (± 1.89) days prior to the surge onset. A second troughin UR power occurred a mean of 2.06 (± 1.02) days after surge onset ($\chi^2 = 5.66$, p = 0.0174,). These stereotyped changes were not present in perimenopausal cycles ($\chi^2 = 0.37$, p = 0.5354, for the same comparisons) (Fig. 2C).

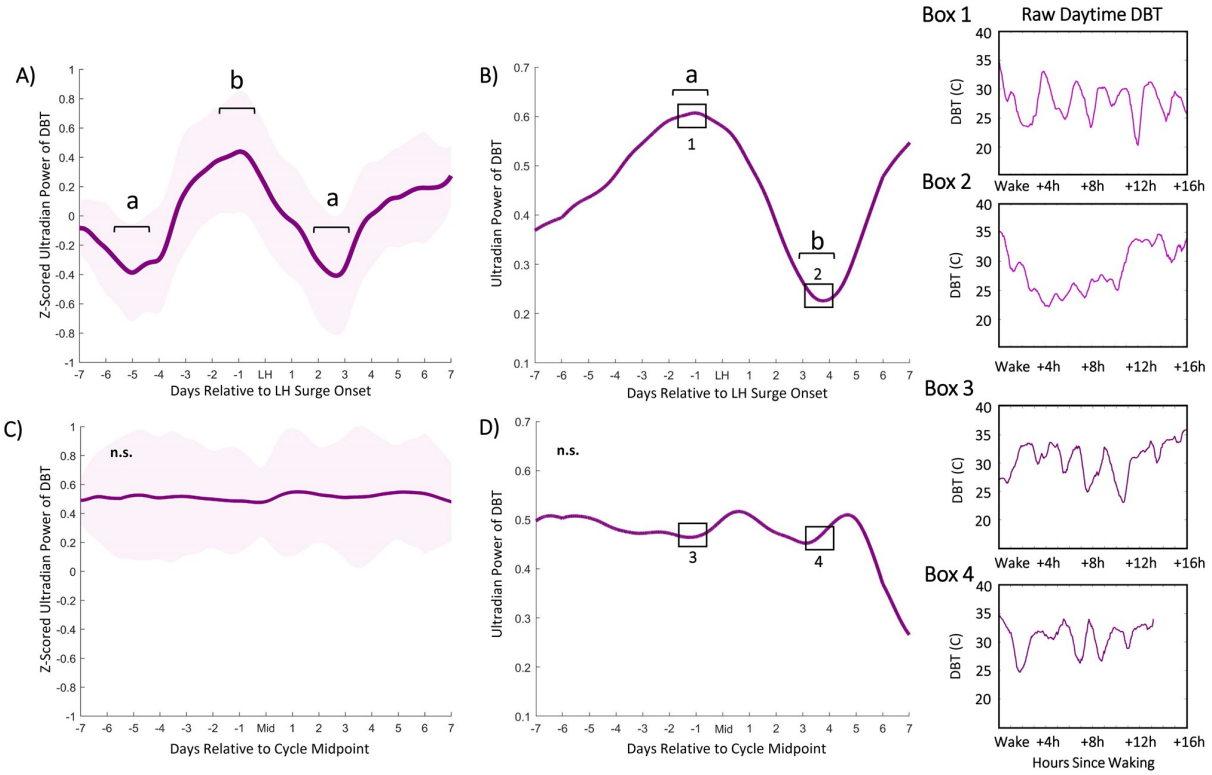


**Figure 2. Ultradian power of DBT anticipates LH surge onset. Mean DBT ultradian power (z-scored) ± standard deviation for premenopausal cycles (A) within one week of LH surge onset and perimenopausal cycles (C) within one week of mid cycle.** DBT UR power peaks exhibit an inflection point 5.82 (± 1.82) days prior to LH onset, a peak a mean of 2.58 (± 1.89) before LH onset on average and a subsequent trough a mean of 2.6 (± 1.02) days after surge onset ($\chi^2$ = 5.66, *p* = 0.0174). Perimenopausal UR power shows no conserved peaks and troughs ($\chi^2$ = 0.37, *p* = 0.5354, for same comparisons). Representative individual example of raw DBT ultradian power within one week of LH surge onset in premenopausal (B) and within one week of mid cycle in perimenopausal (D) cycles. Black squares in (B) and (D) correspond to Boxes 1 & 2 and Boxes 3 & 4, respectively. Boxes show linear waking DBT from which ultradian power in B and D were generated; these days were selected to visually illustrate days of relatively high and low ultradian power in premenopausal cycles, and the same two days in perimenopausal cycles.

Ultradian power of sleeping HRV (RMSSD) also exhibited a stereotyped fluctuation preceding LH surge onset in premenopausal (Fig. 3A,B), but not perimenopausal (Fig. 3C,D), cycles. Ultradian HRV (RMSSD) power showed an inflection point with a mean of 5.82 (± 1.53) nights prior to LH surge onset, a subsequent peak with a mean of 2.58 (± 1.59) nights prior to the surge onset and a trough a mean of 2.11 (± 1.27) days after surge onset. ($\chi^2$ = 4.91, p = 0.034). These stereotyped changes were not present in perimenopausal cycles ($\chi^2$ = 0.4797, p = 0.57) (Fig. 3C). Ultradian power of HR and circadian power of DBT did not show a significant pattern of change preceding the LH surge ($\chi^2$ = 0.3 and 1.12, p = 0.581 and 0.2899), nor mid cycle in perimenopausal individuals ($\chi^2$ = 0.02 and 1.65, p = 0.8798 and 0.1984, respectively) (See Supplemental Figs. 2 and 3). No significant trends were observed in sleep metrics captured once per night (See Supplemental Fig. 1). Linear means of nightly HR and HRV, and continuous DBT did not yield consistent patterns of change relative to surge onset or peri- menopausal midcycle (Supplemental Figs. 4–6).

**Inflection points and subsequent peaks of DBT and HRV ultradian power anticipate LH surge onset.** In premenopausal women, the first inflection point of DBT and HRV (RMSSD) UR power occurred between -8 and -2 days prior to surge onset, whereas the subsequent peak in UR power for both metrics occurred between -6 days before to 2 days after LH surge onset (Fig. 4). 85% of cycles exhibited the first inflection point by 4 days prior to the surge, with 100% showing this inflection by 2 days prior to the surge. The peak of UR power occurred at least 1 day prior to the surge in 82% of cycles. Together, these inflection points and subsequent peaks in UR power of HRV (RMSSD) and DBT uniquely anticipated the LH surge days before its onset (see "Discussion" for potential relevance to the fertile window).

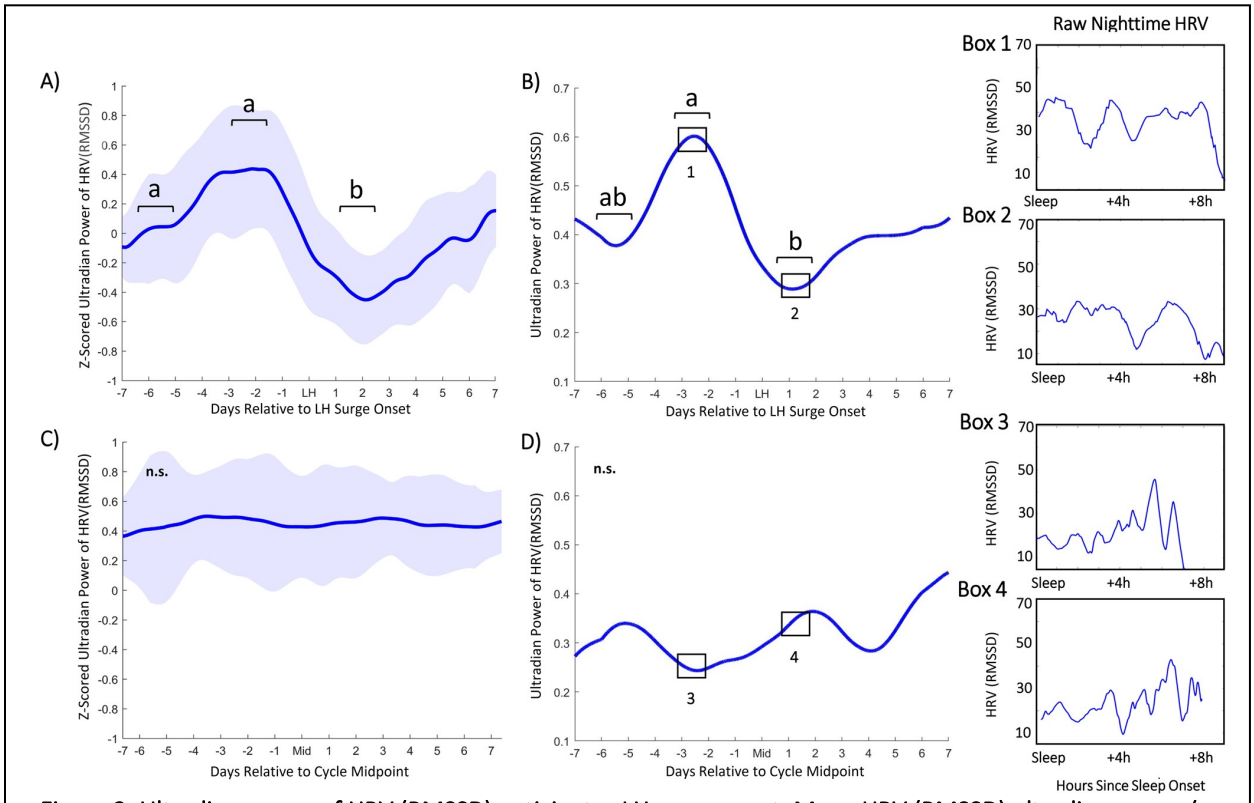


**Figure 3. Ultradian power of HRV (RMSSD) anticipates LH surge onset. Mean HRV (RMSSD) ultradian power (z-scored) ± standard deviation for premenopausal cycles (A) within one week of LH surge onset and perimenopausal cycles (C) within one week of mid cycle.** Ultradian HRV (RMSSD) power inflects an average of 5.82 (± 1.53) nights prior to LH surge onset, exhibits a subsequent peak an average of 2.58 (± 1.59) days prior to the surge onset and a trough an average of 2.11 (± 1.27) days after surge onset. ($\chi 2 = 4.91$, $p = 0.034$,). These stereotyped changes are not present in perimenopausal cycles ($\chi 2 = 0.4797$, $p = 0.57$). Representative individual example of HRV (RMSSD) ultradian power within one week of LH surge onset in premenopausal (B) and perimenopausal (D) cycles. Black boxes in (B) and (D) correspond to Boxes 1 & 2 and Boxes 3 & 4, respectively. Boxes show linear sleeping HRV (RMSSD) signal from which (B) and (D) were generated, illustrating days of relatively high and low ultradian power in ovulatory cycles, and the same two days in perimenopausal cycles.

## 4.5 Discussion and Conclusions

The present findings reveal stereotyped fluctuations in DBT and HRV (RMSSD) UR power that anticipate 100% of LH surge onsets, a key component of female health and fertility. By contrast, changes in DBT circadian rhythm power were not predictive of the LH surge, suggesting that URs are uniquely coupled to the pre-ovulatory time of the menstrual cycle. Likewise, discrete, nightly behavioral, and physiological measures did not anticipate the surge, suggesting that continuous measures of physiological output provide signals more amenable to LH surge anticipation. Finally, these features did not occur stereotypically in perimenopausal cycles with respect to mid cycle. These findings point to peripheral URs as oscillations that are coupled to menstrual cycle physiology and that have the potential to contribute to the development of tools for estimating the female fertile window.

Although the underlying physiological mechanisms that lead to systematic changes in UR power in DBT require further investigation, much is known about general changes in body temperature across the menstrual cycle. Estrogens lower, and progestins raise, body temperature[53,72]. Accordingly, body temperature reaches a minimum, with minimum core circadian amplitude, during the late follicular phase and rises in the core, mouth, and skin following ovulation[73]. Body temperature also broadly reflects metabolic rate, which is elevated in the late follicular and luteal phases[74]. In mice, the structure of core temperature URs allows for the detection of female reproductive state, with a high plateau of temperature and trough of UR power during the active phase indicative of the LH surge and ovulation[13,75]. Most human studies to date have focused on core temperature, measured via an ingestible device that travels through the GI tract[73], intravaginal or rectal sensor[76], or oral thermometer[60]. However, ultradian, circadian, and ovulatory rhythms in temperature are readily observed at the periphery, providing several advantages: (1) DBT has higher amplitude fluctuations than core body temperature, making URs and CRs easier to detect[77], (2) changes in DBT may correlate with sleep stage[78], and (3) DBT is in circadian antiphase to core temperature, but shows the same general trend across the menstrual cycle, suggesting com- parable reliability[77]. It is possible that rising UR power of DBT before the LH surge reflects higher UR power of reproductive hormones during this time.

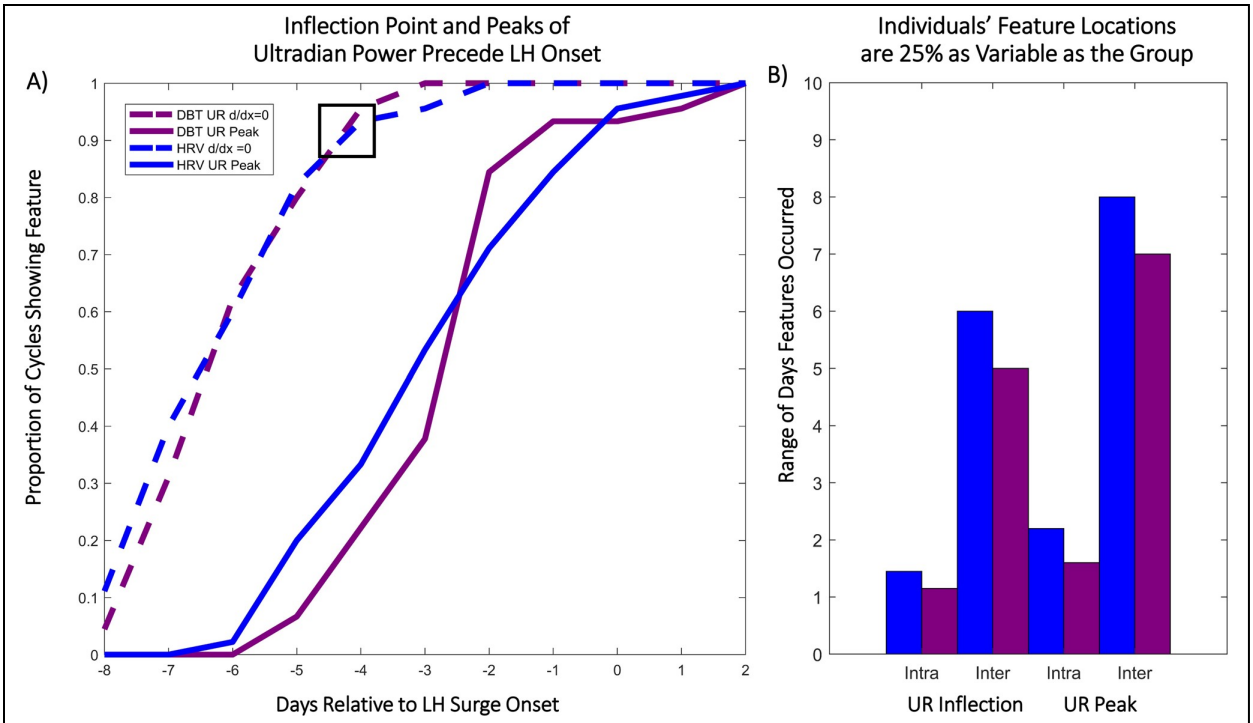


**Figure 4.** Inflection Points and Peaks of Ultradian Power Anticipate the LH Surge Within and Across Individuals. (**A**) Cumulative histogram indicates the proportion of cycles showing an inflection point on a given day relative to LH surge onset (blue = HRV (RMSSD), maroon = DBT, dashed = inflection point, solid = subsequent peak). Box indicates that on day LH—4, ~ 90% of individuals had shown the HRV and DBT first inflection point. (**B**) Intra-vs. inter-individual range of days over which inflection points ("UR Inflection") and subsequent peaks ("UR Peak") of ultradian DBT and HRV power occurred. The range intra-individual range (2–3 cycles per individual) is 25% the size of the inter-individual range (45 total cycles).

Whereas body temperature is the most commonly used non-hormonal output in menstrual cycle tracking, previous studies have found that HRV also changes by cycle phase and may therefore be a candidate for surge anticipation[79]. Parasympathetic input to the heart dominates during the follicular phase, lowering resting heart rate and elevating HRV (RMSSD)[57]. Sympathetic input to the heart dominates during the luteal phase, elevating heart rate and depressing HRV (RMSSD)[11,57]. Consequently, HRV (RMSSD) varies ~ 10 ms from the follicular to the luteal phase[11], with a marked decrease in the latter portion of the cycle[52]. These fluctuations may be more difficult to detect during a short daytime recording window, and are impacted by daytime activities, making sleep an ideal window over which to look for unmasked features[45]. Natural negative controls illustrating reproductive and metabolic influences on HRV patterns are that (1) LH pulsatility is disrupted in obese and diabetic women[80,81], and (2) mid cycle and luteal fluctuations in HRV are absent in polycystic ovarian syndrome (PCOS), a leading cause of female infertility[58,59]. In the present study, sleeping HRV (RMSSD) UR power rose in the late follicular phase, peaked near the LH surge, and dropped sharply before rising into the early luteal phase. Although the present study lacks sufficient power to evaluate other potential patterns that may be relevant to the menopausal transition, the preliminary absence of comparable features in perimenopausal individuals suggests that

this group deserves further study. Together, signal processing of DBT and HRV could yield actionable information for individuals and clinicians wishing to estimate the "fertile window". However, there are several challenges inherent to accurately defining the female fertile window.

The fertile window (the time during which a woman may become pregnant) depends upon many factors, including (1) the timing of the LH surge, (2) the subsequent time of the release of the ovum or ovulation, (3) the presence of a viable corpus luteum releasing adequate progesterone[38], (4) the duration of time sperm can survive in the female body, which is dependent both on sufficient number and quality of sperm and on the appropriate vaginal environment (e.g., pH)[22,82], and 5) quality of the uterine environment. Most investigations report the highest probability of fertility as the 5 days preceding ultrasound-determined day of ovulation (USDO)[83], but actual days on which an individual may become pregnant are much more variable, with pregnancy occurring up to 11 days prior to ovulation to 5 days after ovulation[71].

Some of the reported variability in the fertile window likely results from discrepancies in language used to describe both human ovulation and the fertile window itself[84]. Despite their namesake, home "ovulation tests" that identify supra-threshold LH concentrations do not measure ovulation, which may occur many days after and occasionally a few days *before* LH surge onset[71]. Despite this variability, the fertile window is often treated as predictable, with definitions including the 5–6 days prior to the LH surge as a proxy for ovulation[85], the first day of slippery clear cervical fluid through LH surge onset[86], the total days of slippery clear cervical fluid[87], day 10–17 of the cycle[88], and retrospective measures of salivary ferning[85], basal body temperature[64,89], and progesterone metabolites (e.g.,[90]). Today, many online and app-based ovulation prediction algorithms are validated using day of cycle or LH data alone, in the absence of hormone measures or USDO[2,83,84,91]. Additionally, extant data sets regularly report excluding 20–50% of collected data due to cycle irregularities, without determining if given cycles were hormonally aberrant[71,92–94]. Together, the confounding of the LH surge with ovulation and the variable criteria used to define the fertile window make it difficult to accurately determine the variance, and contributors to variability, of fertility relative to the LH surge or ovulation. Despite these discrepancies, the possibility that UR features anticipate the onset of the LH surge by a few to several days suggests applicability for family planning. When one considers the additional time between LH surge onset and ovulation, these features may anticipate much to all of the fertile window. If confirmed in larger cohorts, this method would constitute the earliest method of predicting a definitive event at any point within the fertile window.

Open source, non-invasive methods for predicting the LH surge as a marker of likely future ovulation are not currently available[71], but the present findings indicate that the onset of the LH surge may be anticipated days in advance by automated detection of changes in ultradian

power of DBT and HRV (RMSSD). These changes consistently anticipate LH surge onset in women of a variety of ages, cycle lengths, surge timing and duration. The frequency band of 2–5 h examined in the present investigation was not specifically selected for the present group of participants but chosen based on the peak frequency band observed across physiological systems[14,25,56], suggesting potentially broad applicability. Due to the high demand for accurate methods of fertility assessment, such novel methods carry the responsibility to clearly report the aspects of reproductive physiology that are detected and the methods by which detection is achieved once algorithms are tested on large populations[68,84,91]. Future work will determine the extent to which these ultradian rhythm-based methods of menstrual cycle monitoring generate accurate predictions in larger, more diverse cohorts. In particular, the study of a greater number of cycles within individuals may enable personalization of relevant features. With these data, methods such as empirical mode decomposition for selection of tailored ultradian bands, or machine learning based methods for assessment across many different features at once, may result in greater specificity or longer predictive windows. These features could potentially be used on their own, with minimal user input (e.g., tracking of dates of menstruation), or in combination with other FAM methods. Ideally, such methods could be widely employed on wearable devices such as the Oura Ring, or on future generations of convenient and precise body temperature and HRV sensors. Together, these findings may guide further research aimed at understanding how hormones, metabolism, and the autonomic nervous system temporally interact; and may aid the development of open-source, non-invasive methods of fertility awareness.

4.6 Acknowledgements The authors would like to thank the participants in the study for their interest, careful longitudinal self-tracking, and excellent questions and feedback. We also thank Dr. Linda Wilbrecht and Dr. Andrew Ahn for their helpful suggestions on an earlier version of this manuscript.

## 4.7 Supplemental Figures

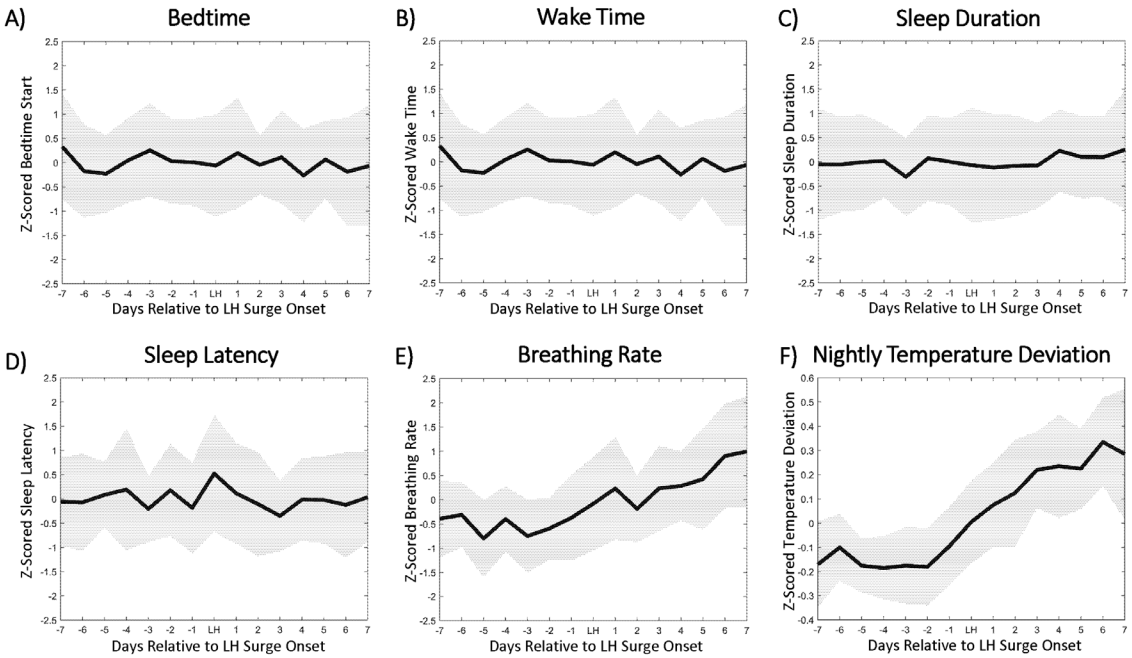


**Supplemental Figure 1. Sleep timing, duration, latency, breathing rate and temperature deviation do not anticipate the LH surge.** Bedtime (A), wake time (B), sleep duration (C) and sleep latency (D) do not show reliable changes relative to LH surge onset in premenopausal individuals. Breathing rate (E) and nightly temperature deviation (F, see methods) do not anticipate the surge, but exhibit an upward trend following the surge.

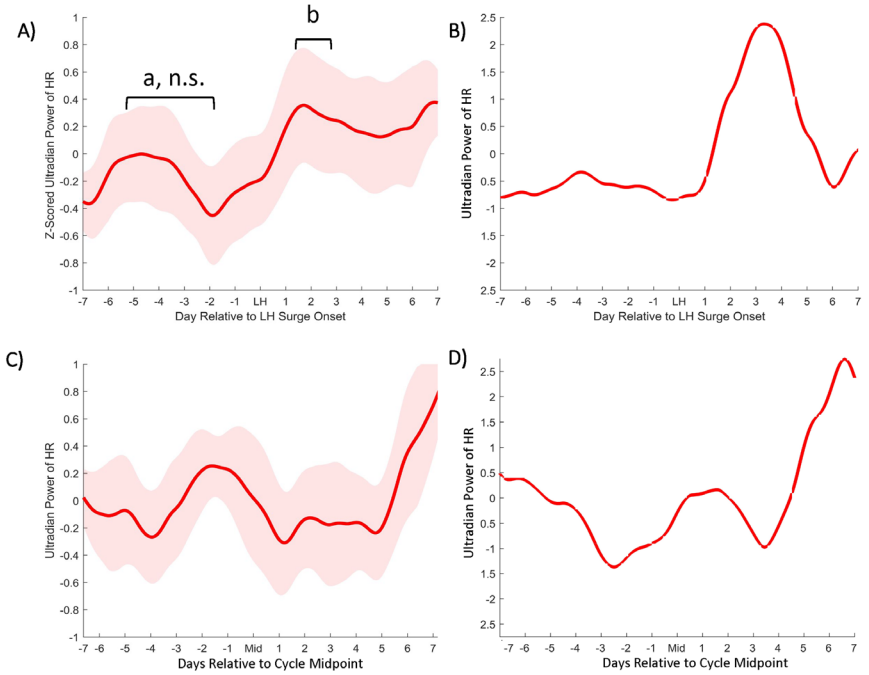


**Supplemental Figure 2. Heart rate ultradian power does not anticipate LH surge onset.** Mean sleeping heart rate ultradian power ± standard deviation for premenopausal cycles (A) within one week of LH surge onset and perimenopausal cycles (C) within one week of mid cycle. HR ultradian fluctuations do not anticipate the LH surge ($p>0.05$) but exhibit a significant elevation 2-3 days after the surge ($\chi^2 = 0.3$, $p=0.04$ ). Representative individual examples of HR ultradian power within one week of LH surge onset or mid cycle in premenopausal (B) and perimenopausal (D) cycles, respectively.

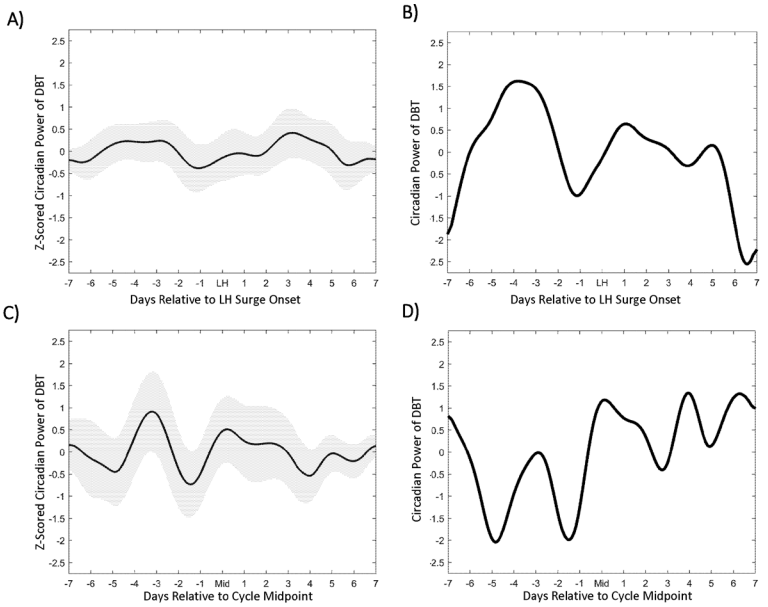


**Supplemental Figure 3. Circadian power of body temperature does not change stereotypically around LH surge onset.** Mean DBT circadian power ± standard deviation for premenopausal cycles (A) within one week of LH surge onset and perimenopausal cycles (C) within one week of mid cycle do not exhibit significant stereotyped fluctuations relative to LH surge onset or mid cycle. Individuals varied widely (examples B and D).

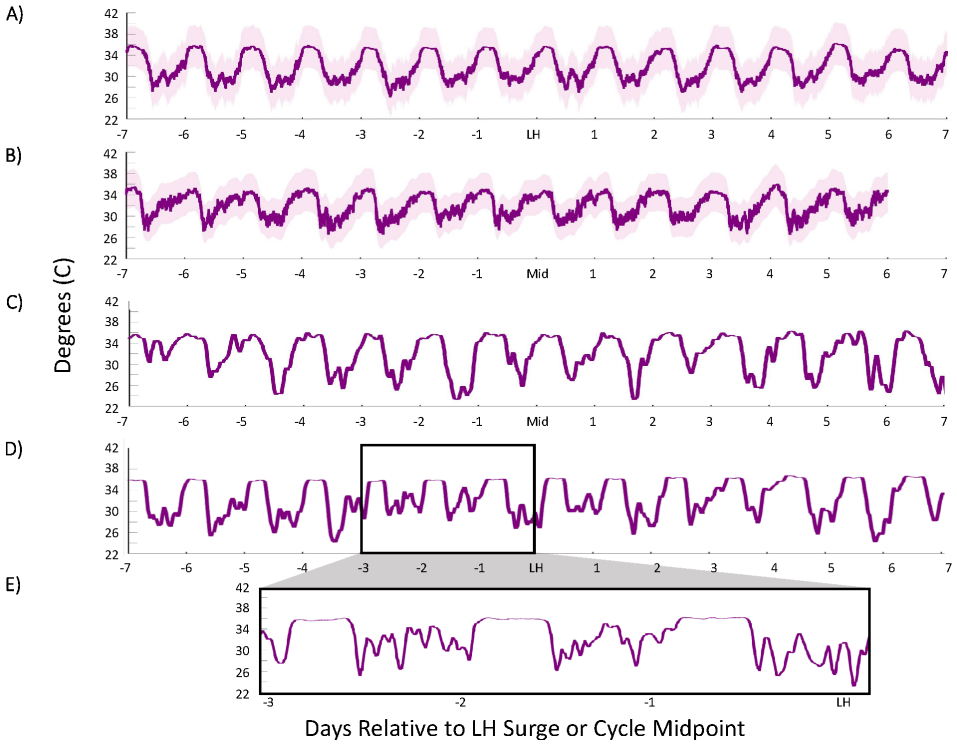


**Supplemental Figure 4. Linear average of DBT relative to LH surge onset in premenopausal and mid cycle in perimenopausal individuals.** Mean (A), ± standard deviation (shaded) of linear DBT around LH surge onset. Perimenopausal mean (B) ± standard deviation (shaded) of linear DBT surrounding mid cycle (note two perimenopausal cycles were very short, with only 6 days after midcycle occurring before next menses), and individual example (C). Individual example of DBT around LH surge onset (D) and zoomed window in this individual from LH-3 days to LH illustrating the presence of high amplitude URs during the day and a relatively high plateau during sleep (E).

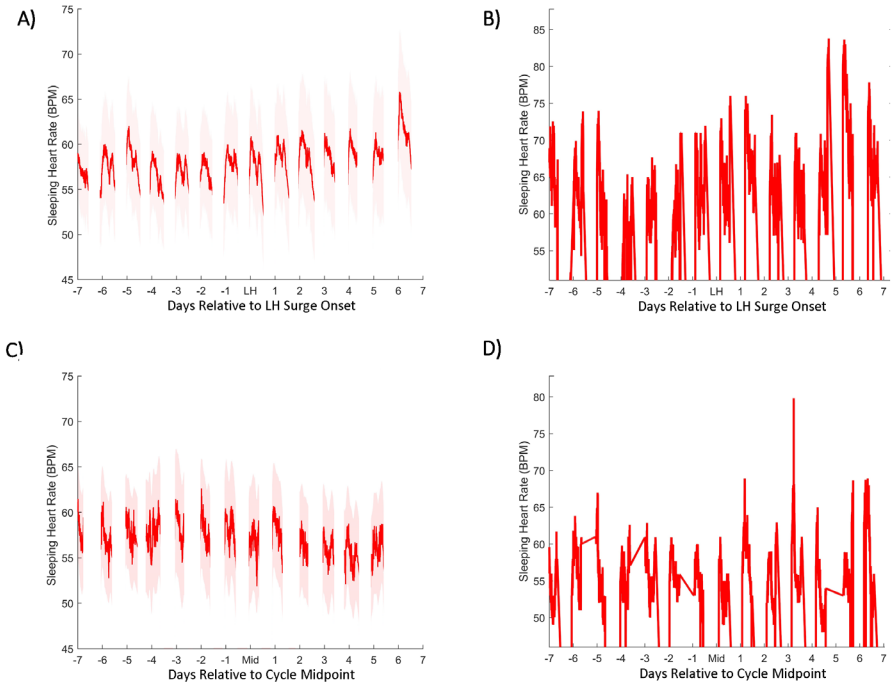


**Supplemental Figure 5. Linear average of sleeping HR relative to LH surge onset in premenopausal and mid cycle in perimenopausal individuals.** Premenopausal average (A), ± standard deviation (shaded) of linear sleeping HR surrounding LH surge onset, and individual example (B). Perimenopausal average (C) ± standard deviation (shaded) of linear HR surrounding mid cycle, and individual example (D).

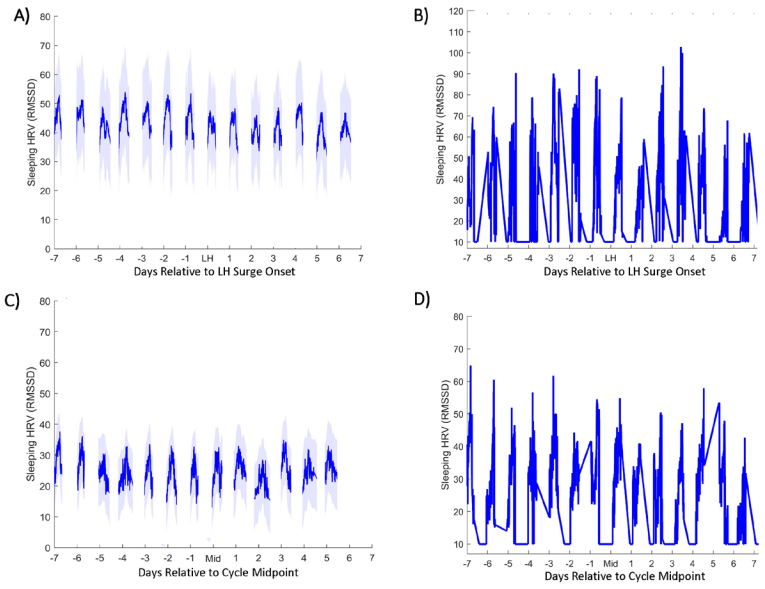


**Supplemental Figure 6. Linear average of sleeping HRV (RMSSD) relative to LH Surge onset in premenopausal and mid cycle in perimenopausal individuals.** Premenopausal average (A), ± standard deviation (shaded) of linear sleeping HRV surrounding LH surge onset, and individual example (B). Perimenopausal average (C) ± standard deviation (shaded) of linear HRV surrounding mid cycle, and individual example (D).

## 4.8 References


Grimes, D. A., Gallo, M. F., Grigorieva, V., Nanda, K. & Schulz, K. F. Fertility awareness-based methods for contraception: systematic review of randomized controlled trials. *Contraception* 72, 85–90 (2005).

Shilaih, M. *et al.* Modern fertility awareness methods: Wrist wearables capture the changes of temperature associated with the menstrual cycle. *Biosci. Rep.* https://doi.org/10.1042/BSR20171279 (2017) (Epub ahead of print).

Mørch, L. S. *et al.* Contemporary hormonal contraception and the risk of breast cancer. *N. Engl. J. Med.* 377, 2228–2239 (2017).

Marsden, J. Hormonal contraception and breast cancer, what more do we need toknow?. *Post Reprod. Health* 23, 116–127 (2017).

Gnoth, C., Frank-Herrmann, P., Schmoll, A., Godehardt, E. & Freundl, G. Cycle characteristics after discontinuation of oral contraceptives. *Gynecol. Endocrinol.* 16, 307–317 (2002).

Delbarge, W. *et al.* Return to fertility in nulliparous and parous women after removal of the GyneFix intrauterine contraceptive system. *Eur. J. Contracept. Reprod. Health Care Off. J. Eur. Soc. Contracept.* 7, 24–30 (2002).

Bradshaw, H. K., Mengelkoch, S. & Hill, S. E. Hormonal contraceptive use predicts decreased perseverance and therefore per- formance on some simple and challenging cognitive tasks. *Horm. Behav.* 119, 104652 (2020).

Pletzer, B. A. & Kerschbaum, H. H. 50 years of hormonal contraception—time to find out, what it does to our brain. *Front. Neurosci.* 8, 256 (2014).

Skovlund, C. W., Mørch, L. S., Kessing, L. V., Lange, T. & Lidegaard, Ø. Association of hormonal contraception with suicide attempts and suicides. *Am. J. Psychiatry* 175, 336–342 (2018).

Skovlund, C. W., Mørch, L. S., Kessing, L. V. & Lidegaard, Ø. Association of hormonal contraception with depression. *JAMA Psychiatry* 73, 1154–1162 (2016).

Brar, T. K., Singh, K. D. & Kumar, A. Effect of different phases of menstrual cycle on heart rate variability (HRV). *J. Clin. Diagn. Res. JCDR* 9, CC01-04 (2015).

Smarr, B. L., Zucker, I. & Kriegsfeld, L. J. Detection of successful and unsuccessful pregnancies in mice within hours of pairing through frequency analysis of high temporal resolution core body temperature data. *PLoS ONE* 11, e0160127 (2016).

Smarr, B. L., Grant, A. D., Zucker, I., Prendergast, B. J. & Kriegsfeld, L. J. Sex differences in variability across timescales in BALB/c mice. *Biol. Sex Differ.* 8, 7 (2017).

Grant, A. D., Wilsterman, K., Smarr, B. L. & Kriegsfeld, L. J. Evidence for a coupled oscillator model of endocrine ultradian rhythms. *J. Biol. Rhythms* 33, 475–496. https://doi.org/10.1177/0748730418791423 (2018).

Baerwald, A. R., Adams, G. P. & Pierson, R. A. Ovarian antral folliculogenesis during the human menstrual cycle: a review. *Hum. Reprod. Update* **18**, 73–91 (2012).

Ferreira, S. R. & Motta, A. B. Uterine function: from normal to polycystic ovarian syndrome alterations. *Curr. Med. Chem.* **25**, 1792–1804 (2018).

Simonneaux, V., Bahougne, T. & Angelopoulou, E. Daily rhythms count for femalefertility. *Best Pract. Res. Clin. Endocrinol. Metab.* **31**, 505–519 (2017).

Robker, R. L., Hennebold, J. D. & Russell, D. L. Coordination of ovulation and oocyte maturation: a good egg at the right time. *Endocrinology* **159**, 3209–3218 (2018).

Zhang, S. *et al.* Changes in sleeping energy metabolism and thermoregulationduringmenstrual cycle. *Physiol. Rep.* **8**, e14353 (2020).

Yeung, E. H. *et al.* Longitudinal study of insulin resistance and sex hormones over the menstrual cycle: the biocycle study. *J. Clin. Endocrinol. Metab.* **95**, 5435–5442 (2010).

Tada, Y. *et al.* The impact of menstrual cycle phases on cardiac autonomic nervous system activity: an observational study con- sidering lifestyle (diet, physical activity, and sleep) among female college students. *J. Nutr. Sci. Vitaminol. (Tokyo)* **63**, 249–255 (2017).

Stanford, J. B. Revisiting the fertile window. *Fertil. Steril.* **103**, 1152–1153 (2015).

Shannahoff-Khalsa, D. S., Kennedy, B., Yates, F. E. & Ziegler, M. G. Ultradian rhythms of autonomic, cardiovascular, and neu- roendocrine systems are related in humans. *Am. J. Physiol.* **270**, R873-887 (1996).

Shannahoff-Khalsa, D. S., Kennedy, B., Yates, F. E. & Ziegler, M. G. Low-frequency ultradian insulin rhythms are coupled to cardiovascular, autonomic, and neuroendocrine rhythms. *Am. J. Physiol. Regul. Integr. Comp. Physiol.* **272**, R962–R968 (1997).

Brandenberger, G., Simon, C. & Follenius, M. Ultradian endocrine rhythms: a multioscillatory system. *J. Interdiscip. Cycle Res.* **18**, 307–315 (1987).

Zavala, E. *et al.* Mathematical modelling of endocrine systems. *Trends Endocrinol. Metab.* **30**, 244–257 (2019).

Clarke, I. J., Thomas, G. B., Yao, B. & Cummins, J. T. GnRH secretion throughout the ovine estrous cycle. *Neuroendocrinology* **46**, 82–88 (1987).

Gore, A. C., Windsor-Engnell, B. M. & Terasawa, E. Menopausal increases in pulsatile gonadotropin-releasing hormone release in a nonhuman primate (*Macaca mulatta*). *Endocrinology* **145**, 4653–4659 (2004).

Moenter, S. M., Caraty, A., Locatelli, A. & Karsch, F. J. Pattern of gonadotropin-releasing hormone (GnRH) secretion leading up to ovulation in the ewe: existence of a preovulatory GnRH surge. *Endocrinology* **129**, 1175–1182 (1991).

Backstrom, C., McNeilly, A. S., Leask, R. & Baird, D. Pulsatile secretion of LH, FSH, Prolactin, oestradiol, and progesterone during the human menstrual cycle. *Clin. Endocrinol. (Oxf.)* **17**, 29–42 (1982).

Rossmanith, W. G. *et al.* Pulsatile cosecretion of estradiol and progesterone by the midluteal phase corpus luteum: temporal link to luteinizing hormone pulses. *J. Clin. Endocrinol. Metab.* **70**, 990–995 (1990).

Vugt, D. A. V., Lam, N. Y. & Ferin, M. Reduced frequency of pulsatile luteinizing hormone secretion in the luteal phase of the rhesus monkey involvement of endogenous opiates. *Endocrinology* **115**, 1095–1101 (1984).

Booth, R. A. Jr. *et al.* Mode of pulsatile follicle-stimulating hormone secretion in gonadal hormone-sufficient and-deficient women–a clinical research center study. *J. Clin. Endocrinol. Metab.* **81**, 3208–3214 (1996).

Genazzani, A. D. *et al.* FSH secretory pattern and degree of concordance with LH in amenorrheic, fertile, and postmenopausal women. *Am. J. Physiol. - Endocrinol. Metab.* **264**, E776–E781 (1993).

Pincus, S. M., Padmanabhan, V., Lemon, W., Randolph, J. & Rees Midgley, A. Follicle- stimulating hormone is secreted more irregularly than luteinizing hormone in both humans and sheep. *J. Clin. Invest.* **101**, 1318–1324 (1998).

Yen, S. S. C., Tsai, C. C., Naftolin, F., Vandenberg, G. & Ajabor, L. Pulsatile patterns of gonadotropin release in subjects with and without ovarian function. *J. Clin. Endocrinol. Metab.* **34**, 671–675 (1972).

Licinio, J. *et al.* Synchronicity of frequently sampled, 24-h concentrations of circulating leptin, luteinizing hormone, and estradiol in healthy women. *Proc. Natl. Acad. Sci. USA* **95**, 2541–2546 (1998).

Soules, M. R., Clifton, D. K., Cohen, N. L., Bremner, W. J. & Steiner, R. A. Luteal phase deficiency: abnormal gonadotropin and progesterone secretion patterns. *J. Clin. Endocrinol. Metab.* **69**, 813–820 (1989).

Veldhuis, J. D. *et al.* Physiological profiles of episodic progesterone release during the midluteal phase of the human menstrual cycle. *J. Clin. Endocrinol. Metab.* **66**, 414–421 (1988).

Filicori, M., Butler, J. P. & Crowley, W. F. Neuroendocrine regulation of the corpus luteum in the human. Evidence for pulsatile progesterone secretion. *J. Clin. Invest.* **73**, 1638–1647 (1984).

Genazzani, A. D., Guardabasso, V., Petraglia, F. & Genazzani, A. R. Specific concordance index defines the physiological lag between LH and progesterone in women during the midluteal phase of the menstrual cycle. *Gynecol. Endocrinol.* **5**, 175–184 (1991).

Nóbrega, L. H. C. *et al.* Analysis of testosterone pulsatility in women with ovulatory menstrual cycles. *Arq. Bras. Endocrinol. Metabol.* **53**, 1040–1046 (2009).

Healy, D. L., Schenken, R. S., Lynch, A., Williams, R. F. & Hodgen, G. D. Pulsatile progesterone secretion: its relevance to clinical evaluation of corpus luteum function. *Fertil. Steril.* **41**, 114–121 (1984).

Shechter, A., Boudreau, P., Varin, F. & Boivin, D. B. Predominance of distal skin temperature changes at sleep onset across menstrual and circadian phases. *J. Biol. Rhythms* **26**, 260–270 (2011).

Leicht, A. S., Hirning, D. A. & Allen, G. D. Heart rate variability and endogenous sex hormones during the menstrual cycle in young women. *Exp. Physiol.* **88**, 441–446 (2003).

Chen, W., Kitazawa, M. & Togawa, T. HMM-based estimation of menstrual cycle from skin temperature during sleep. In *2008 30th Annual International Conference of the IEEE Engineering in Medicine and Biology Society* **2008**, 1635–1638 (2008). https:// doi.org/10.1109/IEMBS.2008.4649487.

Charkoudian, N., Hart, E. C. J., Barnes, J. N. & Joyner, M. J. Autonomic control ofbody temperature and blood pressure: influ- ences of female sex hormones. *Clin. Auton. Res.* **27**, 149–155 (2017).

de Zambotti, M., Willoughby, A. R., Sassoon, S. A., Colrain, I. M. & Baker, F. C. Menstrual cycle-related variation in physiological sleep in women in the early menopausal transition. *J. Clin. Endocrinol. Metab.* **100**, 2918–2926 (2015).

de Zambotti, M., Nicholas, C. L., Colrain, I. M., Trinder, J. A. & Baker, F. C. Autonomic regulation across phases of the menstrual cycle and sleep stages in women with premenstrual syndrome and healthy controls. *Psychoneuroendocrinology* **38**, 2618–2627 (2013).

Stein, P. K. *et al.* Circadian and ultradian rhythms in heart rate variability. *Biomed. Tech. (Berl)* **51**, 155–158 (2006).

Stein, P. K. *et al.* Circadian and ultradian rhythms in cardiac autonomic modulation. *Conf. Proc. Annu. Int. Conf. IEEE Eng. Med. Biol. Soc. IEEE Eng. Med. Biol. Soc. Annu. Conf.* **1**, 429–432 (2006).

Visrutha, K., Harini, N., Ganaraja, B., Pavanchand, A. & Veliath, S. A study of cardiac autonomic control and pulmonary func- tions in different phases of menstrual cycle. *Int. J. Appl. Biol. Pharm. Technol.* **3**, 306–311 (2012).

Buxton, C. L. & Atkinson, W. B. Hormonal factors involved in the regulation of basal body temperature during the menstrual cycle and pregnancy. *J. Clin. Endocrinol. Metab.* **8**, 544–549 (1948).

Fredholm, B. B., Johansson, S. & Wang, Y.-Q. Adenosine and the regulation of metabolism and body temperature. *Adv. Phar- macol. San Diego Calif* **61**, 77–94 (2011).

Stuckey, M. I., Kiviniemi, A., Gill, D. P., Shoemaker, J. K. & Petrella, R. J. Associations between heart rate variability, metabolic syndrome risk factors, and insulin resistance. *Appl. Physiol. Nutr. Metab. Physiol. Appl. Nutr. Metab.* **40**, 734–740 (2015).

Goh, G. H., Maloney, S. K., Mark, P. J. & Blache, D. Episodic ultradian events—ultradian rhythms. *Biology* **8**, 15 (2019).

Sato, N., Miyake, S., Akatsu, J. & Kumashiro, M. Power spectral analysis of heart rate variability in healthy young women during the normal menstrual cycle. *Psychosom. Med.* **57**, 331–335 (1995).

Uckuyu, A., Toprak, E., Ciftci, O. & Ciftci, F. C. The fluctuation in the heart rate variability throughout ovulation induction cycle: is the case different in polycystic ovary syndrome?. *Gynecol. Obstet.* **3**, 1–5 (2013).

Yildirir, A., Aybar, F., Kabakci, G., Yarali, H. & Oto, A. Heart rate variability in young women with polycystic ovary syndrome. *Ann. Noninvasive Electrocardiol.* **11**, 306–312 (2006).

Kräuchi, K. *et al.* Diurnal and menstrual cycles in body temperature are regulated differently: a 28-day ambulatory study in healthy women with thermal discomfort of cold extremities and controls. *Chronobiol. Int.* **31**, 102–113 (2014).

Uchida, Y., Atsumi, K., Takamata, A. & Morimoto, K. The effect of menstrual cycle phase on foot skin temperature during mild local cooling in young women. *J. Physiol. Sci. JPS* **69**, 151–157 (2019).

Baker, F. C. & Driver, H. S. Circadian rhythms, sleep, and the menstrual cycle. *Sleep Med.* **8**, 613–622 (2007).

Bauman, J. E. Basal body temperature: unreliable method of ovulation detection. *Fertil. Steril.* **36**, 729–733 (1981).

Quagliarello, J. & Arny, M. Inaccuracy of basal body temperature charts in predicting urinary luteinizing hormone surges. *Fertil. Steril.* **45**, 334–337 (1986).

de Zambotti, M., Rosas, L., Colrain, I. M. & Baker, F. C. The sleep of the ring: comparison of the ŌURA sleep tracker against polysomnography. *Behav. Sleep. Med.* **17**, 1–15. https://doi.org/10.1080/15402002.2017.1300587 (2017).

Hasselberg, M. J., McMahon, J. & Parker, K. The validity, reliability, and utility of the iButton for measurement of body tempera- ture circadian rhythms in sleep/wake research. *Sleep Med.* **14**, 5–11 (2013).

Gear, A. J. C. H. J. C. H. Wearables are totally failing the people who need them most. *WIRED* https://www.wired.com/2014/11/ where-fitness-trackers-fail/.

Epstein, D. A. *et al.* Examining menstrual tracking to inform the design of personal informatics tools. *Proc. SIGCHI Conf. Hum. Factors Comput. Syst. CHI Conf.* **2017**, 6876–6888 (2017).

Bashan, A., Bartsch, R. P., Kantelhardt, J. W., Havlin, S. & Ivanov, P. C. Network physiology reveals relations between network topology and physiological function. *Nat. Commun.* **3**, 702 (2012).

Bartsch, R. P., Liu, K. K. L., Bashan, A. & Ivanov, P. C. Network physiology: how organ systems dynamically interact. *PLoS ONE* **10**, e0142143 (2015).

Direito, A., Bailly, S., Mariani, A. & Ecochard, R. Relationships between the luteinizing hormone surge and other characteristics of the menstrual cycle in normally ovulating women. *Fertil. Steril.* 99, 279-285.e3 (2013).

Williams, H., Dacks, P. A. & Rance, N. E. An improved method for recording tail skin temperature in the rat reveals changes during the Estrous cycle and effects of ovarian steroids. *Endocrinology* 151, 5389–5394 (2010).

Coyne, M. D., Kesick, C. M., Doherty, T. J., Kolka, M. A. & Stephenson, L. A. Circadian rhythm changes in core temperature over the menstrual cycle: method for noninvasive monitoring. *Am. J. Physiol.-Regul. Integr. Comp. Physiol.* 279, R1316–R1320 (2000).

Solomon, S. J., Kurzer, M. S. & Calloway, D. H. Menstrual cycle and basal metabolic rate in women. *Am. J. Clin. Nutr.* 36, 611–616 (1982).

Sanchez-Alavez, M., Alboni, S. & Conti, B. Sex- and age-specific differences in core body temperature of C57Bl/6 mice. *Age Dordr. Neth.* 33, 89–99 (2011).

Shechter, A. & Boivin, D. B. Sleep, hormones, and circadian rhythms throughout the menstrual cycle in healthy women and women with premenstrual dysphoric disorder. *Int. J. Endocrinol.* 2010, e259345 (2010).

Szymusiak, R. Body temperature and sleep. *Handb. Clin. Neurol.* 156, 341–351 (2018).

Henane, R., Buguet, A., Roussel, B. & Bittel, J. Variations in evaporation and body temperatures during sleep in man. *J. Appl. Physiol.* 42, 50–55 (1977).

Schmalenberger, K. M. *et al.* A systematic review and meta-analysis of within-person changes in cardiac vagal activity across the menstrual cycle: implications for female health and future studies. *J. Clin. Med.* 8, 1946 (2019).

Jain, A. *et al.* Pulsatile luteinizing hormone amplitude and progesterone metabolite excretion are reduced in obese women. *J. Clin. Endocrinol. Metab.* 92, 2468–2473 (2007).

van Leckwyck, M. *et al.* Decreasing insulin sensitivity in women induces alterations in LH pulsatility. *J. Clin. Endocrinol. Metab.* 101, 3240–3249 (2016).

Lessey, B. A. & Young, S. L. What exactly is endometrial receptivity?. *Fertil. Steril.* 111, 611–617 (2019).

Faust, L. *et al.* Findings from a mobile application-based cohort are consistent with established knowledge of the menstrual cycle, fertile window, and conception. *Fertil. Steril.* 112, 450-457.e3 (2019).

Setton, R., Tierney, C. & Tsai, T. The accuracy of web sites and cellular phone applications in predicting the fertile window. *Obstet. Gynecol.* 128, 58–63 (2016).

Su, H.-W., Yi, Y.-C., Wei, T.-Y., Chang, T.-C. & Cheng, C.-M. Detection of ovulation, a review of currently available methods. *Bioeng. Transl. Med.* 2, 238–246 (2017).

Keulers, M. J., Hamilton, C. J. C. M., Franx, A., Evers, J. L. H. & Bots, R. S. G. M. The length of the fertile window is associated with the chance of spontaneously conceiving an ongoing pregnancy in subfertile couples. *Hum. Reprod. Oxf. Engl.* **22**, 1652–1656 (2007).

Ecochard, R., Duterque, O., Leiva, R., Bouchard, T. & Vigil, P. Self-identification of the clinical fertile window and the ovulation period. *Fertil. Steril.* **103**, 1319-1325.e3 (2015).

Wilcox, A. J., Dunson, D. & Baird, D. D. The timing of the "fertile window" in the menstrual cycle: day specific estimates from a prospective study. *BMJ* **321**, 1259–1262 (2000).

Moghissi, K. S. Accuracy of basal body temperature for ovulation detection. *Fertil. Steril.* **27**, 1415–1421 (1976).

Newman, M., Pratt, S. M., Curran, D. A. & Stanczyk, F. Z. Evaluating urinary estrogen and progesterone metabolites using dried filter paper samples and gas chromatography with tandem mass spectrometry (GC–MS/MS). *BMC Chem.* **13**, 20 (2019).

Freis, A. *et al.* Plausibility of menstrual cycle apps claiming to support conception. *Front. Public Health* **6**, 98 (2018).

Renaud, R. L. *et al.* Echographic study of follicular maturation and ovulation during the normal menstrual cycle. *Fertil. Steril.* **33**, 272–276 (1980).

Queenan, J. T. *et al.* Ultrasound scanning of ovaries to detect ovulation in women. *Fertil. Steril.* **34**, 99–105 (1980).

Polan, M. L. *et al.* Abnormal ovarian cycles as diagnosed by ultrasound and serum estradiol levels. *Fertil. Steril.* **37**, 342–347 (1982).

Choe, E. K., Lee, N. B., Lee, B., Pratt, W. & Kientz, J. A. Understanding quantified-selfers' practices in collecting and exploring personal data. In *Proceedings of the 32nd annual ACM conference on human factors in computing systems*, 1143–1152 (2014).

Grant, A. D., Wolf, G. I. & Nebeker, C. Approaches to governance of participant-led research: a qualitative case study. *BMJ Open* **9**, e025633 (2019).

Vayena, E. & Tasioulas, J. Adapting standards: Ethical oversight of participant-led health research. *PLoS Med.* **10**(3), e1001402. https://doi.org/10.1371/journal.pmed.1001402 (2013).

Maijala, A., Kinnunen, H., Koskimäki, H., Jämsä, T. & Kangas, M. Nocturnal finger skin temperature in menstrual cycle tracking: ambulatory pilot study using a wearable Oura ring. *BMC Womens Health* **19**, 150 (2019).

Grant, A. D. & Wolf, G. I. Free-living humans cross cardiovascular disease risk categories due to daily rhythms in cholesterol and triglycerides. *J. Circadian Rhythms* **17**, 3 (2019).

Greshake Tzovaras, B. *et al.* Open humans: a platform for participant-centered research and personal data exploration. *GigaS- cience* **8**, giz076 (2019).

Roos, J. *et al.* Monitoring the menstrual cycle: Comparison of urinary and serum reproductive hormones referenced to true ovulation. *Eur. J. Contracept. Reprod. Health Care Off. J. Eur. Soc. Contracept.* 20, 438–450 (2015).

Barron, M. L., Vanderkolk, K. & Raviele, K. Finding the fertile phase: low-cost luteinizing hormone sticks versus electronic fertility monitor. *MCN. Am. J. Matern. Child Nurs.* 43, 153–157 (2018).

Leise, T. L. Wavelet analysis of circadian and ultradian behavioral rhythms. *J. Circadian Rhythms* 11, 5 (2013).

Lilly, J. M. & Olhede, S. C. Generalized morse wavelets as a superfamily of analytic wavelets. *IEEE Trans. Signal Process.* 60, 6036–6041 (2012).

# 5. Multi-Timescale Rhythmicity of Blood Glucose and Insulin Delivery Reveals Key Advantages of Hybrid Closed Loop Therapy

## 5.1 Abstract

**Background:** Blood glucose and insulin exhibit coordinated daily and hourly rhythms in people without diabetes (nonT1D). Although the presence and stability of these rhythms are associated with euglycemia, it is unknown if they (1) are preserved in individuals with type 1 diabetes (T1D) and (2) vary by therapy type. In particular, Hybrid Closed Loop (HCL) systems improve glycemia in T1D compared to Sensor Augmented Pump (SAP) therapies, but the extent to which either recapitulates coupled glucose and insulin rhythmicity is not well described. In HCL systems, more rapid modulation of glucose via automated insulin delivery may result in greater rhythmic coordination and euglycemia. Such precision may not be possible in SAP systems. We hypothesized that HCL users would exhibit fewer hyperglycemic event, superior rhythmicity, and coordination relative to SAP users.

**Methods:** Wavelet and coherence analyses were used to compare glucose and insulin delivery rate (IDR) within-day and daily rhythms, and their coordination, in 3 datasets: HCL (n = 150), SAP (n = 89), and nonT1D glucose (n = 16).

**Results:** Glycemia, correlation between normalized glucose and IDR, daily coherence of glucose and IDR, and amplitude of glucose oscillations differed significantly between SAP and HCL users. Daily glucose rhythms differed significantly between SAP, but not HCL, users and nonT1D individuals.

**Conclusions:** SAP use is associated with greater hyperglycemia, higher amplitude glucose fluctuations, and a less stably coordinated rhythmic phenotype compared to HCL use. Improvements in glucose and IDR rhythmicity may contribute to the overall effectiveness of HCL systems.

## 5.2 Introduction

In people without diabetes, blood glucose, insulin, and other metabolic outputs (e.g., glucagon) are rhythmically regulated at multiple timescales[1–4]. Prominent timescales include the day (circadian rhythm(s); CR, 23-25 h)[5–7] and within-a-day (ultradian rhythm(s); UR, ~1-6 h)[2,4]. CRs are maintained by a hierarchy consisting of a master brain clock in the suprachiasmatic nucleus of the hypothalamus that coordinates the activity of subordinate central and peripheral cellular oscillators[8–11]. Although mechanisms of UR generation are still under investigation, these oscillations are nearly ubiquitous in metabolic and endocrine systems and are thought to be generated centrally and reinforced peripherally[12–14]. At both timescales, exogenous signals such as food intake and light act as cues to synchronize internal systems with respect to the 24 h day[5,15–20].

Stability and in-range amplitude of CRs and URs are associated with better health outcomes. At the CR timescale, stable sleep-wake schedule and time restricted eating are associated with improved glycemia in individuals without diabetes or in those with Type 2 Diabetes (T2D)[15,21–24]. Circadian oscillators within pancreatic beta islet cells modulate insulin secretion throughout the day, with disruption to these rhythms resulting in oxidative stress and diabetes in animal models[25–27]. Additionally, time of day modulates the response of muscle and adipose tissue to insulin, with more efficient glucose uptake during the daytime hours[28,29]. At the UR timescale, a pulse of glucose followed promptly by a pulse of insulin can more expediently trigger glucose uptake, thereby preventing glucose from rising out of the euglycemic range[5]. Conversely, a pulse of glucose followed by a delayed or blunted pulse of insulin is more likely to result in hyperglycemia[30], a dynamic observed previously in individuals with T2D[31]. Together, metabolic health does not merely reflect healthy levels of key factors, but coordinated rhythmic patterns of intake, absorption, and production.

Biological rhythms and coordination of glucose and insulin have been studied only to a limited extent in people with T1D, with previous studies largely restricted to modelling[32–35]. People with T1D likely exhibit widely varying glucose and insulin dynamics in comparison to nonT1D and T2D individuals, due to the latter's temporal pattern of endogenous insulin production and sensitivity. As a result, understanding 1) the timing of glucose and insulin delivery fluctuation, and 2) any preservation of endogenous glucose rhythms in people with T1D, is critical for understanding the efficacy of current treatments and designing effective future therapies.

For people with T1D, insulin is delivered exogenously under varying protocols, ranging from multiple daily injections to Sensor Augmented Pump (SAP) therapy and Hybrid Closed Loop (HCL) therapy. In SAP therapy, an insulin pump delivers a pre-programmed basal rate of insulin which is supplemented by manual bolusing as needed for meals or corrections. In HCL therapy, glucose data is fed into an algorithm that directly determines insulin delivery adjustments up to every five minutes and is supplemented by manual bolusing for meals by the user. This process allows for frequent adjustment of insulin delivery, greater personalization, and is associated with greater safety, improved glycemia, and superior A1c as compared to SAP therapy[36–48].

Much remains to be learned about how T1D therapies temporally coordinate with metabolic physiology, the mechanisms responsible for the particular effectiveness of HCL, and how the growing diversity of HCL systems could be further improved. A key difference between SAP and HCL systems is that, in SAP therapy, glucose does not automatically influence insulin administration, whereas, in HCL therapy, glucose algorithmically determines insulin delivery. A possible downstream effect of these two methods of insulin administration is a difference in temporal coordination between glucose and insulin delivery rate (IDR) which may generate differences in the amplitude and stability of glucose rhythms. Understanding potential rhythmic differences between users of SAP and HCL and any relationship between rhythmicity and glycemia may enhance our understanding of how HCL achieves its success and suggest avenues for future improvements and personalization.

T1D rhythmicity can now be studied for the first time in a large, longitudinal dataset of SAP and HCL continuous glucose monitor (CGM) and insulin pump data to better characterize therapy outcomes beyond A1c and time in range. Additionally, the increased usage of CGMs by individuals without diabetes now allows for glucose timeseries and rhythmicity comparisons among people with and without T1D. We hypothesized that glycemia and rhythmicity vary widely among T1D individuals, but that HCL system use results in patterns of rhythmic change in glucose and insulin delivery, such as high glucose-insulin delivery temporal coordination and linear correlation relative to SAP[1,2,5,49,50]. Specifically we hypothesized that: 1) HCL users would show fewer instances of hyperglycemia compared to SAP, consistent with previous findings[36,37,39]; 2) glucose levels and insulin delivery rate would be more strongly correlated in HCL than SAP users; 3) such coordination, if present, may be associated with greater correlation of rhythmicity at higher frequencies in HCL (as these frequencies of change are enabled stably by HCL systems) than SAP users, and 4) HCL users would exhibit stronger temporal coordination between glucose and IDR compared to SAP users. To examine these possibilities, we used wavelet and wavelet coherence analyses to compare glucose and insulin delivery data sets.

## 5.3 Materials and Methods

Ethical Approval and Data Access. T1D data used in this study (1-SRA-2019-821-S-B) were licensed by JDRF from the Tidepool Big Data Donation Project[51], a Type 1 Diabetes data organization service. NonT1D data used in this study were made available through Open Humans[52], a service that allows individuals to anonymously donate their biometric data[53]. Because all data were anonymized and retrospective, IRB approval was not required.

Inclusion Criteria and Data Cleaning. Data were included from SAP and HCL users with at least 1 month of data without gaps of > 12 h at any point during the month (n=89 SAP, n=150 HCL). In wavelet analyses, data were further restricted to users who consistently logged > 4 CGM readings per hour (n=144 HCL, n=82 SAP); the vast majority of data points were logged approximately every five minutes. CGM data from n=16 nonT1D individuals from the Quantified Self Blood Glucose Data Set were included. Data were not cleaned of outliers as we intended to capture all variance within the data but were z-scored for wavelet coherence analyses and wavelet scatter plots. There

were no age, sex, or parity restrictions (see Demographic data). Data were interpolated to a standard of five minute resolution for analysis.

Data Analysis. All code and data needed to recapitulate these analyses are available on AG's Github[54]. Code was written in MATLAB 2020a, 2020b (MathWorks, Natick, MA), and Python 3 (Python Software Foundation, Wilmington, DE). Wavelet transformation (WT) code was modified from the Jlab toolbox and from Dr. Tanya Leise [55]. WT was used to assess the structure of URs and CRs of blood glucose and IDR timeseries, and wavelet coherence was utilized to assess the relationship between rhythms in glucose and rhythms in IDR. In contrast to signal processing methods that transform a signal into frequency space without temporal position (e.g., Fourier transform using sine wave components of infinite length), wavelets are constructed with amplitude diminishing to 0 in both directions from center, enabling frequency and amplitude calculation at a given position (See: Supplemental Figure 1).

Additionally, wavelets enable variation of window length when calculating power at different frequencies, enabling more accurate assessment of power at each frequency. Wavelets can assume many functions (e.g., Mexican hat, square wave, Morse); the present analyses use a Morse wavelet with a low number of oscillations (defined by $\beta$ and $\gamma$), analogous to wavelets used in previous circadian applications[55,56]. Morse Wavelet parameters of $\beta=5$ and $\gamma=3$ describe the frequencies of the two waves superimposed to create the wavelet, and which have successfully been used on biological timeseries [56–58]. This low number of oscillations enhances detection of contrast and transitions. The maximum for each point in time within the band of the wavelet matrix rhythms of each hour (e.g., 2-3 h) was taken in order to create linear representations of UR WT power over time. Bands analyzed here corresponded with the daily ultradian peak power observed in URs across many physiological systems (2-5 h), with a slight shift (omission of 1 h) and expansion (inclusion of up to 6 h) in supplemental figures to account for the onset and duration of insulin action in people with T1D [12,13,59]. The band of the wavelet matrix corresponding to 23-25 h was assessed to represent circadian rhythmicity. Because WTs exhibit artifacts at the edges of the data being transformed, only the WT of the second through the second to last days of data were analyzed further. After WT, wavelet matrices were down-sampled to every 10th point for ease of visualization in scatter plots. Wavelet coherence was assessed using the MATLAB "wcoherence" package by Dr. Aslak Grinsted [60,61]. Briefly, wavelet coherence enables the assessment of the extent to which two signals share power at a timescale (here, circadian) at a given moment, and the consistency of their phase relationship [61–63]. Thus, coherence between IDR and endogenous glucose rhythms was assessed despite the delay from subcutaneous insulin delivery to absorption into the bloodstream.

Statistics. Distributions of glucose were differentiated by group by extracting skewness of each individual's proportionally scaled glucose distribution using the MATLAB function "skewness". A Kruskal Wallis test (non-parametric ANOVA) was then used to compare skewness of individuals by group (HCL vs. SAP vs. NonT1D). Linear regression was used to generate correlations of z-scored glucose and z-scored IDR, and of glucose and insulin UR power, using the MATLAB function "fitlm". Area under the curve was used to represent an individual's amplitude of daily and hourly glucose rhythms and, separately, circadian coherence. Kruskal Wallis tests were used to compare areas under the curve by group for circadian glucose oscillation amplitude and ultradian glucose oscillation amplitude differences from NonT1D "baseline", and to compare circadian coherences. Each statistic utilized 1 number representing each individual per group, per comparison. Corrections for multiple comparisons used Dunn's test within the MATLAB function "multcompare"; where all groups differed significantly, the largest p-value was reported. Findings were considered statistically significant when $p<0.05$.

## 5.4 Results

Demographics. The T1D dataset comprised a wide age range of individuals, most diagnosed with T1D at a young age. Notably, ethnicity data were not collected by Tidepool, and reporting of sex was optional. Demographics, including the percentage of individuals who opted not to report sex in each group, are listed in Table 1.

| | *n*-Value | Mean Age (stdev) | % Female, Male, Unlisted | Years Living with Diabetes (stdev) |
|---|---|---|---|---|
| SAP | 89 | 34.4 (20.6) | 13,23,64 | 18.4 (16.9) |
| HCL | 150 | 28.5 (16.2) | 44,32,24 | 15.3 (12.0) |
| Non-T1D | 16 | 33.6 (13.9) | 56,44,0 | 0 (0) |

Table 1: Demographics. Age, sex (when listed), and years living with diabetes of individuals by group.

HCL Use is Associated with Improved Glycemia. HCL use reduces hyperglycemia [36–39,64–68]. Specifically, SAP system users exhibit a broader, right shifted distribution of glucose in comparison to HCL system users, indicating greater hyperglycemia (>7.8 mmol/L); SAP, HCL, and nonT1D glucose distributions differed significantly from one another ($\chi^2$=57.86, p<3*10$^{-4}$). Hypoglycemia was rare in both T1D datasets (<5% of all data points for either group) (**Figure 1**).

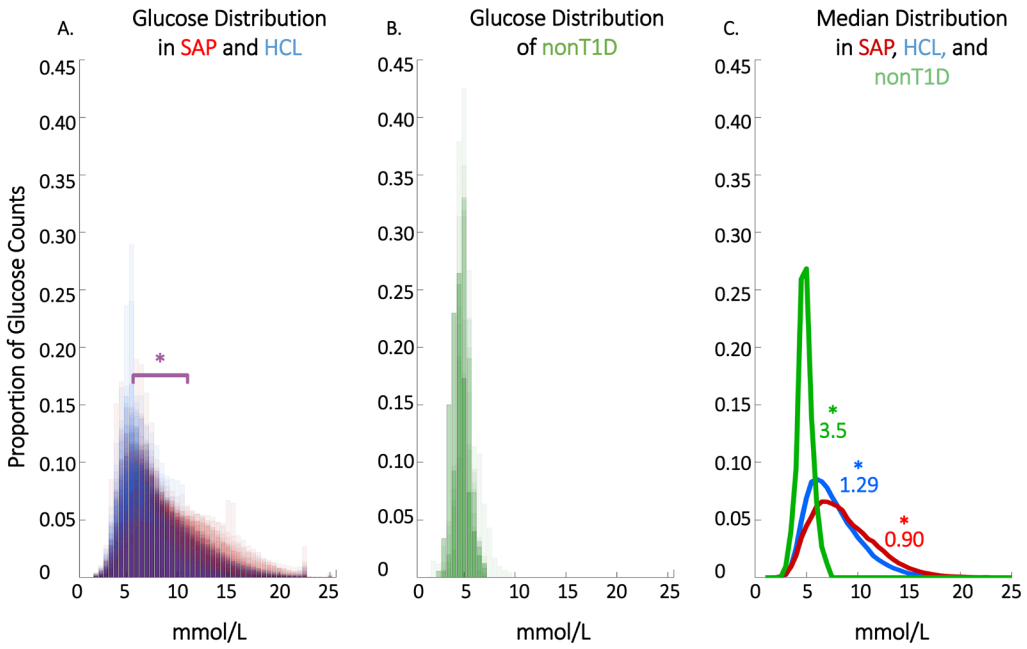


**Figure 1: HCL Systems Reduce Hyperglycemia.** A) Proportional counts of glucose distributions of all individuals with T1D using SAP and HCL systems. Note that counts are scaled such that each individual contributes the same proportion of total data. SAP system users exhibit greater hyperglycemia (>7.8 mmol/L); SAP, HCL and, nonT1D glucose distributions differed significantly. Hypoglycemic events (<4mmol/L) comprised <5% of all data points for either T1D dataset. B) Proportional counts of nonT1D glucose distributions. C) Median distributions for each dataset. *Significantly different from other groups in the same figure panel p<0.05.

Linear and Rhythmic Correlation of Glucose and Insulin Delivery Rate are Increased in HCL Users. HCL increases the correlation between normalized glucose and IDR levels (SAP $r^2$=0.002; p=0.119; HCL $r^2$=0.015; p=1.26*10$^{-5}$) and the correlation between glucose and insulin high frequency URs (SAP $r^2$ =0.002; p=0.127; HCL $r^2$ =0.084; p=5.6*10$^{-22}$) compared to SAP (SAP metrics are uncorrelated). (**Figure 2**). This difference was not restricted to the 2 to 3 h ultradian band (**Supplemental Figure 2**).

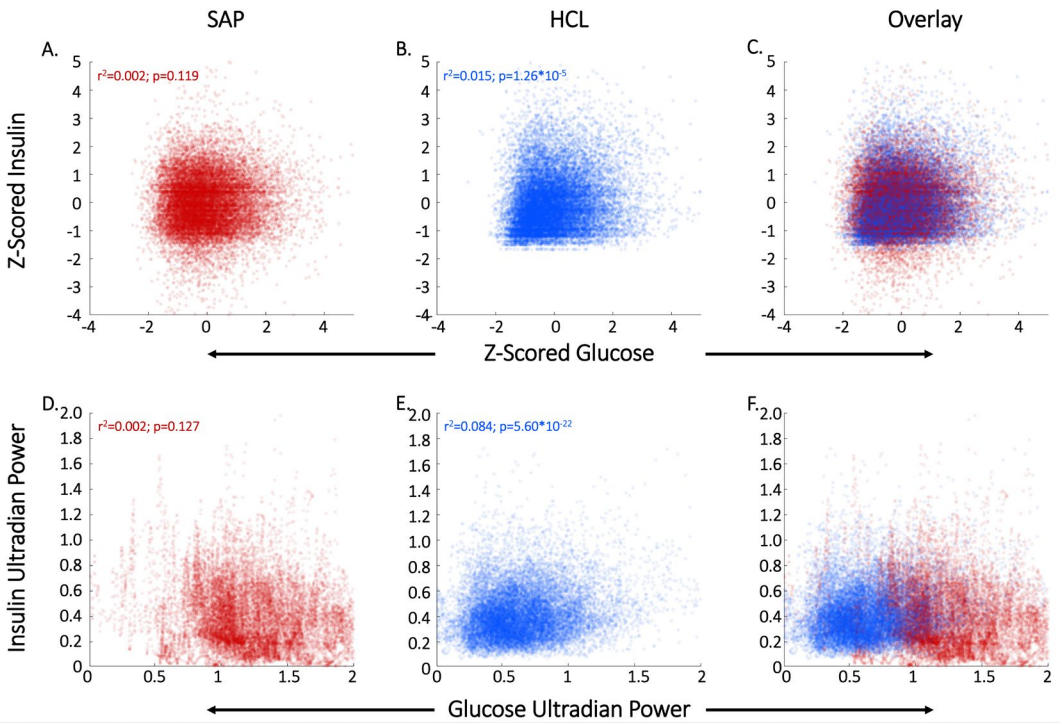


**Figure 2: HCL Increases Correlation of Glucose and Insulin Levels and Ultradian Rhythmicity.** SAP users exhibit uncorrelated normalized glucose and insulin levels (A) and uncorrelated URs of glucose and insulin (D). Glucose and its rhythms assume a wide spectrum of values for each of the standard doses of insulin rates provided by the pump, leading to the striped appearance of the correlations. By contrast, Hybrid Closed Loop users exhibit correlated normalized glucose and insulin levels (B) and correlated ultradian rhythms of glucose and insulin (E). Overlays of normalized glucose and insulin (C) and ultradian rhythms (F) emphasize group differences.

HCL Use is Associated with Lower Amplitude Circadian and Ultradian Glucose Deviations than SAP. SAP glucose CR and UR amplitude is significantly higher than that of HCL or nonT1D ($\chi^2$=140 p< $4.41*10^{-4}$, $\chi^2$=73.5, p<$1.11*10^{-4}$ , respectively). (**Figure 3A**). HCL CR amplitude is not significantly different from nonT1D CR amplitude (p=0.206). Together, HCL users are more similar than SAP users to the canonical nonT1D phenotype of glucose rhythmic amplitude.

HCL Exceeds SAP Wavelet Coherence of Circadian Rhythms of Glucose and Insulin Delivery Rate. HCL users exhibit greater coherence between circadian rhythms of glucose and insulin delivery rate ($\chi^2$=29.12, p=$6.80*10^{-8}$) (**Figure 3B**). Finally, HCL improves the correlation between glucose and insulin circadian rhythms (SAP $r^2$ = 0.002, p=0.141; HCL $r^2$=0.083, p=$1.13*10^{-21}$) (**See Supplemental Figure 2**). These findings indicate that the relationship between glucose and insulin in HCL users more closely resemble that expected in nonT1D than SAP users[1,5,7,69].

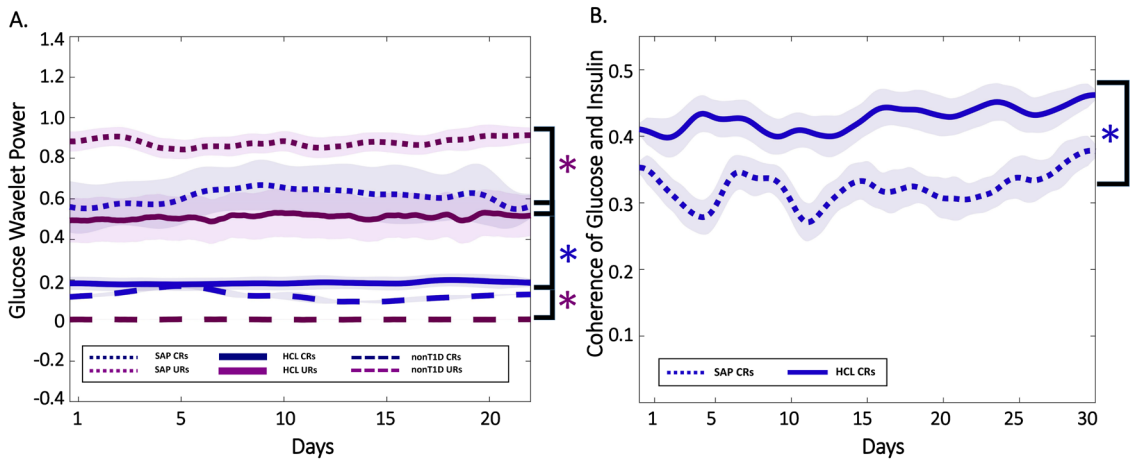


**Figure 3: HCL Use Decreases Amplitude of Glucose Oscillations and Increases Glucose-Insulin Coherence Compared to SAP.** The amplitude of HCL users' glucose CRs (blue) and URs (maroon) (solid), and those of nonT1D (dashed) and SAP (dotted) users' (A). Transparent shading indicates standard deviation (SD). SAP glucose CR and UR amplitude is significantly higher than that of HCL or nonT1D. HCL CR amplitude is not significantly different from nonT1D CR amplitude. Mean± STD of circadian wavelet coherence for HCL (solid) and SAP (dotted) users (B). Circadian (blue) coherence of glucose and insulin in HCL (solid) and SAP (dotted) users. Transparent shading indicates SD. Although both HCL and SAP individuals exhibit lower coherence than would be expected in nonT1D individuals, HCL CR coherence is significantly greater than SAP CR coherence. *Significantly different from other groups indicated in the same figure panel $p<0.05$.

## 5.5 Discussion and Conclusions

The present findings reveal that glycemia, biological rhythms in glucose and IDR, and rhythmic coherence vary significantly by T1D therapy type. In conjunction with lower incidence of hyperglycemia, HCL system use is associated with lower amplitude rhythmic fluctuation at the CR and UR timescales, a stronger association between glucose and IDR, and increased coherence of glucose and IDR circadian rhythms. The lack of a significant amplitude difference between HCL and nonT1D individuals is encouraging. Although much research is aimed at raising the amplitude of biological rhythms, the nonT1D data provide a context for illustrating that a reduction of rhythmic amplitude with preservation of rhythmic stability may be desirable in SAP systems, and in HCL systems at the UR timescale. Together, HCL systems appear to recapitulate glucose levels and rhythms to a greater extent than SAP systems.

The biological rhythm and insulin delivery metrics in the present investigation differ from those typically used to assess the efficacy of T1D therapies (e.g., A1c and time in range). In contrast to insulin release in nonT1D individuals, absorption of insulin delivered subcutaneously results in smoothed levels of the hormone reaching the bloodstream with a delay[70,71]. Such delays can also occur for measurements of interstitial glucose, relative to circulating levels[72,73]. Although these delays may hamper the interpretation of rhythms in insulin delivery rate, the present findings argue that this variable can be informative. The observation that glucose and IDR oscillate at the

same frequencies and are temporally coordinated argues that the algorithmic coupling of glucose to delivered insulin can be stably maintained in both outputs, and therefore that central insulin maintains aspects of this 2-5 h and 24 h rhythmicity.

Because timeseries metrics assess key aspects of glucose-insulin regulation, CRs and URs, they may be useful for further comparison of different HCL systems or for reviewing efficacy at different time points after adoption of HCL. Consideration of rhythms in, and coordination of, glucose and insulin may enable better understanding of how algorithmic changes to HCL systems result in improvement or deterioration of glycemia and may guide protocols to help individuals more quickly achieve euglycemic status after changes in therapy. Additionally, available data on the number of interactions required both by users of HCL and SAP therapies may help differentiate outcomes and highlight possible improvements based on the number of interactions required to achieve euglycemia. In each of these cases, attempts to understand and improve therapies may be more successful if both the levels and rhythmic patterning of glucose and insulin administration are evaluated.

Additional factors, such as sex and age, likely impact rhythmicity of glucose and insulin[74–77]. For example, adolescence is a time of restructuring of circadian and ultradian rhythmicity, and, in females, the emergence of a monthly timescale of rhythmicity in the form of the ovulatory cycle (or its suppression by the use of hormonal contraceptives)[78]. Likewise, aging (e.g., menopause, andropause) is a time of endocrine, metabolic, and rhythmic change as circadian rhythms lose coherence and decrease in amplitude[79–82]. These changes to hormones, metabolism and their temporal structures may require different algorithms to customize therapy for different age groups, sexes, and hormonal milieus. Future explorations of donated T1D and nonT1D timeseries will be essential to understanding individual differences in glucose-insulin dynamics and to creating more effective, personalized HCL algorithms.

## Limitations

These analyses were limited to the HCL systems present in the Tidepool HCL dataset and may not apply to all HCL systems. Additionally, analyses were conducted on basal-rate and temporary basal-rate delivered insulin data. This analysis excludes manual bolus data. More specifically, corrections for out of range glycemia are delivered by either bolus or temporary basal rates manually by SAP users whereas temporary basal rates likely make up a larger proportion of 'corrections' for out of range glucose levels in HCL users, depending on their HCL and the available settings. Thus, future analyses will evaluate rhythmic features with the addition of manual boluses in both datasets. Finally, subcutaneously delivered insulin takes time to reach the bloodstream, and subcutaneously measured glucose may not capture changes at the highest frequencies in general circulation[70–73]. The true relationship between circulating insulin after administration and circulating glucose requires longitudinal evaluation in a clinical setting, and future work modelling these delays[32,83,84] in real-world conditions.

## Conclusions

HCL use is associated with beneficial outcomes and rhythmic dynamics that more closely resemble nonT1D individuals, including: 1) a significantly lower incidence of hyperglycemia compared to SAP users, consistent with previous reports, 2) lower amplitude glucose oscillations at the circadian and ultradian timescales than SAP users, 3) a greater correlation of glucose and IDR than SAP users, 4) a higher correlation of ultradian rhythms of glucose and ultradian rhythms of IDR than SAP users, and 5) greater rhythmic coordination of glucose and IDR at the circadian and ultradian timescales compared to SAP users. Together, these results illustrate that HCL use is associated with both improved glycemia and stronger coordination between key rhythmic patterns of glucose and insulin administration.

## 5.6 Acknowledgements

We thank Dr. Benjamin Smarr for his helpful input on figure design and Dr. Andrew Ahn for his helpful comments on an early version of this manuscript. We would like to thank Mrs. Annamarie Sucher-Jones for her editorial assistance. Supported by JDRF grant 1-SRA-2019-821-S-B.

## 5.7 Supplemental Figures

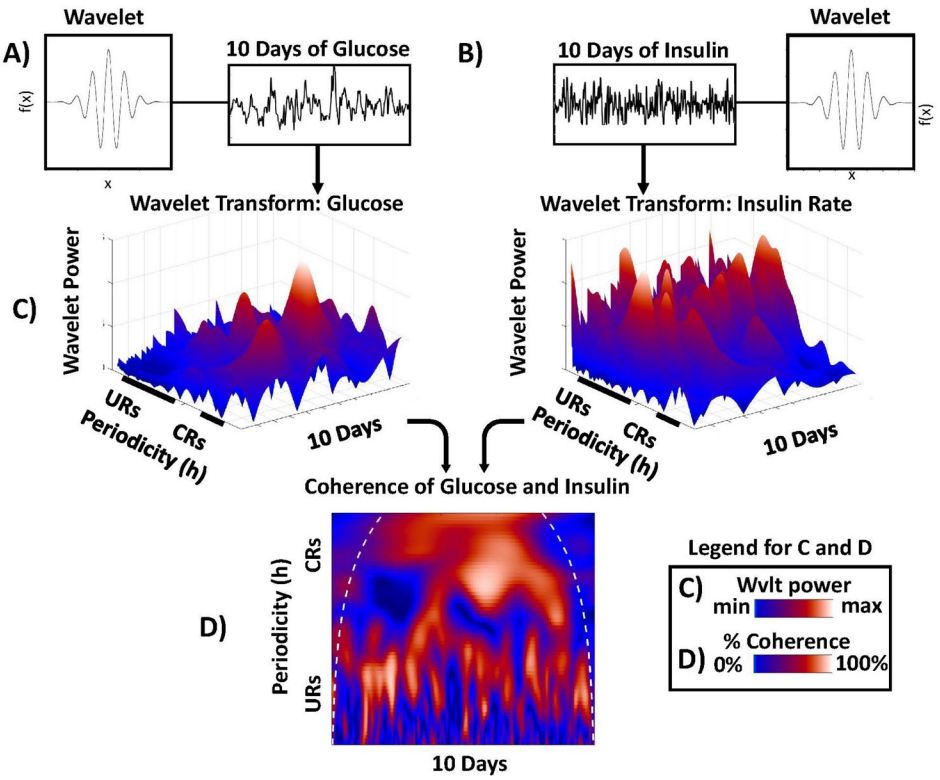


**Supplemental Figure 1: Example of Wavelet Analysis.** Morse wavelets (A) estimate rhythmic strength in glucose or insulin data (a combination of signal amplitude and oscillation stability) by assessing the fit of a wavelet stretched in window and in the x and y dimensions to a signal (B). The output (C) is a matrix of wavelet power, periodicity, and time (days). Transform of example HCL data illustrates predominantly circadian power in glucose, and predominantly 1-6 h ultradian power in insulin. Color map indicates wavelet power (synonymous with Y axis height). Wavelet coherence (D) enables assessment of rhythmic interactions between glucose and insulin; here, glucose and insulin rhythms are highly correlated at the ultradian and circadian timescales.

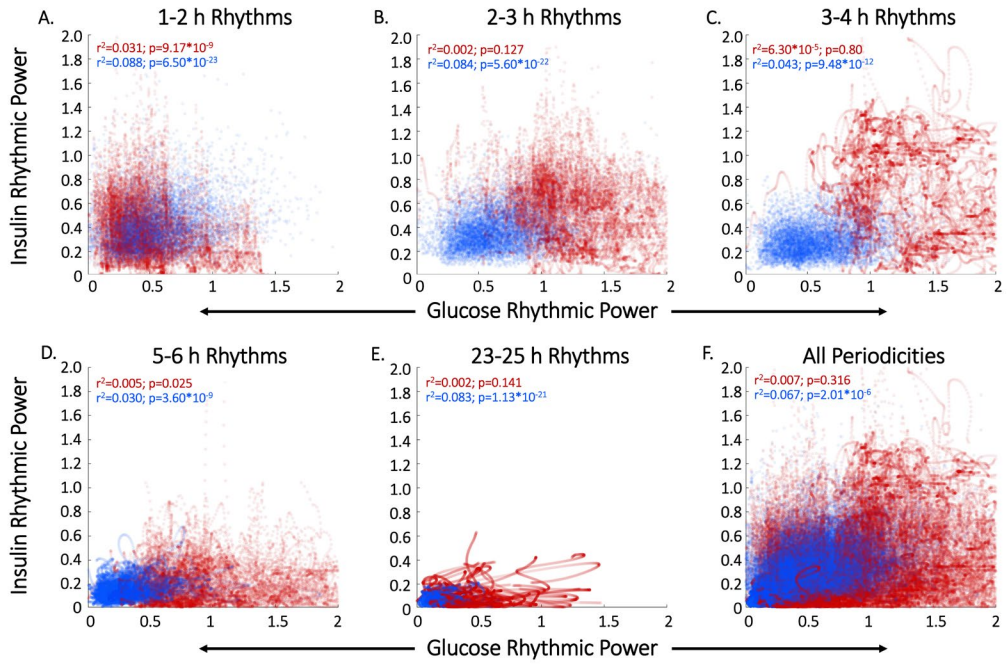


**Supplemental Figure 2: Glucose and Insulin Rhythms Exhibit Greater Correlation and Tighter Range in HCL than SAP.** Scatter plots of rhythmic power of glucose and insulin for HCL (blue) and SAP (red) data across periodicities (A-E) and overlaid at all periodicities. HCL use is associated with a significant correlation between glucose and insulin circadian rhythms (E). Correlation across all periodicities is greater in HCL users.

## 5.8 References


1. Kolopp M, Bicakova-Rocher A, Reinberg A, et al. Ultradian, circadian and circannual rhythms of blood glucose and injected insulins documented in six self-controlled adult diabetics. *Chronobiol Int*. 1986;3(4):265-280.
2. Simon C, Brandenberger G, Follenius M. Ultradian oscillations of plasma glucose, insulin, and C-peptide in man during continuous enteral nutrition. *J Clin Endocrinol Metab*. 1987;64(4):669-674.
3. Minamitani N, Chihara K, Kaji H, Kodama H, Kita T, Fujita T. Ultradian rhythm of growth hormone secretion in unrestrained, conscious male rabbits: role of endogenous somatostatintdagger. *J Neuroendocrinol*. 1989;1(2):147-151. doi:10.1111/j.1365-2826.1989.tb00094.x
4. Kern W, Offenheuser S, Born J, Fehm HL. Entrainment of ultradian oscillations in the secretion of insulin and glucagon to the nonrapid eye movement/rapid eye movement sleep rhythm in humans. *J Clin Endocrinol Metab*. 1996;81(4):1541-1547. doi:10.1210/jcem.81.4.8636364
5. Mejean L, Bicakova-Rocher A, Kolopp M, et al. Circadian and ultradian rhythms in blood glucose and plasma insulin of healthy adults. *Chronobiol Int*. 1988;5(3):227-236.
6. Bandín C, Scheer F a. JL, Luque AJ, et al. Meal timing affects glucose tolerance, substrate oxidation and circadian-related variables: A randomized, crossover trial. *Int J Obes 2005*. 2015;39(5):828-833. doi:10.1038/ijo.2014.182
7. Van Cauter E, Blackman JD, Roland D, Spire JP, Refetoff S, Polonsky KS. Modulation of glucose regulation and insulin secretion by circadian rhythmicity and sleep. *J Clin Invest*. 1991;88(3):934-942. doi:10.1172/JCI115396
8. Rutter J, Reick M, McKnight SL. Metabolism and the control of circadian rhythms. *Annu Rev Biochem*. 2002;71:307-331. doi:10.1146/annurev.biochem.71.090501.142857
9. Panda S. Circadian physiology of metabolism. *Science*. 2016;354(6315):1008-1015. doi:10.1126/science.aah4967
10. Hastings MH, Maywood ES, Brancaccio M. Generation of circadian rhythms in the suprachiasmatic nucleus. *Nat Rev Neurosci*. 2018;19(8):453-469. doi:10.1038/s41583-018-0026-z
11. Takahashi JS. Transcriptional architecture of the mammalian circadian clock. *Nat Rev Genet*. 2017;18(3):164-179. doi:10.1038/nrg.2016.150
12. Goh GH, Maloney SK, Mark PJ, Blache D. Episodic Ultradian Events—Ultradian Rhythms. *Biology*. 2019;8(1):15. doi:10.3390/biology8010015
13. Grant AD, Wilsterman K, Smarr BL, Kriegsfeld LJ. Evidence for a Coupled Oscillator Model of Endocrine Ultradian Rhythms. *J Biol Rhythms*. 2018;33(5):475-496. doi:10.1177/0748730418791423
14. Prendergast BJ, Zucker I. Ultradian rhythms in mammalian physiology and behavior. *Curr Opin Neurobiol*. 2016;40:150-154. doi:10.1016/j.conb.2016.07.011
15. Longo VD, Panda S. Fasting, Circadian Rhythms, and Time-Restricted Feeding in Healthy Lifespan. *Cell Metab*. 2016;23(6):1048-1059. doi:10.1016/j.cmet.2016.06.001
16. Brodsky VY. Circahoralian (Ultradian) metabolic rhythms. *Biochem Mosc*. 2014;79(6):483-495. doi:10.1134/S0006297914060017

17. Porcellati F, Lucidi P, Bolli GB, Fanelli CG. Thirty Years of Research on the Dawn Phenomenon: Lessons to Optimize Blood Glucose Control in Diabetes. *Diabetes Care*. 2013;36(12):3860-3862. doi:10.2337/dc13-2088
18. Rakshit K, Qian J, Colwell CS, Matveyenko AV. The islet circadian clock: entrainment mechanisms, function and role in glucose homeostasis. *Diabetes Obes Metab*. 2015;17 Suppl 1:115-122. doi:10.1111/dom.12523
19. Stephan FK. The "other" circadian system: food as a Zeitgeber. *J Biol Rhythms*. 2002;17(4):284-292. doi:10.1177/074873040201700402
20. Morin LP. A Path to Sleep Is through the Eye. *eNeuro*. 2015;2(2). doi:10.1523/ENEURO.0069-14.2015
21. Arble DM, Bass J, Behn CD, et al. Impact of Sleep and Circadian Disruption on Energy Balance and Diabetes: A Summary of Workshop Discussions. *SLEEP*. 2015;38(12):1849-1860. doi:10.5665/sleep.5226
22. Hatori M, Vollmers C, Zarrinpar A, et al. Time-Restricted Feeding without Reducing Caloric Intake Prevents Metabolic Diseases in Mice Fed a High-Fat Diet. *Cell Metab*. 2012;15(6):848-860. doi:10.1016/j.cmet.2012.04.019
23. Asher G, Sassone-Corsi P. Time for food: the intimate interplay between nutrition, metabolism, and the circadian clock. *Cell*. 2015;161(1):84-92. doi:10.1016/j.cell.2015.03.015
24. Chaix A, Manoogian ENC, Melkani GC, Panda S. Time-Restricted Eating to Prevent and Manage Chronic Metabolic Diseases. *Annu Rev Nutr*. 2019;39:291-315. doi:10.1146/annurev-nutr-082018-124320
25. Bass MP Kathryn Moynihan Ramsey, Biliana Marcheva, Joseph. Circadian Transcription from Beta Cell Function to Diabetes Pathophysiology - Mark Perelis, Kathryn Moynihan Ramsey, Biliana Marcheva, Joseph Bass, 2016. *J Biol Rhythms*. Published online July 15, 2016. Accessed September 22, 2020. https://journals-sagepub-com.libproxy.berkeley.edu/doi/10.1177/0748730416656949?url_ver=Z39.88-2003&rfr_id=ori%3Arid%3Acrossref.org&rfr_dat=cr_pub++0pubmed
26. Wei H, Zapata RC, Lopez-Valencia M, et al. Dopamine D2 receptor signaling modulates pancreatic beta cell circadian rhythms. *Psychoneuroendocrinology*. 2020;113:104551. doi:10.1016/j.psyneuen.2019.104551
27. Lee J, Ma K, Moulik M, Yechoor V. Untimely oxidative stress in β-cells leads to diabetes - Role of circadian clock in β-cell function. *Free Radic Biol Med*. 2018;119:69-74. doi:10.1016/j.freeradbiomed.2018.02.022
28. Carrasco-Benso MP, Rivero-Gutierrez B, Lopez-Minguez J, et al. Human adipose tissue expresses intrinsic circadian rhythm in insulin sensitivity. *FASEB J Off Publ Fed Am Soc Exp Biol*. 2016;30(9):3117-3123. doi:10.1096/fj.201600269RR
29. Basse AL, Dalbram E, Larsson L, Gerhart-Hines Z, Zierath JR, Treebak JT. Skeletal Muscle Insulin Sensitivity Show Circadian Rhythmicity Which Is Independent of Exercise Training Status. *Front Physiol*. 2018;9:1198. doi:10.3389/fphys.2018.01198
30. Yu H, Jia W, Bao Y, Lu J, Wu H, Xiang K. [Insulin ultradian pulse model of individuals with overweight and impaired glucose tolerance]. *Zhonghua Yi Xue Za Zhi*. 2006;86(20):1405-1409.

31. O'Meara NM, Sturis J, Van Cauter E, Polonsky KS. Lack of control by glucose of ultradian insulin secretory oscillations in impaired glucose tolerance and in non-insulin-dependent diabetes mellitus. *J Clin Invest*. 1993;92(1):262-271. doi:10.1172/JCI116560
32. Li J, Kuang Y, Mason CC. Modeling the glucose-insulin regulatory system and ultradian insulin secretory oscillations with two explicit time delays. *J Theor Biol*. 2006;242(3):722-735. doi:10.1016/j.jtbi.2006.04.002
33. Kissler SM, Cichowitz C, Sankaranarayanan S, Bortz DM. Determination of personalized diabetes treatment plans using a two-delay model. *J Theor Biol*. 2014;359:101-111. doi:10.1016/j.jtbi.2014.06.005
34. Palerm CC, Zisser H, Jovanovič L, Doyle FJ. A Run-to-Run Control Strategy to Adjust Basal Insulin Infusion Rates in Type 1 Diabetes. *J Process Control*. 2008;18(3-4):258-265. doi:10.1016/j.jprocont.2007.07.010
35. Visentin R, Dalla Man C, Kudva YC, Basu A, Cobelli C. Circadian Variability of Insulin Sensitivity: Physiological Input for In Silico Artificial Pancreas. *Diabetes Technol Ther*. 2015;17(1):1-7. doi:10.1089/dia.2014.0192
36. Provenzano V, Guastamacchia E, Brancato D, et al. Closing the Loop with OpenAPS in People with Type 1 Diabetes—Experience from Italy. *Diabetes*. 2018;67(Supplement 1). doi:10.2337/db18-993-P
37. Lewis DM, Swain RS, Donner TW. Improvements in A1C and Time-in-Range in DIY Closed-Loop (OpenAPS) Users. *Diabetes*. 2018;67(Supplement 1). doi:10.2337/db18-352-OR
38. Petruzelkova L, Soupal J, Plasova V, et al. Excellent Glycemic Control Maintained by Open-Source Hybrid Closed-Loop AndroidAPS During and After Sustained Physical Activity. *Diabetes Technol Ther*. 2018;20(11):744-750. doi:10.1089/dia.2018.0214
39. Bong Choi S, Shil Hong E, Hee Noh Y. Open Artificial Pancreas System Reduced Hypoglycemia and Improved Glycemic Control in Patients with Type 1 Diabetes | Diabetes. Published July 2018. Accessed September 10, 2020. https://diabetes.diabetesjournals.org/content/67/Supplement_1/964-P
40. Lewis DM. *Automated Insulin Delivery*.; 2019. Accessed September 10, 2020. https://www.artificialpancreasbook.com/
41. Forlenza GP, Ekhlaspour L, Breton M, et al. Successful At-Home Use of the Tandem Control-IQ Artificial Pancreas System in Young Children During a Randomized Controlled Trial. *Diabetes Technol Ther*. 2019;21(4):159-169. doi:10.1089/dia.2019.0011
42. Pinsker JE, Müller L, Constantin A, et al. Real-World Patient Reported Outcomes and Glycemic Results with Initiation of Control-IQ Technology. *Diabetes Technol Ther*. Published online August 26, 2020. doi:10.1089/dia.2020.0388
43. Knebel T, Neumiller JJ. Medtronic MiniMed 670G Hybrid Closed-Loop System. *Clin Diabetes Publ Am Diabetes Assoc*. 2019;37(1):94-95. doi:10.2337/cd18-0067
44. Lal RA, Basina M, Maahs DM, Hood K, Buckingham B, Wilson DM. One Year Clinical Experience of the First Commercial Hybrid Closed-Loop System. *Diabetes Care*. 2019;42(12):2190-2196. doi:10.2337/dc19-0855
45. Tauschmann M, Thabit H, Bally L, et al. Closed-loop insulin delivery in suboptimally controlled type 1 diabetes: a multicentre, 12-week randomised trial. *The Lancet*. 2018;392(10155):1321-1329. doi:10.1016/S0140-6736(18)31947-0

46. Thabit H, Tauschmann M, Allen JM, et al. Home Use of an Artificial Beta Cell in Type 1 Diabetes. http://dx.doi.org/10.1056/NEJMoa1509351. doi:10.1056/NEJMoa1509351
47. Hanaire H, Franc S, Borot S, et al. Efficacy of the Diabeloop closed-loop system to improve glycaemic control in patients with type 1 diabetes exposed to gastronomic dinners or to sustained physical exercise. *Diabetes Obes Metab*. 2020;22(3):324-334. doi:https://doi.org/10.1111/dom.13898
48. Benhamou P-Y, Franc S, Reznik Y, et al. Closed-loop insulin delivery in adults with type 1 diabetes in real-life conditions: a 12-week multicentre, open-label randomised controlled crossover trial. *Lancet Digit Health*. 2019;1(1):e17-e25. doi:10.1016/S2589-7500(19)30003-2
49. Simon C, Brandenberger G. Ultradian Oscillations of Insulin Secretion in Humans. *Diabetes*. 2002;51(suppl 1):S258-S261. doi:10.2337/diabetes.51.2007.S258
50. Simon C. Ultradian pulsatility of plasma glucose and insulin secretion rate: circadian and sleep modulation. *Horm Res*. 1998;49(3-4):185-190. doi:10.1159/000023169
51. Tidepool Blog. Accessed November 3, 2020. https://www.tidepool.org/bigdata
52. Home - Open Humans. Accessed November 3, 2020. https://www.openhumans.org/
53. Activity detail - Open Humans. Accessed November 3, 2020. https://www.openhumans.org/direct-sharing/projects/on-site/continuous-glucose-monitor-data-donation/
54. azuredominique. *Azuredominique/Type-1-Diabetes*.; 2020. Accessed November 3, 2020. https://github.com/azuredominique/type-1-diabetes
55. Leise TL. Wavelet analysis of circadian and ultradian behavioral rhythms. *J Circadian Rhythms*. 2013;11:5. doi:10.1186/1740-3391-11-5
56. Smarr BL, Grant AD, Zucker I, Prendergast BJ, Kriegsfeld LJ. Sex differences in variability across timescales in BALB/c mice. *Biol Sex Differ*. 2017;8:7. doi:10.1186/s13293-016-0125-3
57. Lilly JM, Olhede SC. Generalized Morse Wavelets as a Superfamily of Analytic Wavelets. *IEEE Trans Signal Process*. 2012;60(11):6036-6041. doi:10.1109/TSP.2012.2210890
58. Leise TL. Chapter Five - Wavelet-Based Analysis of Circadian Behavioral Rhythms. In: Sehgal A, ed. *Methods in Enzymology*. Vol 551. Circadian Rhythms and Biological Clocks, Part A. Academic Press; 2015:95-119. Accessed May 18, 2016. http://www.sciencedirect.com/science/article/pii/S0076687914000123
59. Brandenberger G, Simon C, Follenius M. Ultradian endocrine rhythms: A multioscillatory system. *J Interdiscip Cycle Res*. 1987;18(4):307-315. doi:10.1080/09291018709359958
60. Grinsted A, Moore JC, Jevrejeva S. Application of the cross wavelet transform and wavelet coherence to geophysical time series. *Nonlinear Process Geophys*. 2004;11(5/6):561-566.
61. Cui R, Zhang M, Li Z, et al. Wavelet coherence analysis of spontaneous oscillations in cerebral tissue oxyhemoglobin concentrations and arterial blood pressure in elderly subjects. *Microvasc Res*. 2014;93:14-20. doi:10.1016/j.mvr.2014.02.008
62. Grinsted A. Application of the cross wavelet transform and wavelet coherence to geophysical time series. Published December 24, 2004. Accessed October 18, 2018. https://www.glaciology.net/publication/2004-12-24-application-of-the-cross-wavelet-transform-and-wavelet-coherence-to-geophysical-time-series/
63. Tankanag AV, Grinevich AA, Kirilina TV, Krasnikov GV, Piskunova GM, Chemeris NK. Wavelet phase coherence analysis of the skin blood flow oscillations in human. *Microvasc Res*. 2014;95:53-59. doi:10.1016/j.mvr.2014.07.003

64. Litchman ML, Lewis D, Kelly LA, Gee PM. Twitter Analysis of #OpenAPS DIY Artificial Pancreas Technology Use Suggests Improved A1C and Quality of Life. *J Diabetes Sci Technol*. Published online September 10, 2018:1932296818795705. doi:10.1177/1932296818795705
65. Koutsovasilis A, Sotiropoulos A, Pappa M, et al. Clinical evaluation of a closed-loop insulin delivery system on glycaemic control in adults with type 1 diabetes - Virtual Meeting | EASD. Accessed September 22, 2020. https://www.easd.org/virtualmeeting/home.html#!resources/clinical-evaluation-of-a-closed-loop-insulin-delivery-system-on-glycaemic-control-in-adults-with-type-1-diabetes-134c4ad2-53f1-4698-927f-5bd287a76a5d
66. Mader IS-F Anna K Schütz, Marlies Eichner, Julia K. Two Subsequent Pregnancies in a Woman With Type 1 Diabetes: Artificial Pancreas Was a Gamechanger - Ingrid Schütz-Fuhrmann, Anna K. Schütz, Marlies Eichner, Julia K. Mader, 2020. *J Diabetes Sci Technol*. Published online February 14, 2020. Accessed September 22, 2020. https://journals-sagepub-com.libproxy.berkeley.edu/doi/10.1177/1932296820906219
67. Zabinsky J, Howell H, Ghezavati A, Nguyen A, Wong J. 988-P: Do-It-Yourself Artificial Pancreas Systems for Type 1 Diabetes Reduce Hyperglycemia without Increasing Hypoglycemia | Diabetes. Accessed September 22, 2020. https://diabetes.diabetesjournals.org/content/69/Supplement_1/988-P
68. Volkova AR, Chernaya M, Vlasova KA. Experience of using insulin therapy with the closed loop method among patients with type 1 diabetes mellitus in Russia. In: BioScientifica; 2020. doi:10.1530/endoabs.70.AEP329
69. Sadacca LA, Lamia KA, deLemos AS, Blum B, Weitz CJ. An intrinsic circadian clock of the pancreas is required for normal insulin release and glucose homeostasis in mice. *Diabetologia*. 2011;54(1):120-124. doi:10.1007/s00125-010-1920-8
70. Heinemann L, Nosek L, Kapitza C, Schweitzer M-A, Krinelke L. Changes in Basal Insulin Infusion Rates With Subcutaneous Insulin Infusion: Time until a change in metabolic effect is induced in patients with type 1 diabetes. *Diabetes Care*. 2009;32(8):1437-1439. doi:10.2337/dc09-0595
71. Hildebrandt P, Birch K, Jensen BM, Kühl C, Brange J. Absorption of Subcutaneously Infused Insulin: Influence of the Basal Rate Pulse Interval. *Diabetes Care*. 1985;8(3):287-289. doi:10.2337/diacare.8.3.287
72. Cengiz E, Tamborlane WV. A Tale of Two Compartments: Interstitial Versus Blood Glucose Monitoring. *Diabetes Technol Ther*. 2009;11(Suppl 1):S-11-S-16. doi:10.1089/dia.2009.0002
73. Jansson PA, Fowelin J, Smith U, Lönnroth P. Characterization by microdialysis of intracellular glucose level in subcutaneous tissue in humans. *Am J Physiol*. 1988;255(2 Pt 1):E218-220. doi:10.1152/ajpendo.1988.255.2.E218
74. Briski KP, Alhamami HN, Alshamrani A, Mandal SK, Shakya M, Ibrahim MHH. Sex Differences and Role of Estradiol in Hypoglycemia-Associated Counter-Regulation. *Adv Exp Med Biol*. 2017;1043:359-383. doi:10.1007/978-3-319-70178-3_17
75. Chan Z, Chooi YC, Ding C, et al. Sex Differences in Glucose and Fatty Acid Metabolism in Asians Who Are Nonobese. *J Clin Endocrinol Metab*. 2019;104(1):127-136. doi:10.1210/jc.2018-01421

76. Basu A, Dube S, Basu R. Men Are from Mars, Women Are from Venus: Sex Differences in Insulin Action and Secretion. *Adv Exp Med Biol*. 2017;1043:53-64. doi:10.1007/978-3-319-70178-3_4
77. Gehrand AL, Hoeynck B, Jablonski M, et al. Sex differences in adult rat insulin and glucose responses to arginine: programming effects of neonatal separation, hypoxia, and hypothermia. *Physiol Rep*. 2016;4(18). doi:10.14814/phy2.12972
78. Nokoff N, Thurston J, Hilkin A, et al. Sex Differences in Effects of Obesity on Reproductive Hormones and Glucose Metabolism in Early Puberty. *J Clin Endocrinol Metab*. 2019;104(10):4390-4397. doi:10.1210/jc.2018-02747
79. Mirmiran M, Swaab DF, Kok JH, Hofman MA, Witting W, Van Gool WA. Circadian rhythms and the suprachiasmatic nucleus in perinatal development, aging and Alzheimer's disease. *Prog Brain Res*. 1992;93:151-162; discussion 162-163.
80. van den Berg R, Noordam R, Kooijman S, et al. Familial longevity is characterized by high circadian rhythmicity of serum cholesterol in healthy elderly individuals. *Aging Cell*. 2017;16(2):237-243. doi:10.1111/acel.12547
81. Hale GE, Hughes CL, Burger HG, Robertson DM, Fraser IS. Atypical estradiol secretion and ovulation patterns caused by luteal out-of-phase (LOOP) events underlying irregular ovulatory menstrual cycles in the menopausal transition. *Menopause N Y N*. 2009;16(1):50-59. doi:10.1097/GME.0b013e31817ee0c2
82. Manoogian ENC, Panda S. Circadian rhythms, time-restricted feeding, and healthy aging. *Ageing Res Rev*. 2017;39:59-67. doi:10.1016/j.arr.2016.12.006
83. Huard B, Bridgewater A, Angelova M. Mathematical investigation of diabetically impaired ultradian oscillations in the glucose-insulin regulation. *J Theor Biol*. 2017;418:66-76. doi:10.1016/j.jtbi.2017.01.039
84. Zavala E, Wedgwood KCA, Voliotis M, et al. Mathematical Modelling of Endocrine Systems. *Trends Endocrinol Metab*. 2019;30(4):244-257. doi:10.1016/j.tem.2019.01.008